ISSN: 2588-5596

JGT

Journal of Gas Technology

Volume 9 . Issue 2 . Winter 2024 . www.jgt.irangi.org

Journal of Gas Technology, JGT

Volume 9, Issue 2, Winter 2024

Publisher
Iranian Gas Institute

Contact Information
http://jgt.irangi.org
Email: ijgt.igi@gmail.com

EISSN: 2588-5596

Open Access Journal
Journal of Gas Technology is a peer reviewed, open access journal.

JOURNAL OF GAS TECHNOLOGY

Volume 9, Issue 2, Winter 2024

Annual Names of Reviewers

Ali Vatani
University of Tehran

Mastaneh Hajipour
Islamic Azad University, Science and Research Branch

Saeid Jamshidi
Sharif University of Technology

Morteza Zivdar
University of Sistan and Baluchestan

Amir Hossein Mohammadi
University of KwaZulu-Natal, South Africa

Sadegh Etedali
Birjand University of Technology

Mohammad Foroughi
University of Tehran

Masoud Aghajani
Petroleum University of Technology

Hossein Sanghtarash
Islamic Azad University Bandar Abbas Branch

Hosseinali Rahdar
University of Zabol

Vahid Haddadi Asl
Amirkabir University of Technology

Yahya Balouchi
University of Sistan and Baluchestan

Ail Hassani Joshaghani
Islamic Azad University, Arak Branch

Masoud Bijani
Garmsar University

Mahdi Elyasi Kojabad
Behbahan Khatam Alanbia University of Technology

Reza Lotfi Mayan Sofla
Sahand University of Technology

Kioumars Taheri
National Iranian Oil Company

Masoud Dorfeshan
Behbahan Khatam Alanbia University of Technology

Alimorad Rashidi
Research Institute of Petroleum Industry

Table of Contents

Identifying and Ranking the Factors Influencing the Determination of the "Delivery Point" in International Natural Gas Sales Contracts (Case Study: Natural Gas Sales Contracts in LNG state) 5

Mohammad Reza Alimardan, Abbas KazemiNajafabaddi , Mohammad Reza Seyed Hashemi Touloun, Seyed Asghar Hendi, Mohamad Mahdi Hajian

Enhanced CO_2 Separation Using Pebax Membrane Modified with Ethylene Glycol Monophenyl Ether 28

Mahdi Elyasi Kojabad, Parya Amirabedi, Masoud Dorfeshan

Application of Ultrasonic Waves on the Demulsification (Dehydration) of Crude Oil 39

Asieh Hafezi, Amir Hossein Saeedi Dehaghani, Serveh Abdollahi, Mehdi Razavifar

Optimisation of Steel Pipe-Rack Structures in the Oil Industry Using Metaheuristic Algorithms 54

Ruholamin Chatrazar, Hamed Ghohani Arab, Mahmoud Miri

The Impression of Roughness on Flow Pattern and Performance of Axial Gas Cyclone Along with Erosion Rate 70

Masoud Dorfeshan, Sattar Moghaddam, Farzad Parvaz

JOURNAL OF GAS TECHNOLOGY

Volume 9 / Issue 2 / Winter 2024 / Pages 5-27

Journal Home page: http://jgt.irangi.org

Identifying and Ranking the Factors Influencing the Determination of the "Delivery Point" in International Natural Gas Sales Contracts (Case Study: Natural Gas Sales Contracts in LNG state)

Mohammad Reza Alimardan[1], Abbas Kazemi Najafabadi[2*], Mohammad Reza Seyed Hashemi Touloun[3], Seyed Asghar Hendi[4], Mohamad Mahdi Hajian[5]

1. Ph.D. Student, Department of Law and Political Science, Faculty of Law, Allameh Tabataba'i University, Tehran, Iran
2. Associate Professor, Department of Law and Political Science, Faculty of Law, Allameh Tabataba'i University Tehran, Iran
3. Assistant Professor, Department of Management, Sohrevardi Institute of Higher Education, Qazvin, Iran
4. Faculty Member, Research institute of Petroleum Industry, Tehran, Iran
5. Assistant Professor, Department of Law and Political Science, Faculty of Law, Allameh Tabataba'i University Tehran, Iran

ARTICLE INFO

ORIGINAL RESEARCH ARTICLE

Article History:
Received: 15 July 2024
Revised: 02 October 2024
Accepted: 27 November 2024

Keywords:
Natural gas
Liquefied natural gas (LNG)
Natural gas sales and transmission contract
Delivery Point
Contractual factors
Contingent factors

DOR: 20.1001.1/jgt.2025.2030090.1038

ABSTRACT

The analysis of the global environment of the energy industry and its developments shows that natural gas is the shaper of the world's energy future. The future of Iran, as the owner of the world's first gas resources, is undeniably tied to a category called "Natural gas". New developments, such as the environmental conditions of the world, the consequences of the war between Russia and Ukraine, the tensions in the Middle East region, and the prediction of a rise in the global price of crude oil in the near future have also increased the role and importance of natural gas. According to the analysis of British Petroleum (BP) and the International Energy Agency (IEA), the trend of natural gas consumption will continue at a faster pace until 2030. Therefore, in order to maintain Iran's superior position in the world markets and to timely use the advantage of the country's gas reserves so as to turn these reserves into more value-added capital, we need to further develop country's technical, political, marketing, legal, infrastructures etc. One of the main components of the legal infrastructure to create and develop market share in the global natural gas markets is to pay attention to the issue of how to design and regulate international natural gas sales contracts in accordance with the transfer method and the basic bottlenecks in it. One of the most important bottlenecks in international contracts for the sale of natural gas is the design and determination of the "Delivery Point", which can be different in different contracts, according to the method of transfer and the contingent factors of each contract. In this research, in order to identify the factors influencing the determination of the "Delivery Point" in the international contracts for the sale of natural gas in LNG form, the research literature was reviewed and interviews were conducted with experts, and the conceptual model of the research and their measurement indicators were designed. The collected indicators were distributed among the members of the statistical community in the form of a researcher-made questionnaire and their opinions were collected. According to the findings of this research, the results of the T-test indicated that the five main factors defined for this research are effective, according to the members of the study's statistical population, in determining the delivery point in international natural gas sales contracts with an emphasis on the LNG method. On the other hand, the Friedman ranking test was used to rank these factors in terms of their level of importance. Based on the test results, the contractual factor had the highest mean rank and, consequently, the greatest importance. The political, geographical, technical, and economic factors followed in terms of importance, respectively.

How to cite this article
M.R. Alimardan, M.R. Syed Hashemi Toloun, A. Kazemi Najafabadi, S.A. Hendi, M.M. Hajian. Identifying and Ranking the Factors Influencing the Determination of the "Delivery Point" in International Natural Gas Sales Contracts (Case Study: Natural Gas Sales Contracts in LNG state). Journal of Gas Technology. 2024; 9(2): 5-27. (https://www.jgt.irangi.org/article_723161.html)

* Corresponding author.
E-mail address: kazemi_najaf@atu.ac.ir, (A. Kazemi Najafabadi).

Available online 30 December 2024

1. Introduction

Natural gas plays an important role in meeting global energy needs. It can be transported through pipelines (Local or international) or in the form of liquefied natural gas (LNG). The construction of gas and LNG infrastructure requires large investments, which are concluded from the very first days through long-term contracts with reliable buyers. Historically, there was only one long-term segment for gas and LNG sales. This is how the delivery of LNG cargo, and gas export through the pipeline, were executed with a significant amount of contracts and financial shares that were closed through these contracts. In the 1990s, short-term markets began to emerge, providing new contractual arrangements for the sale of gas and LNG. As a result, the contract landscape for international gas and LNG transactions has become more diverse. Despite the growing role of spot or short-term transactions, a significant volume of gas and LNG is still traded under long-term contracts. After Russia's invasion of Ukraine, these traditional agreements may become even more important. This is due to the increasing geopolitical uncertainties and the need to ensure long-term energy security. Long-term contracts provide buyers and sellers with confidence that supply and demand will be predictable in the future, especially in conditions where political or economic disruptions could affect short-term markets (IEA, 2022). Furthermore, following Russia's invasion of Ukraine, many European countries have sought to reduce their dependence on Russian gas and diversify their energy supply sources. This has led to an increase in demand for long-term contracts with other gas producers, particularly through LNG methods. These contracts not only guarantee energy security but also help countries avoid price volatility in short-term markets (BP, 2023). Consequently, long-term contracts have gained greater importance as a key tool for managing geopolitical and economic risks in the global gas and LNG industry.

Therefore, we see an increase in the interest of various actors, including energy market participants, regulators, as well as the general public, in long-term gas and LNG supply contracts (Ason, 2022). The past few years have also seen significant advances in liquefied natural gas (LNG) processing and distribution technologies, which have opened up new avenues for reliable energy supply at affordable prices. As a result, the number of LNG consuming countries has increased from 15 countries in 2005 to 48 countries in 2023 (IEA, 2023; Msakni & Haouari, 2018). Interestingly, natural gas is the only fossil fuel whose share of primary energy consumption is expected to increase. The International Energy Agency recently estimated that global demand for natural gas is expected to increase. For some emerging economies, this growth is even more impressive. As an example, China is expected to account for 40% of the global growth. One of the reasons for this growth in China is its interest in natural gas, which is and will be supplied from Russia because natural gas is considered the cleanest fossil fuel (Msakni & Haouari, 2018). Additionally various gas producing export countries such as Australia, America and Russia are launching huge plans to increase their capacity of LNG production by spending the required large investment. Therefore, it is important to pay attention to the legal issues of international natural gas sales agreements (GSA). The terms of international natural gas sales contracts are very important from a financial, legal and even political point of view, because gas contracts can have a significant impact on the economic future of countries due to their high financial volume. In the international gas sales contracts and specifically in the LNG state, there are many administrative, technical and legal bottlenecks: In international LNG sales contracts, key bottlenecks include complex regulatory approvals, technical challenges

in liquefaction and transportation, legal disputes over jurisdiction, price negotiation complexities, and ensuring long-term supply security amidst geopolitical risks, which are necessary to be investigated further, in order to avoid any implementation problems and the resulting consequences. I knowing and avoiding the bottlenecks of international natural gas sales contracts, can it greatly help to facilitate these types of contracts? One of the main bottlenecks in international natural gas sales contracts is the category of determining the "Delivery Point". Considering the special characteristics of natural gas, every international contract for the sale of natural gas has its own special conditions which naturally require attention and consideration. In all international contracts for the sale of natural gas, the issue of determining the "Delivery Point" is one of the most important issues, which is influenced by various geographical, political, economic, and other factors. From the legal point of view, the point of delivery or delivery of the goods is the point where the goods are in a state where the buyer can exercise ownership rights over them. Due to the lack of previous research resources in this field (IEA, 2021; Wood, 2018) we, in this research, seek to explain and analyze the concept of the "Delivery Point" in international gas sales contracts and explain the factors affecting the determination of the "Delivery Point" with an emphasis on the LNG along with their related indicators. And we also rank these factors based on their importance in international gas sales contracts.

2. Problem Definition

With the passage of time and in different eras, different fuels have been used, from wood to coal, oil and its derivatives, and natural gas. This rotation from wood to coal and from coal to oil and natural gas is due to each energy source having different characteristics compared to its previous source. For example, the more favorable a fuel source is in terms of the amount of energy it releases, in terms of the technological needs of the day and in terms of the environment, the more attention and use that source has. Amongst all energy carriers, natural gas is more important and desirable because it has the highest ratio of hydrogen to carbon among fuels (Alikhani, 2016: 290; Busby, 2016; Seyedhashemi Toulon, 2019). Natural gas has a history of thousands of years, but its importance as a fuel used in our lives began in the early 1930s. At the end of the 20th century, it became clear that natural gas has become a very necessary and vital energy source in most of the industrialized world (Busby, 2010: 26; Demirbas, 2006).

Due to the following reasons, the role and importance of natural gas is increasing:

- Day by day, more natural gas resources are being discovered (IEA, 2023; BP, 2022), so that natural gas will become one of the most important natural fuel energy carriers in the 22nd century.
- By reducing carbon dioxide and stabilizing the entry of greenhouse gases into the atmosphere, natural gas can have a positive effect on the growing trend of global warming.
- Natural gas is a carrier of energy that can be used in many technologies and different parts of different industries as well as in household uses (IEA, 2022, EIA, 2023).
- If natural gas can be transferred through the global gas supply network, many people can get benefit from it. In this regard, Russia is still the largest exporter of natural gas in the world, most of which has been transported through pipelines and then in the form of LNG. But after the war in Ukraine, the export of Russian gas has been limited. Currently, Russia has a gas lock of about 75 to 85 billion cubic meters and does not know where to use this gas (Fars news Agency, 2023).

However, in fact, natural gas has its own issues for consideration. For example, the supply and demand of natural gas in the world markets is less than oil, and its transfer from one place to another is very expensive and difficult. But since most of the natural gas fields in the world are far from the consumption market, the costs related to the production, processing and transportation of natural gas are high. In such a situation, gas transmission by means of new solutions along with cost reduction is of particular importance. This problem has caused the creation of different methods for natural gas transmission. Pipelines and LNG are among the most important and widely used natural gas transportation methods. Investigations have shown that it is possible and practical to transfer natural gas to long distances at a lower price through LNG. LNG transportation costs per mile are lower than pipeline. Another major advantage of this method is the easier transportation of liquefied natural gas to long distances and the reduction of political problems in terms of crossing international waters (Qanvati-Nasab, 2021: 36-29; Rahimi and Dehghani, 2019: 14-22).

On the other hand, the amount of energy that natural gas releases in a certain volume is less. However, due to the continuous increase in the price of oil and environmental concerns about the level of air pollution, natural gas has become one of the most important sources of clean energy in the world. Also, the consequences of the war between Russia and Ukraine and the lack of a vision for the end of the war, as well as the sanctions imposed against Russia, have caused global imbalances in the players of the energy industry (Alikhani, 2016: 2; Hirani). et al., 2016). Price volatility and supply disruptions following Russia's invasion of Ukraine have negatively affected the performance of several gas and LNG supply contracts. Parties to gas contracts have also faced unprecedented demands from regulators regarding their contractual rights. The prolonged period of market uncertainty has led to an increased emphasis on risk management activities by industry participants and has recently led to a significant increase in disputes under long-term contracts. In parallel, the urgent need to reduce dependence on Russian gas imports has sparked a search for additional supplies and led to the signing of dozens of new LNG contracts this year, including more than 25 signed by US producers (for more than 35 million metric tons per year). Although the legal and commercial aspects of these new contracts are generally confidential, the reported contract terms (mostly between 15 and 25 years) and the estimated average new contract duration of nearly 20 years indicate a significant increase in long-term contracts. This in turn means a deviation from the previous trend in favor of shorter deals (Ason, 2022: 17-18).

But in general, based on the statistics and the results of expert studies regarding the advantages and disadvantages of natural gas, it can be argued that natural gas is facing an increasing acceptance at the global level and a certain trend. natural gas has become an essential energy source in most of the industrialized world (U.S. Energy Information Administration (EIA), 2006; Mitchell et al., 2012; Roberts, 2014: 135; Robinson and Holland, 2021; Rahimi, 2016: 98; Seyedhashmi Toulon, 2019: 25; Shiriavskaya et al., 2021: 2). Many countries are lucky enough to have at least some natural gas reserves, but there are other countries such as Japan that have to import almost all the gas they need. Most of the places containing rich oil resources also have natural gas resources. Russia, the Middle East (specially Iran & Qatar), Mexico, some parts of South America and the countries located on the edge of the North Sea of Europe are among these (Busby, 1380: 17). But the distribution of natural gas reserves in the world is asymmetric and due to the set of positive characteristics of natural gas, the global demand for it is increasing (Roberts, 2014: 135;

Augusta et al., 2021: 5). For example, based on the analysis provided by the BP Energy Studies Center, in the time horizon of 2035, natural gas will have the highest consumption growth rate, which will be supported by strong supply growth (BP, 2016). It is especially supported by American shale gas and LNG liquefied gas and by environmental policies (Hajian and Mousavi, 2015: 82).

On the other hand, in recent years, in addition to its conventional sources, gas production has become possible from unconventional sources as well (Samadi and Meibodi, 2014). As the first holder of conventional gas reserves in the world and the fourth producer, Iran intends to increase its share in the global gas trade by entering the gas competition. Meanwhile, according to the latest estimates made by BP in 2023, Iran has the first natural gas reserves in the world (18%) (BP, 2023; EIA, 2023). Finally, it can be concluded in this section that the current developments in the field of world energy diplomacy indicate that in the not so distant years, there will be countries with superior economic power that dominate the world's energy resources, especially oil and gas. Therefore, identifying and providing the necessary infrastructure for the production, marketing and global sale of natural gas will be one of the priorities of the National Iranian Oil Company (NIOC), (Stevens, 2015: 2; Shiravi, 2012).

In this regard, one of the most important areas that can maintain Iran's public and national interests in the field of economy and politics at the international level is the commercialization of energy, including gas supply through sales contracts of which gas transfer is an important factor in this regard. (Hajian and Mousavi, 2015: 82). Meanwhile, in the studies conducted by the European Parliament, it has been determined that there is a possibility of exporting gas to Europe from 12 countries. Iran is one of these countries and has the suitable source of gas supply to this continent. Europe is looking for the diversification of energy supply sources of the green continent and Iran will also find a suitable capacity to increase gas exports with the development of new phases of South Pars which can be connected to the European gas network from eight routes (Mohammadi et al., 2015: 2). Russia's various political challenges with the European Union and the interruption of Russian natural gas exports to Europe several times since 2006, the consequences of Russia's war with Ukraine and the surplus of Russia's gas balance, the tensions in the Middle East and the forecast increase in global oil prices. It has set a special position for Iran's gas export and considering the transferring is an important issue. Because of several disputes with Turkey in sales contract and different aspects to this business, Iran has to look for other transmission methods, the other choice is LNG transmission. All these arguments indicate that the future of Iran is undeniably tied to a category called "gas". Therefore, it is necessary to carry out basic studies and measures in all the infrastructural aspects of this industry. Contracts for the sale and transfer of natural gas are always among the most important contracts in the world's oil and gas industry, and due to the growing use of natural gas fuel instead of oil, the importance of such contracts is becoming more and more clear (NikBakhsh Sharafshade, 2013: 1; Ason, 2022).

Long-term gas and LNG supply contracts, which serve as the main examples of international gas contracts, contain strong provisions that define the rights and obligations of the parties. International gas contracts operate in a dynamic market environment. There are many challenges facing these contracts, which always require improvement of contract conditions and sometimes immediate responses from the parties (Ason, 2022). Therefore, one of these basic challenges is paying attention to the legal issues of international gas sales contracts. Paying attention to the bottlenecks of international natural gas sales contracts can greatly help in facilitating these types

of contracts. One of the main bottlenecks in international natural gas sales contracts is the category of determining the "Delivery Point". Considering the special characteristics of natural gas, every international contract for the sale of natural gas has its own conditions and naturally requires special attention and considerations. In all international contracts for the sale of natural gas, the issue of determining the "Delivery Point" is one of the most important issues, which is influenced by various geographical, political, economic, and other factors. From the legal point of view, the point of delivery or delivery of the goods is the point where the goods are in a state where the buyer can exercise ownership rights over them. The term transfer of ownership has the meaning that a person, by virtue of a contract or a deed, transfers the ownership of which he has a financial burden to another person, so that his ownership is lost as soon as this transfer is made and the ownership of another person or persons takes the place of his ownership (Qanawati, 2013: 30). Due to the lack of research resources in this field, in this research, we seek to explain and analyze the concept of the "Delivery Point" in international gas sales contracts and explain the factors affecting the determination of the "Delivery Point" along with the indicators related to them, as well as the ranking. These factors are based on the level of importance in international gas sales contracts.

3. Research Literature Review

International gas sales contracts include agreements and commitments between countries or international companies for the purchase and sale of natural gas. These contracts are usually signed for a long period of time and based on specific contract terms. International gas sales contracts can be signed bilaterally or multilaterally between countries. In bilateral agreements, only two countries are involved, while in multilateral agreements, several countries may be involved. The things that are usually considered in international gas sales contracts are:

- Gas price: Contracts usually determine the conditions for determining the price of gas. This price may be fixed or determined based on some market indicators.
- Volume and delivery time: Contracts usually specify how much gas should be delivered and when.
- Payment conditions: Contracts also determine conditions for payment to the seller. These conditions may include determining the time of payment and the method of payment.
- Contract conditions: Contracts usually also specify other conditions, such as: conditions for the transfer of gas ownership ("Delivery Point"), obligations related to gas quality and responsibilities of the parties to the contract. Considering the importance of gas in the energy industry, concluding gas contracts is a necessity in order to ensure the establishment of international cooperation, guarantee energy supply and industrial development.

One of the key points in international gas contracts is transparency. These contracts must have full transparency and assure the parties that all the terms and conditions in these contracts are correctly foreseen. One of the main bottlenecks in natural gas sales contracts is the issue of determining the "Delivery Point". Therefore, according to the nature of the topic of this research, the research literature is divided into two main parts. In the first part, we analyze and explain the legal nature of the concept of delivery and submission in different legal systems, and then in the second part of the research background, we try to explain the factors affecting the determination of the "Delivery Point" in international gas

sales contracts. We use the pipeline and LNG transmission, and at the end of this section, the conceptual model of the research, which is a combination of the research background and experts' opinion, is presented.

3.1. The First Part of the Background of the Research: Analysis and Explanation of the Legal Nature of Delivery and Submission

All legal systems agree that the purpose of the sales contract is to transfer ownership from the seller to the buyer. However, legal systems differ on when and how to transfer ownership, so that the drafters of the Vienna Convention in 1980 preferred to be silent about the time of transfer of ownership in the international sale of goods. In fact, in the analysis of the transfer of ownership process, we are faced with two basic questions:

- Does the sales contract itself directly cause the transfer of ownership without the need of any intermediary?
- Does the sales contract create the transfer of ownership immediately?

The answers of legal systems to these two questions are not the same. Some consider the transfer of ownership to be a direct and immediate effect of the sale contract, and others consider other legal actions necessary in addition to the sale contract to realize the transfer of ownership (Amini, 2012: 36; Faizi-Chekap and Mousavi, 1400). The transfer of ownership is the main purpose of sale in all legal systems, but the time of transfer of ownership to the buyer is different in different legal systems according to the type of goods (Qanvati, 2012: 59; Faizi-Chekap and Mousavi, 1400). Ownership may be transferred to the buyer upon conclusion of the contract, delivery of the goods, completion of the contract, or at any time agreed upon by the parties. The relationship between delivery and ownership is well reflected in the Rome legal system, since in Rome law, ownership is transferred to the buyer upon delivery of the goods. Surrender is an important step in sales contracts, because the buyer can exercise most aspects of his ownership rights on the seller when the seller is in his possession and control by real and material or hypothetical and immaterial handover. In this regard, it is necessary to examine the relationship between the concepts of surrender and ownership in the legal systems of Iran, England and the International Sales Convention (Vienna Convention). Of course, the Vienna Convention, because it does not contain provisions regarding the transfer of ownership, can be less effective in this direction than the laws of England and Iran (Olumi-Yazdi, 2001: 67; Faizi-Chekap and Mousavi, 2020). Regarding the determination of the time and legal analysis of the ownership transfer process in sales contracts, there is a fundamental difference between two views: the view that considers the sale contract insufficient for the transfer of ownership and the view that considers the sale contract sufficient for the transfer of ownership. German laws on one hand and French and Iranian laws on the other hand are good examples to explain these two views. Carefully in the analytical bases regarding the time and manner of transfer of ownership in sales contracts in the three legal systems of Germany, France and Iran, it shows well that the fundamental difference is actually the degree of adherence of each system to two important legal principles, i.e. respect for freedom and independence of will and guaranteeing security of transactions and protection of third parties return on the other hand. Affected by their historical, economic and social conditions, some systems have paid more attention to the first principle and others to the second principle (Amini, 2004: 173). In general, and by examining different analysis regarding the nature of submission in different legal systems, it can be concluded

that there are similar elements in the concept of submission in different legal systems, which are somehow compatible with the Vienna Convention. Surrender, whether physical and material or hypothetical and judicial, in most legal systems indicates the transfer of control of the seller to the buyer. Before handing over, although the buyer acquires the property of the seller, the effects and manifestations of this ownership, especially in relation to third parties, are revealed by handing over. A transfer of ownership, when not accompanied by a surrender, will have no significant effect. Surrender, whether physical or judicial, enables the buyer to exercise his ownership rights over the seller. Surrender occurs when the seller stops exercising control and possession and places the seller in a situation that allows the buyer to exercise this control. In this sense, delivery is different from bill and receipt of goods. The issue is the time and method of transferring ownership to the buyer. The Vienna Convention has left the answer to these two questions to the domestic law of the country whose law can be applied as the governing law of the contract. In English law, the parties can agree on the time of transfer of ownership from the seller to the buyer, but if the subject of the contract is a general obligation or a general contract, it is not possible to transfer ownership before determining and assigning one of the general persons to the contract. In Iranian law, ownership is transferred at the same time as the sale is concluded, provided that the seller has the ability to transfer. The parties can also agree on the transfer of ownership at another time, provided that the subject of the sale contract can accept the transfer at that time. Iranian law is similar to English law because the total ownership of the seller cannot be transferred to the buyer in either of the two systems. But the difference between English and Iranian law is that in English law, the parties can agree on the transfer of ownership before concluding the contract, while in Iranian law, the parties cannot retroactively apply the effect of the contract. In any case, the differences are small and uniform regulations such as the Vienna Convention, which cleverly refrained from raising the issue of the time of ownership transfer, are compatible with both systems (Olumi-Yazdi, 2010: 92-92). Finally, it can be concluded in this part of the research literature that determining the transfer point of contractual liability risk in international gas sales and transportation contracts is very important in the political and economic situation of the owners of these tanks and the contractors of these contracts. In addition, how the risk is distributed and the point of its transfer will affect the contractual and financial situation surrounding the aforementioned contracts. In natural gas sales and transportation projects through pipeline or LNG, the parties to the contract usually foresee the point of transfer of ownership, risk and goods in the contract, and in case the governing law is not determined and the territorial regulations are silent, the provisions of the Vienna Convention and Incoterms regarding the transfer of liability risk can govern these contracts (FeiziChekap and Mousavi, 2020). In energy transfer projects, which involve the sea transport of goods by ship, the point of transfer of contractual responsibility will be according to the agreement of the will of the parties or the provisions of maritime transport conventions or other relevant international regulations. In the Vienna Convention, the main rule in determining the point of transfer of liability is that it is transferred by submitting the risk, but there are exceptional cases for determining the point of risk transfer, where another solution is accepted, which is the time of concluding the contract, as far as today LNG sales is in CIF term and usually is not transferred to another place as reselling, title transfer letter and Authorization To Sell and Collect letter has not an important role in LNG business as in the other fossil energy carriers.

3.2. The Second Part of the Background of the Research: Factors Affecting the Determination of the "Delivery Point" in International Contracts for the Sale of Natural Gas

The international contract for the sale of natural gas or the agreement for the sale and purchase of natural gas will determine a certain point, usually called the point of delivery or sometimes called the point of sale, at which point the seller's obligations to deliver the gas to the buyer will be implemented.. This point requires precise definition, as does the nature of the seller's delivery obligation. The point of delivery will be identified in a relevant agreement with a lexical explanation and possibly by adding an outline to show the necessary details (Roberts, 2014: 135). The "Delivery Point" is a point that is clearly defined and at that point, the ownership and risk of the sold gas is transferred from the seller to the buyer. In international contracts for the sale of natural gas, often a detailed plan of the pipeline systems and facilities related to the "Delivery Point" completes the definition of the "Delivery Point". The specifications of the "Delivery Point" often include the specifications of the delivery pressure, or its minimum and maximum values, as well as the quality specifications that are directly mentioned in the contract or indirectly by referring to the agreement related to the transportation (Wood, 2018; IGU, 2021). The "Delivery Point" is the point where the gas is transferred from the seller to the buyer and is the focal point between the upstream and downstream interests. The "Delivery Point" is usually defined in the international natural gas sales contract as a precise geographic location and a specific point between the seller's gas production facility and the buyer's gas facility. Also, the "Delivery Point" can be defined and determined among the gas transportation facilities. The definition of the "Delivery Point" is often accompanied by an outline in the international gas sales contract for graphic representation. The "Delivery Point" may be the point of connection of the gas producing equipment to the pipeline that delivers the gas through these facilities, which is often called the "plant gate" or "backdoor sales" (Roberts, 2014: 135).

3.2.1. Types of "Delivery Point" Modes in International Gas Sales Contracts Through the Pipeline

In the international contracts for the sale of natural gas by pipeline, the process of gas transfer and delivery is carried out through pipelines, so there are at least five different modes in the definition and determination of the "Delivery Point", which are mentioned in this section.

1. Gas delivery at the seller's production facility: as shown in (Figure 1), in this case, the gas "Delivery Point" is determined at the outlet of the natural gas seller's facility and from this point, the ownership and the resulting risk is transferred from the seller to the buyer. Naturally, in this situation and according to the situation of the "Delivery Point", the majority of the risks will be borne by the buyer.

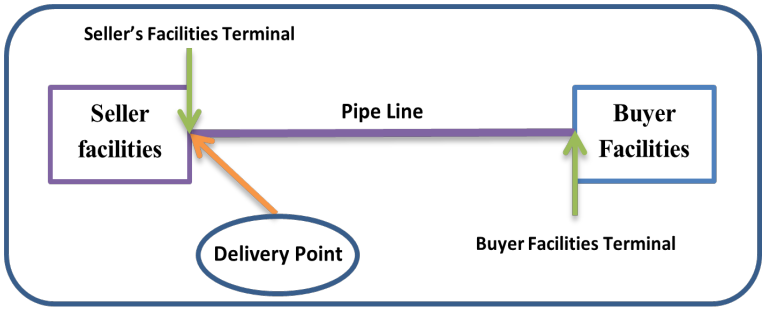

Figure 1: the First Mode of Determining the "Delivery Point": Gas Delivery at the Outlet of the Seller's Facility (Roberts, 2014: 136)

2. Gas delivery at the buyer's delivery facility: as shown in (Figure 2), in this case, the gas "Delivery Point" is determined at the entrance of the buyer's gas delivery facility, and from this point, ownership and risk as a result, it is transferred from the seller to the buyer. Naturally, in this situation and according to the situation of the "Delivery Point", most of the risks will be borne by the seller.

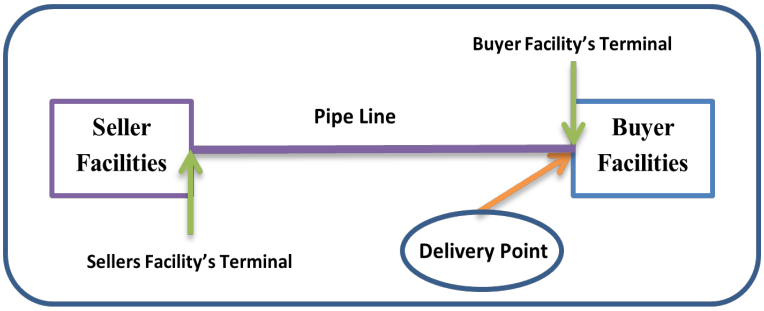

Figure 2. The Second Mode of Determining the "Delivery Point", Gas Delivery at the Buyer's Delivery Facility (Roberts, 2014: 136)

3. Delivery of gas at an alternative "Delivery Point" in the buyer's delivery facility: In the international natural gas sales contract, there may be a specified alternative "Delivery Point" where the buyer's or seller's facilities are designed to meet this possibility. In such a case, this advantage is created for the seller that if there is a problem in the supply of gas at the main "Delivery Point", the delivery of gas will be made through an alternative "Delivery Point", and increasing the overall level of transportation to the buyer is in the seller's favor (Roberts, 2014: 136). Alternative "Delivery Point" formulation assumes that a primary "Delivery Point" is specified in the contract, with an alternative "Delivery Point" (or alternative points), the alternative "Delivery Point" may be defined and determined from the beginning in the contract or during the implementation of the contract will be identified and defined. The alternate "Delivery Point" will actually back up the original "Delivery Point". The international gas sales contract can also have multiple "Delivery Points". Also, the international contract for the sale of natural gas can include a mechanism through which the "Delivery Point" can be changed at different times based on the negotiations between the seller and the buyer and the agreement reached (Roberts, 2014: 136-137).

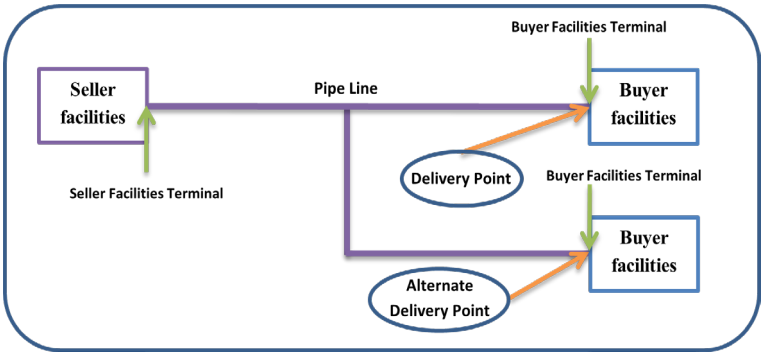

Figure 3. The Third Mode of Determining the "Delivery Point", Gas Delivery at the Alternative "Delivery Point" in the Buyer's Delivery Facility (Roberts, 2014: 136)

4. Gas delivery to the gas transmission network agreed between the seller and the buyer: the "Delivery Point" can be the entry point to a gas transmission network. The buyer can take responsibility for transporting gas through this network and separately, from the gas transmission network, the amount of gas delivered with a certain quality by the seller to the gas transmission network. Taking delivery of gas by the seller to the network creates for the buyer the right to deliver gas from the network in the quantity and quality provided by the seller to the network at a separate "Delivery Point". As a result, the gas transmission network may face an imbalance resulting from the gas withdrawal by the buyer in an amount less or more than the amount delivered by the seller. If such a situation occurs, the contractual requirements will be applied to each of the parties in the international gas sales contract. For example, the buyer has to reserve the capacity of the network for the amount of gas that will be delivered by the seller, to the equivalent amount of gas in order to maintain the integrity of the network. In this case, the buyer must be sure that in the international natural gas sales contract, provisions have been made to cover any liability due to non-delivery of gas or shortfall in gas delivery from the seller to the network. Because in this case, in case of any problem, the gas transmission network will be the party of account with the buyer. In (Figure 4), the mode of gas delivery at the entrance of the gas transmission network is shown.

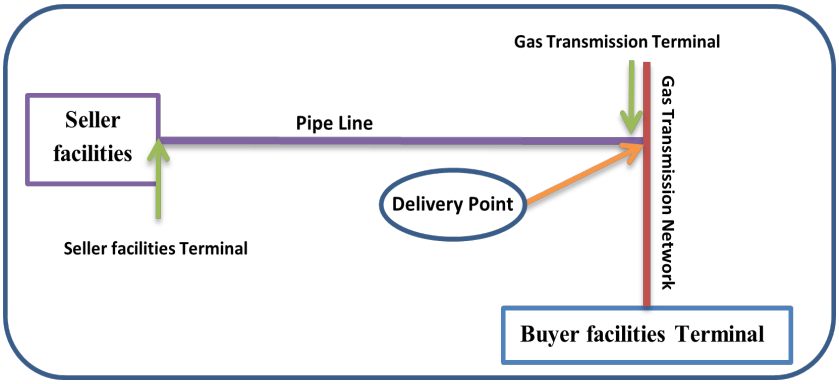

Figure 4. The Fourth Mode of Determining the "Delivery Point", Gas Delivery at the Entrance of the Gas Transmission Network (Roberts, 2014: 137)

5. Delivery of gas by the seller at the destination and at the entry point of the buyer's facility: in this case, the seller's duty is to provide the gas to the buyer at the "Delivery Point", which is defined as a point outside a gas transmission network. In this case, the responsibility of reserving capacity in the gas transmission network as well as the responsibility of delivering gas to the network will be with the seller. Therefore, in this case, the seller must ensure the existence of appropriate mechanisms and guarantees in the international gas sales contract from the buyer to cover any negligence in gas delivery or delivery of gas exceeding the contractual amount. In diagram number (Figure 5), the state of gas delivery at the destination and at the gas "Delivery Point" at the entrance of the buyer's facility is shown (Roberts, 2014: 138-137).

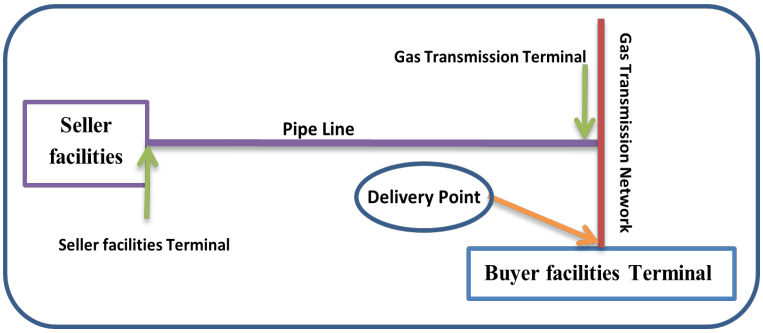

Figure 5. The Fifth Mode of Determining the "Delivery Point", Gas Delivery at the Destination and at the Entrance of the Buyer's Facility

3.2.2. Considerations Related to the "Delivery Point" in International Gas Sales Contracts Through LNG

In order to better explain the considerations related to determining the "Delivery Point" in LNG sales contracts, it is necessary to first familiarize ourselves with the LNG supply chain process and the main challenges in it. As previously mentioned in parts of this research, the role of natural gas in the global energy market has forced the energy industry to launch complex multi-billion-dollar supply chains with the aim of ensuring the timely delivery of LNG around the world with the required volumes and with it is the cheapest cost. Typically, an LNG supply chain consists of the following four main stages:

1. Exploration and Production
2. Processing and liquefaction, in which the natural gas is cooled to minus 162 degrees Celsius and as a result its volume is reduced approximately 600 times
3. Transportation, in which LNG is transported in liquid form using cryogenic ships
4. Regasification and distribution, in which LNG is converted into its gaseous state and distributed to end users (Msakni & Haouari, 2018: 394).

The LNG producer concludes long-term contracts that specify the required monthly or annual delivery quantities at the destination ports (Andersson et al., 2017). It is the producer's responsibility to deliver the LNG to customers while also being responsible for production and inventory management. The producer creates an annual delivery schedule for each customer that specifies the port of loading and unloading for each LNG shipment, as well as the departure and arrival dates for a period of 12 to 18 months (Rakke et al., 2011). Typically, the goal of an annual delivery schedule is to provide long-term contracts at minimum cost. When planning for the annual delivery schedule, inventory management should be considered as it is of critical importance in the LNG industry. The inventory level must be maintained within certain limits. If the inventory level is too high or too low, production may be forced to shut down, which may cause heavy losses and thus be unfavorable. In addition to inventory constraints, the planned annual delivery schedule must be feasible according to ship and hub availability at various ports. It is customary to assign most, but not all, production capacity to medium-term and long-term contracts (Stålhane et al., 2012). For example, Russian liquefaction plants have contracted the Yamal and Sakhalin Energy projects in the form of medium- and long-term contracts, which count for approximately 90 and 95% of annual production, respectively (GIIGNL, 2019). Excess LNG production is usually sold to various spot markets, providing an opportunity for the producer to earn more

or reduce production inventory pressure. Selecting the spot market for service and time is also usually part of the ADP planning process, considering logistic capacity. (Schütz, 2020).

The design, operation and control of these stages creates serious challenges for the scientific and research community. Articles in this field cover three levels of standard decision-making: 1- strategic, 2- tactical and 3- operational. The strategic level focuses on long-term planning of facilities, fleets and infrastructure, as well as on setting up long-term contracts involving periodic deliveries of LNG over long periods of time (typically 20-25 years). The tactical level (mid-term) focuses on the design of an annual delivery plan that specifies delivery quantities along with a practical delivery plan with the aim of implementing long-term (compulsory) contracts with minimal operating costs. The (short-term) operational planning phase aims to create a detailed delivery schedule that takes into account the annual delivery schedule while integrating opportunities to sell excess LNG quantities in the spot market. Typically, the time horizon of an action plan is three months (Msakni & Haouari, 2018: 394).

In this regard, Koza et al. (2017) have investigated the strategic issues caused by the LNG supply chain. The issues identified by the researchers are: 1- The cost of building LNG storage ports in different places in Asia and Europe; 2- Capacity of storage ports and 3- Fleet of LNG ships (owned or leased) to transfer LNG from producer to storage ports (Msakni & Haouari, 2018: 394). For example, one of the features that distinguishes LNG transportation from other marine cargoes is the possibility of using boiled gas. Due to its low boiling point, LNG vaporizes (boils) and the gas from the boiling is usually used as a fuel for the carrier (Goel et al., 2012). Another fundamental problem for the annual delivery schedule with a planning horizon of about one year is that seasonal changes in speed can be expected, which may affect the quality of the solutions. The use of fixed sailing time may also cause scheduling problems in practice, so seasonal sailing time should also be considered (Schütz, 2020).

Another major problem in selling LNG with an annual delivery schedule has been inspired by the Yamal project located on the Yamal Peninsula in northern Russia. To transport LNG from Thabita to customers, specially developed ice-cold LNG carriers are needed due to the presence of sea ice. These ice LNG carriers are designed to work in Arctic waters and the northern Sea route, but in open waters, normal LNG carriers perform better. As the eastbound route from Thabita to Asia may not be available during the winter due to environmental conditions, Asian customers are serviced through a transit port in Europe. By using a transshipment port, the producer avoids longer than necessary open-water voyages with ice LNG carriers, as conventional LNG carriers can pick up LNG and deliver it to customers. Direct routes and transfers are different in terms of distance and therefore shipping time as well as costs. Then the manufacturer must decide not only about the departure dates, but also through which route to serve its customers. Introducing a transit port to the network provides more flexibility, but also makes planning the annual delivery schedule more challenging. Another problem with the annual LNG delivery schedule in the transportation sector is that in each shipment, LNG is only allowed to be moved at most once. This problem has appeared in recent years with the entry of the Yamal LNG project into production (Schütz, 2020). Another important consideration that should be considered in the procurement and delivery of LNG is the quasi-monopoly of ownership of the equipment in the hands of major producers, so its transportation is almost impossible for

the manufacturer without a specified ship.

However, most of the literature on LNG supply chain optimization has focused on tactical problems that require the creation of an annual delivery schedule, where the time horizon is usually considered to be 12 months.

In this part of the research, we mainly focus on contractual issues and specifically on the category of determining the "Delivery Point" in LNG sales contracts. Therefore, it is important to emphasize the issues and challenges affecting the determination of the LNG "Delivery Point". Considering the issues and challenges in the field of transportation and delivery of natural gas in the form of LNG, from a technical point of view, the LNG "Delivery Point" is actually the place where LNG is delivered from the carrier ship to the buyer's terminal, located in the connecting flange of the carrier manifold and the discharge system. which is part of the terminal. In other words, the "Delivery Point" in LNG gas transportation is the exit point or the "Delivery Point" of gaseous fuel from the terminal to the transmission system, and in LNG transportation, the ship-to-ship delivery term is impossible and therefore meaningless. The "Delivery Point", in future contracts or other derivatives, is the place where the physical goods underlying the contract are delivered. Buyers of futures contracts seeking to maintain their positions must be prepared to accept delivery and pay the agreed price for the physical commodity. However, the "Delivery Point" only applies to futures contracts that specify the physical delivery of the asset. Contracts that are settled in cash do not involve physical delivery. Therefore, the "Delivery Point" is a vital element in writing LNG sales contracts. The chosen "Delivery Point" affects the net delivery price or cost price of the underlying asset. The delivery conditions also guarantee the value of the delivered goods. With physical delivery, the price of the goods is different according to the transportation costs from the origin to the place of delivery. Therefore, to determine a unit price of a good for contract purposes, the point of delivery is an essential detail. Most futures market operators trade speculatively, and most of them do not consider the delivery of physical goods in future contracts. These speculative buyers buy futures contracts because they believe the price of the underlying commodity will rise, not because they are interested in delivering a few thousand barrels of oil or cubic meters of gas. Delivery requires having the resources to store and market these resources to end buyers. Buyers of futures contracts who wish to receive a physical commodity often hope to lock in the price of the commodity they use in production. By buying a futures contract, they hope to reduce the risk of adverse price changes in an asset (commonly known as "Hedging"). The "Delivery Point" for most natural gas and liquefied natural gas (LNG) futures on the New York Mercantile Exchange is a natural gas pipeline located in Erath, Louisiana (Chen, 2022). Therefore, in LNG sales contracts, due to various technical reasons and the complexity of transportation and delivery, the "Delivery Point" is usually determined at the buyer's entry facility in the destination country.

3.3. The Set of Factors Affecting the Determination of the "Delivery Point" in International Gas Sales Contracts

In general, it can be said that the field of international natural gas sales contracts, both inside and outside the country, has very limited study resources. By reviewing the limited literature of the research, we also realize that in the category of factors affecting the determination of the "Delivery Point" in the international contracts for natural gas carpets, not much has been clearly mentioned. The set of points that can be implicitly extracted from the available sources is that the determination of the "Delivery Point" in international contracts for natural gas can be

different depending on the conditions of each contract and is influenced by geographical, political, economic, technical and other factors, Therefore, in this research, due to the existing limitations, the mixed research method was used. After collecting library information, in-depth interviews with Iran's oil and gas industry experts as a statistical sample, supplementary information, the research was revised and finally the conceptual model of this research which shows the macro factors affecting the determination of the "Delivery Point" as well as their measurement indicators and explains the factors affecting the determination of the "Delivery Point" in international natural gas sales contracts with Emphasis on the LNG method is finalized. In order to test the suitability and validity of the results and findings of this research, a researcher-made questionnaire was designed based on the indicators identified in the qualitative phase of the research. The researcher-made questionnaire was used to collect the opinions of managers, oil and gas industry experts, and academic researchers. Academic staff engaged in teaching and researching in the field of oil and gas in Tehran state universities were distributed and their opinions were collected and analyzed. In (Figure 6), the conceptual model taken from the qualitative part of the research is shown.

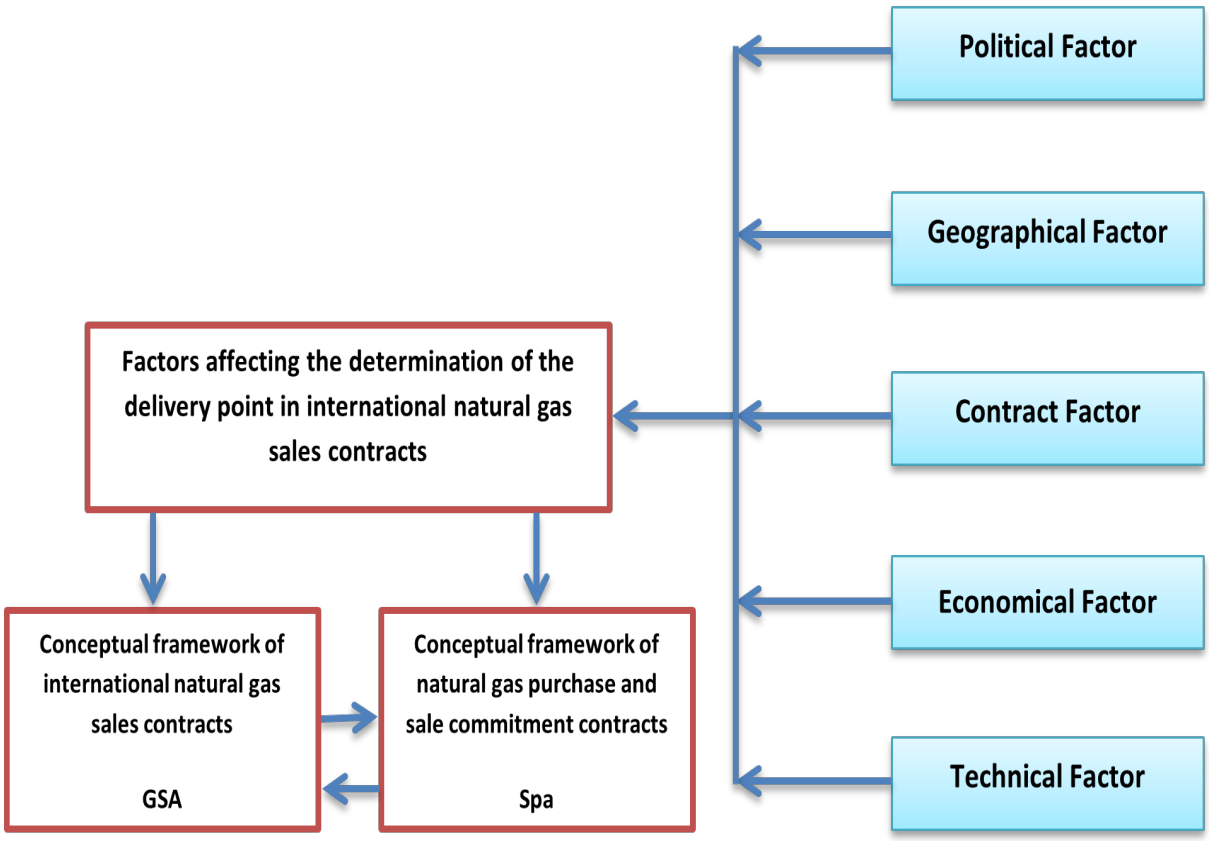

Figure 6. Conceptual Model of the Research: the Set of Macro Factors Affecting the Determination of the "Delivery Point" in International Contracts for the Sale of Natural Gas Using the LNG Method

As shown in (Figure 6), a total of 5 categories of main macro factors affecting the determination of the "Delivery Point" in international gas sales contracts along with the measurement indicators of these factors were identified in the qualitative part of the research and designed. The measurement indices of each of these factors are also shown in (Table 1).

Table 1. ?

The title of the Factor	Measurement indicators
Indicators for measuring the political factor (9 indicators)	1. The degree of political dependence of the seller and buyer countries on the sale and purchase of natural gas 2. The state of international relations between the seller and buyer countries of natural gas 3. Regional and extra-regional political blocs in the world that somehow affect the political relations of countries 4. The state of political relations between natural gas seller and buyer countries 5. History and extent of political differences between natural gas seller and buyer countries 6. Regional and extra-regional security situation. between the countries that sell and buy natural gas 7. The domestic political situation governing the countries that sell and buy natural gas 8. The state of economic and political ideology of the countries that sell and buy natural gas 9. The state of political stability in the countries that sell and buy natural gas.
Indicators for measuring the geographical factor (4 indicators)	1. The size of the geographical distance between the seller country and the buyer of natural gas 2. Having a common water or land border between the seller country and the buyer of natural gas 3. The existence of networks, ports and infrastructures of gas transmission lines in the geographical area between the seller. and the buyer of natural gas 4. The state and natural features of the geographic distance between the country of the seller and the buyer of natural gas.
Contractual factor measurement indicators (6 indicators)	1. The type of contract agreed for the sale of natural gas (gas field assignment contract to the buyer, gas supply and delivery contract, LNG method) 2. The legal system in each of the natural gas seller and buyer countries 3. The gas price formula mechanism and Payment of the gas price from the buyer to the seller 4. The status of the designed guarantee mechanisms (the obligation to receive) in the gas sale contract 5. The law governing the international gas sale contract, as well as the law governing the settlement of disputes 6. The penalty mechanism and procedure determined in the international natural gas sales contract.
Technical factor measurement indicators (6 indicators)	1. The volume and amount of natural gas agreed to be delivered from the seller to the buyer of natural gas 2. The quality standards agreed for the delivery of natural gas from the seller to the buyer of natural gas 3. The state of the calorific value of the natural gas agreed to be delivered from the seller to the buyer Natural gas 4. The lifespan and condition of the pipelines used to transfer gas from the seller to the buyer of natural gas 5. Environmental issues and restrictions raised in each of the natural gas seller and buyer countries 6. The location of the system Measurement in the process of natural gas delivery from the seller to the buyer.
Indicators for measuring the economic factor (4 indicators)	1. The current situation of supply and demand in the international markets of natural gas in the world and the region 2. The situation of the price of natural gas in the international markets of natural gas in the world and the region 3. The economic situation of the countries that sell and buy natural gas in terms of parameters Macroeconomics (income, foreign exchange reserves, etc.) 4. The role of the government in the economy of countries that sell and buy natural gas.

4. Field Study and Research Data Collection Process

In this research, the socio-statistics investigated includes managers of the oil industry, internal experts who have a history of scientific and executive activity in the Iranian oil and gas industry and also academic faculty members of Tehran, Allameh Tabatabai and Shahid Beheshti universities, who are engaged in research and scientific and executive activities in the fields of economics and oil and gas law. According to the definition of the statistical population of the research and also due to the limitation in access to all members of the statistical population, a non-probability sampling method was used. Finally, the possibility of face-to-face interview and completion of the questionnaire was provided to 30 people and the research questionnaire was completed by them. The final research questionnaire consists of 2 parts. In the first part of the questionnaire, individual characteristics were examined through qualitative questions created by the researcher. The second part of the final research questionnaire includes the indicators collected from the research literature and the qualitative part of the research that was obtained through interviews with experts, which was then used to obtain the opinion of the members of the statistical community about the factors and indicators that are effective in determining the "Delivery Point" which is provided in international natural gas sales contracts. This section includes 29 questions that were finalized after a trial implementation phase. Also, in this research, to determine the range of questionnaire answers, we tried to use the methods that lead to the desired results. Therefore, a five-point Likert response scale was used for this purpose. The validity of the questionnaire has been examined based on content validity and construct validity. Content validity was confirmed through the expert opinion of experts as well as the expert opinion of researchers. Confirmatory factor analysis (CFA) technique has also been used to check construct validity. In this research, due to the multi-level model and the multiplicity of model indicators, Partial Least Squares (PLS) method using SMARTPLS version 2 software was used to validate the model. The PLS estimation method determines the coefficients in such a way that the resulting model has the most power of interpretation and explanation, meaning that the model can predict the final dependent variable with the highest precision and accuracy. As shown in (Table 2) and (Table 3), all correlation coefficients are positive and significant at an error level of less than 1%.

Table 2. Validity, Reliability and Descriptive Index of the Research Conceptual Model

Variables	AVE	AVE	R^2	Cronbach's alpha	GOF
Political factor	0.562	0.895	0.684	0.870	0.622
Geographical factor	0.509	0.912	0.699	0.893	
Contractual Factor	0.570	0.929	0.608	0.915	
Technical Factor	0.572	0.929	0.655	0.913	
Economical Factor	0.796	0.970	0.000	0.969	

Table 3. Correlation Matrix and Separate Validity for the Conceptual Model of the Research

Hidden Variables	(1)	(2)	(3)	(4)	(5)
Political factor	0.794				
Geographical factor	0.601	0.714			
Contractual Factor	0.533	0.658	0.755		
Technical Factor	0.635	0.668	0.609	0.756	
Economical Factor	0.640	0.572	0.400	0.397	0.714

* All correlation coefficients are significant at the error level of less than 1%.

** The root mean square root shows the average explained variance (AVE).

The correlation matrix provides valuable insights into the relationships between the latent variables in the conceptual model. The strong correlations between factors like Political, Geographical, and Contractual highlight their interdependence in natural gas agreements. Meanwhile, the Economical Factor stands out as a distinct but still significant component. These findings can guide further analysis and decision-making in the context of international natural gas sales contracts.

5. Inferential Analysis of Research Data

In this research, the collected data were summarized and classified using descriptive statistics indicators such as frequency distribution table setting, graph drawing, calculation of central and dispersion indices. In order to select the generalities of the inferential statistics test (parametric or non-parametric statistics), a normality test was performed on the research data. The preference of the researcher is to use the parametric part of inferential statistics to answer the research questions. Because parametric statistics have more diversity and higher accuracy. The main condition for using parametric statistics is the normality of the distribution of data collected for research. Kolmogorov-Smirnov test was used to determine the normality of the research data (Momeni, 2016). The results of the normality test showed that the research data follows the normal distribution, so the use of the parametric part of inferential statistics is allowed. Therefore, in this research, sample T-Tech tests have been used to identify factors affecting the determination of the "Delivery Point" in international natural gas sales contracts. Friedman's test was also used to rank the identified factors in terms of importance. The first main question raised in this research is what are the factors influencing the determination of the "Delivery Point" in international natural gas sales contracts? In order to answer this research question, one-sample t-test (t-test) was used. This test forms two hypotheses for and against. In the zero hypothesis, the determined factors defined in the research are assumed to be effective, and in the one hypothesis, which is known as the opposite hypothesis, the defined factors are not assumed to be effective. The results of a sample T-Tech test to answer the research question are shown in (Table 4).

Table 4. The Results of the t-test to Identify Factors Affecting the Determination of the "Delivery Point" in Contracts

Description	Amount	Degrees of freedom	T	Average	Difference in averages	Standard deviation	Significant level
Political agent	30	29	11.973	3.8344	.83444	.38172	.000
Geographical factor	30	29	8.259	3.7767	.77667	.51507	.000
Contract agent	30	29	11.912	3.9800	.98000	.45059	.000
Technical agent	30	29	.107	3.0133	.01333	.68568	.016
Economic factor	30	29	1.792	3.2333	.23333	.71310	.014

The t value calculated for the 5 factors of the conceptual model of the research is greater than the t value of the normal distribution table (1.96) and the significance level is also less than (0.05) (Momeni, 2016). According to these results, it can be concluded that all the 5 main

factors that make up the conceptual model of the research are effective in determining the "Delivery Point" in international natural gas sales contracts according to the members of the statistical community studied. The second main question raised in this research, which we seek to answer, is the ranking of factors affecting the "Delivery Point" in international gas sales contracts in terms of their importance in the studied statistical population. To answer this research question, Friedman's ranking test was used. The results of the Friedman test for the ranking of the factors are shown in the (Table 3).

Table 5. Friedman's Test Results for Ranking the Factors Affecting the Determination of the "Delivery Point"

Title of Factors	(Mean Rank)
Political factors	4.63
Geographic factors	4.23
Contract agents	4.85
Technical factors	2.95
Economic factors	2.38

As shown in (Table 5), the contractual factor with an average rank (4.85) has the highest importance. Also, the political factor is ranked second with an average rating (4.63). The geographical factor with an average rating (4.23) ranks third, and the technical factor ranks fourth with an average rating (2.95) and finally the economic factor with an average rating (2.38) is placed in the fifth place. It should be kept in mind that the unit of analysis in this research is the organization; therefore, the calculated framework is based on organizational level variables and extra-organizational variables are not included in this framework.

6. Conclusion and Suggestions

In this research, we seek to explain and analyze the factors influencing the determination of the "Delivery Point" in international contracts for the sale of natural gas, emphasizing the LNG state. Due to the lack of research resources in this field, it is necessary to use mixed and discovery-based research methods in order to conduct the research. Therefore, in order to identify the factors influencing the determination of the "Delivery Point" in international contracts for the sale of natural gas, and, after studying the research literature, in-depth interviews were conducted with experts in the oil and gas industry as well as negotiators of international contracts for the sale of natural gas. Members of the scientific boards of faculties of state universities in Tehran were interviewed and finally the conceptual model of the research along with the measurement indicators of each department was finalized. In order to increase the scientific validity of the conceptual model of this research, a survey was conducted among the members of the research statistical community about the indicators and factors of the model in the form of a researcher-made questionnaire. The results of the t-test showed that the 5 main factors defined for this research are effective in determining the "Delivery Point" in international natural gas sales contracts, emphasizing the LNG method, according to the members of the research statistical community. On the other hand, Friedman's ranking test was used to rank these factors in terms of importance. Based on the results of the test, the contract factor has the highest rank average and is therefore the most important. Political, geographical, technical and economic factors were placed in the next ranks in order of importance. Based on the investigations and studies conducted by the researcher, the results of this research are consistent with the opinion of experts and similar studies and confirm the previous findings. The noteworthy point in this research, which has not been observed in other similar studies and is a kind of innovation specific to this research, is the identification of a relatively complete set of factors affecting the determination of the "Delivery Point" in international contracts for the sale of natural

gas and their complete approval. It is based on the data collected from the statistical population of the research. This research finding is completely unique to this research and has not been observed in other research literature so far. Also, according to the findings of this research, a set of practical suggestions are presented for oil industry managers and negotiators of international contracts for the sale of natural gas:

1. As inferred from the results of this research, the 5 main factors of the conceptual model of this research (contractual, political, geographical, technical and economic factors) as effective factors in determining the "Delivery Point" in international contracts for the sale of natural gas was identified Therefore, considering the importance of determining the "Delivery Point" in the contracts, it is suggested that before conducting any negotiations and setting up the contract for the sale of natural gas, the five factors identified in this research should be carefully and sensitively studied in order to help to make the process of negotiations and setting up the contract more efficient.
2. According to the results of this research, the contractual factor is the most important in determining the "Delivery Point" in international natural gas sales contracts. Political, geographical, technical and economic factors were placed in the next ranks in order of importance. Therefore, it is recommended that the indicators of the contractual agent be analyzed and researched separately and in accordance with the target markets for the sale of natural gas, and the relationships between the indicators planned in this research for the contractual agent are also analyzed and explained
3. Considering the sensitivity and importance of each of the five dimensions identified in this research, it is recommended that each of these factors be investigated and deeply analyzed separately so that more dimensions and angles of the factors should be clarified.
4. It is strongly recommended that the relationship between these factors and their synergism be analyzed in a separate research format. As these factors have a mutual effect on each other in terms of implementation and operation, and, in the case of not paying attention to this key and important category, it is not possible to use the maximum capacity and abilities of these factors in order to determine the optimal "Delivery Point" used in international contracts for the sale of natural gas.
5. It is strongly recommended that recent political developments in the process of power sharing in the world (formation of new corridors) and its impact on international natural gas sales contracts as well as LNG delivery issues should be analyzed in a separate research.
6. According to what was discovered and identified in the case of LNG production in Iran, that due to the lack of free carrier ships and no interest of shipping Iranian produced LNG by International LNG Tanker fleets, the importance of delivery to the buyer's facilities is one of the main challenges of sales during the sanctions. In addition, to receiving the payment from the buyer, will be the provision of LNG carriers and shipment of produced LNG as well as changing documents and origin of the Iranian LNG.

References

Agosta, Alessandro; Boccara, Gillian; Bresciani, Giorgio; Heringa, Berend; Browne, Nicholas (2021). The impact of decarbonization on the gas and LNG industry. McKinsey Insights, McKinsey & Company.

Alikhani, Muhammad (2009). Investigating the

legal status of the sale and price in international gas sales contracts. International Legal Journal, International Legal Affairs Center publication of the Vice President of Legal and Presidential Affairs, year 26, number 4.

Alikhani-Chamgardani, Mohammad (2016). Gas sales contract. Master's thesis, Shahid Beheshti University, Faculty of Law.

Amini, Mansour (2004). Transfer of ownership in sales contracts in the legal systems of Germany, France and Iran. Legal Research Quarterly of Shahid Beheshti University, No. 37.

Andersson, H.; Christiansen, M.; Desaulniers, G.; Rakke, J.G (2017). Creating annual delivery programs of liquefied natural gas. Optim. Eng., 18, 299 - 316. [Google Scholar]

Ason, Agnieszka (2022). International Gas Contracts. Research Paper, Oxford Institute for Energy Studies.

BP p.l.c. (2016). Energy Outlook. Outlook to 2035, 2016 Edition, London, United Kingdom.

BP p.l.c. (2017). BP Statistical Review of World Energy. London, United Kingdom.

Busby, Rebecca L. (2002). Natural gas in non-technical language. Translated by: Alireza Hamidi Younesi, Tehran: Institute of International Energy Studies Publications.

Chapter 4 (2006). Natural Gas. International Energy Outlook, Energy Information Administration Report (An, Official Statistics from U.S Government). (http://www.eia.doe.gov).

Chen, James (2022). "Delivery Point": What It Is, How It Works, Examples. https://www.investopedia.com/terms/d/delivery-point.asp.

Demirbas, A. (2006). The Importance of Natural Gas as a World Fuel. Energy Sources, and Part B: Energy and Planning, Vol.1, No. 4. (Taylor & Francis, Oct-Dec 2006).

Fars news agency (2021). Deciphering the impact of the Ukraine war on the restoration of gas relations between Iran and Turkmenistan. An interview with the head of the International Energy Studies Institute.

GIIGNL. (2019). The LNG Industry GIIGNL Annual Report 2019. The International Group of Liquefied Natural Gas Importers: Neuilly-sur-Seine, France. [Google Scholar]

Goel, V.; Furman, K.C.; Song, J.H.; El-Bakry, A.S (2012). Large neighborhood search for LNG inventory routing. J. Heuristics, 18, 821-848. [Google Scholar]

Haji-Hosseini Baghdadabadi, Tahira; Ghasemi, Abdul Rasul; Mohammadi, Timur (2022). The future study of natural gas consumption in Iran in the horizon of 2030; A scenario-building approach based on the censored regression model. Quarterly Journal of Energy Economics Studies, 18 (73): 1-23.

Hajian, Mohammad Mehdi; Mousavi, Mitra (2015). A comparative study of the legal status of the condition of obligation to receive in gas sales and transmission contracts. Private Law Research Quarterly, Year 5, Number: 16.

Health Effects Institute (2017). State of Global Air 2017. URL<https://www.stateofglobalair.org/sites/default/files/SoGA2017_report.pdf >.

Hosseinzadeh Kashan, Ali; Akbari, Ali Akbar (2016). Natural gas transmission network optimization model - study.

International Energy Agency (IEA). (2021). The role of LNG in the global energy market. Retrieved from https://www.iea.org.

International Energy Agency (IEA). (2022). The role of natural gas in global energy transitions. Retrieved from https://www.iea.org.

International Energy Agency (IEA). (2023). Global energy outlook 2023. Retrieved from https://www.iea.org.

International Gas Union (IGU). (2021). Wholesale gas price formation. Retrieved from https://www.igu.org.

Jazayeri, Ahmed (2015). Gas diplomacy: Europe and turning weaknesses into strengths in the energy crisis. Tehran: Yazda Publications.

Koza, D.F., Ropke, S., Molas, A.B. (2017). The liquefied natural gas infrastructure and tanker fleet sizing problem. Transport. Res. Part E: Logist. Transport. Rev. 99, 96-114 doi:10.1016%2Fj.tre.2017.01.003.

Li, Mingyu, and Peter Schütz (2020). Planning Annual LNG Deliveries with Transshipment. Energies 13, no. 6: 1490. https://doi.org/10.3390/en13061490.

Marcel, Valerie & Mitchell, John V. (2006). Oil Titans: National Oil Companies in the Middle East. Washington D.C: CHATHAM HOUSE and London BROOKINGS INSTITUTION PRESS.

Matthiesen, Henning (2006). To What Extent Do Take-or-Pay Contracts Facilitate the Development of Infant Gas Markets and What Challenges Do They Pose at the Time of Liberalization? CEPMLP Annual Review. (www.dunddee.ac.uk/cepmlp 2006).

Mitchell, John & Marcel, Valérie & Mitchell, Beth (2012). What Next for the Oil and Gas Industry? London, CHATHAM HOUSE, the Royal Institute of International Affairs.

Mohammadi, Teymur; Ghanimi Fard, Hojjat Elah; duty, affection; Javan, Afshin (2015). Simulating the FOB cash price for Iran's natural gas export from the hypothetical northwest hub using the Schwartz-Smith method. Iranian Applied Economic Studies Quarterly, No. 20.

Momeni, Mansour; Qayoumi, Ali (2016). Analyzing statistical data using SPSS. Tehran: Kitab Nou Publications.

Morishima, H. (2006). Natural Gas Bridging to the Future Energy. (http://cat.inist.fr).

Msakni, Mohamed Kais & Haouari, Mohamed (2018). Short-term planning of liquefied natural gas deliveries. Transportation Research Part C: Emerging Technologies, Volume 90, May 2018, Pages 393-410.

Nabi Faizi Checkap, Ghulam; Mousavi, Mitra (2020). The risk transfer point of contractual responsibility in international contracts for the sale and transportation of natural gas from the point of view of the Convention on the International Sale of Goods. Scientific Quarterly of Judicial Law Perspectives, No. (95).

NaturalGas.org (2013). Natural Gas and the Environment. URL<http://naturalgas.org/environment/naturalgas/ >.

Nik-Bakhsh-Sharfshadeh, Ali (2013). Review of natural gas sales and transfer contracts. Master's thesis, University of Tehran, Faculty of Law and Political Sciences.

Pustišek, Andrej & Karasz, Michael (2017). Natural Gas: A Commercial Perspective. Berlin: Springer International Publishing.

Qanawati Nasab, Ali (2020). Investigating hydrate technology and various methods of natural gas transmission. Scientific monthly oil and gas exploration and production. Number (199).

Rahimi, Gholam Ali (2008). Investigating natural gas pricing mechanisms in different regions. Energy Economy Studies, Volume: 4, Number 13.

Rahimi, Gholam Ali, Dehghani, Toraj (2017). LNG import marine terminals; Opportunities and challenges. Scientific monthly oil and gas exploration and production. Number (156).

Rai, Hassan; Nazari, Javad; Sarzahi, Morteza; Maleki, Abbas (2021). The blessing or curse of natural gas in Iran: a prospective study of natural gas exports until 2050. Public Policy Quarterly.

Rakke, J.G.; Stålhane, M.; Moe, C.R.; Christiansen, M.; Andersson, H.; Fagerholt, K.; Norstad, I

(2011). A rolling horizon heuristic for creating a liquefied natural gas annual delivery program. Transp. Res. Part Emerg. Technol, 19, 896-911. [Google Scholar].

Roberts, Peter (2014). Gas and LNG Sales and Transportation Agreements, Principles and Practice, Fourth Edition. SWEET & MAXWELL, THOMSON REUTERS Professional, UK Ltd.

Robinson, J.; Holland, Bill (2021). Natural gas in transition: Upstream faces pressure to cut emissions, go green. S&P Global Platts.

Sakaran, Uma (2016). Research methods in management. Translation: Mohammad Saebi and Mahmoud Shirazi, Tehran: Publications of the Higher Institute of Management and Planning Education and Research, fifth edition.

Samadi, Ali Hossein; You give an imam, Mahdi (2014). Investigating the impact of the expansion of unconventional gas resources on Iran's natural gas production: a system dynamics approach. Iranian energy economy research journal.

Sarmad, Venus; Bazargan, Abbas; Hijazi, Elaha (2009). Research methods in behavioral sciences. Tehran: Aghaz Publishing House, 16th edition.

Seyedhashmi Tolon, Mohammad Reza (2019). Compiling the optimal model of company management in the direction of the internationalization of National Iranian Oil Company. Doctoral thesis, Allameh Tabatabai University, Faculty of Law and Political Sciences.

Shiravi, Abdul Hossein (2012). Oil and gas law. First edition, Tehran: Mizan publication.

Shiryaevskaya, Anna; Stapczynski, Stephan; Koh, Ann (2021). Natural gas prices surge as energy transition-driven demand outstrips supply. World Oil, Houston, Texas.

Stålhane, M.; Rakke, J.G.; Moe, C.R.; Andersson, H.; Christiansen, M.; Fagerholt, K. (2012). A construction and improvement heuristic for a liquefied natural gas inventory routing problem. Comput. Ind. Eng. 2012, 62, 245-255. [Google Scholar]

Stevens, Paul (2015). Prospects for Iran's Oil and Gas Sector. Research paper, Middle East and North Africa Program & Environment. London: Energy and Resources Department, Chatham House, the Royal Institute of International Affairs.

Stevens, Paul (2016). International Oil Companies: The death of the old business Model. Research paper. London: Chatham House, the Royal Institute of International Affairs.

Uzezi Aziano, Ef (2012). Natural Gas Contracts: Do Take or Pay Clauses Fall Foul of The Rule Against Penalties? Journal of Energy and Natural Resources Law, p.8.

Wood, D. (2018). LNG: A nontechnical guide. PennWell Books.

Yazdi Olomi, Hamidreza (2010). The concept of submission and its relationship with the transfer of ownership and risk (including exchange) in the contract of sale. Journal of Law and Policy Research, No. 315.

JOURNAL OF GAS TECHNOLOGY

Volume 9 / Issue 2 / Winter 2024 / Pages 28-38

Journal Home page: http://jgt.irangi.org

Enhanced CO_2 Separation Using Pebax Membrane Modified with Ethylene Glycol Monophenyl Ether

Mahdi Elyasi Kojabad[1*], Parya Amirabedi[1], Masoud Dorfeshan[2]

1. Assistant professor, Department of Chemical Engineering, Faculty of Engineering, Behbahan Khatam Alanbia University of Technology, Behbahan, Iran
2. Assistant professor, Department of Mechanical Engineering, Faculty of Engineering, Behbahan Khatam Alanbia University of Technology, Behbahan, Iran

ARTICLE INFO

ORIGINAL RESEARCH ARTICLE

Article History:
Received: 04 November 2024
Revised: 07 December 2024
Accepted: 30 December 2024

Keywords:
CO_2 separation
Polymer membrane
Polyether block amide
Ethylene glycol monophenyl ether
Trade-off limitation

DOR: 20.1001.1/jgt.2025.2048620.1049

ABSTRACT

CO_2 separation is one of the main challenges of today's world due to the growth of industries. Membrane separation method is a promising method for CO_2 separation, and poly(ether-block-amide) (Pebax) polymer membrane is one of the industrial membranes in this regard. However, this membrane is limited by the permeability-selectivity trade-off, which restricts its wider industrial application. This study aimed to address this limitation by incorporating ethylene glycol monophenyl ether (EGME) as filler in the Pebax membrane. The investigation focused on the impact of EGME on the chemical structure, morphology, physical and thermal properties, as well as the separation characteristics of the polymer. The results showed that by adding EGME, the prepared membrane became more brittle, with increased stiffness, and the tensile strength and Young's modulus of the Pebax/EGME membrane increased by 53 and 99.5 percent, respectively, compared to the pure membrane. Furthermore, the permeability of CO_2 and the CO_2/N_2 selectivity improved by 247% and 49%, respectively, attributed to the interactions between EGME and CO_2 molecules, including Lewis acid-base, dipole-quadrupole, and π-quadrupole interactions. This performance improvement allowed the Pebax/EGME membrane to surpass the Robeson upper bound, overcoming the permeability-selectivity trade-off, indicating the key role of EGME in improving the separation performance of Pebax. Moreover, The separation efficiency of the developed membranes was on par with, and in many cases superior to, the majority of membranes created by other researchers.

How to cite this article
M. Elyasi Kojabad, P. Amirabedi, M. Dorfeshan, Enhanced CO_2 Separation Using Pebax Membrane Modified with Ethylene Glycol Monophenyl Ether. Journal of Gas Technology. 2024; 9(2): 28-38. (https://www.jgt.irangi.org/article_721338.html)

* Corresponding author.
E-mail address: m.elyasi@bkatu.ac.ir, (M. Elyasi Kojabad).

Available online 30 December 2024

1. Introduction

Nowadays, the pollution caused by greenhouse gases represents a significant challenge for nations worldwide. Among these gases, carbon dioxide (CO_2) is particularly detrimental, playing a crucial role in the greenhouse influence and contributing to worldwide warming (Sun et al., 2024). Flue gases are a major source of CO_2 emissions, necessitating the implementation of various removal techniques. Membrane separation technology has developed as a prominent and effective technique in this domain, gaining considerable attention in recent years. The majority of membranes utilized for CO_2 separation are polymer-based, offering numerous advantages such as flexibility and ease of production and modification (Khosravi, 2021). Membranes constructed from the poly(ether-block-amide) (Pebax) copolymer have proven to be particularly effective for CO_2 separation, attracting significant interest from researchers (Afshoun et al., 2017). Pebax is a copolymer composed of polyethylene and polyamide segments, which endows it with mechanical strength and favorable permeability for CO_2 separation due to its distinctive two-part structure. Nonetheless, membranes derived from this copolymer often face challenges related to the trade-off between enhancing selectivity and permeability simultaneously (Kojabad et al., 2024a). To address this issue, researchers have discovered the incorporation of organic or inorganic fillers, amine compounds, carbon-based materials, zeolites, metal oxides, and metal-organic frameworks into the polymer matrix (Elyasi and Norouzi, 2025; Kojabad et al., 2024b; Zhang et al., 2025). This approach improves the interaction between the polymer and gas molecules, so improving both gas separation performance and membrane stability. The collaboration between polymers and fillers leads to the development of membranes characterized by high efficiency, selectivity, and permeability, offering effective solutions for a variety of applications (Narkkun et al., 2023).

The selection of an appropriate compound to incorporate into the polymer matrix is crucial for the development of membranes that exhibit effective separation capabilities. Given that Pebax interacts with CO_2 via its ether groups, the introduction of a compound featuring functional groups with a strong affinity for CO_2 can significantly enhance the permeability (Hosseinkhani et al., 2024). While employing various nanoparticles within the polymer matrix is a viable approach, it presents the challenge of particle aggregation, which can adversely affect the membrane's separation efficiency. Furthermore, although high molecular weight compounds, such as polymers, integrate well with the polymer matrix, their positioning among the polymer chains tends to diminish the fractional free volume, thereby substantially lowering the gas diffusion coefficient. In contrast, low molecular weight compounds that possess functional groups favoring CO_2, when incorporated into the polymer matrix, achieve a favorable distribution and exhibit enhanced mobility, ultimately contributing positively to the increase in gas permeability (Setiawan and Chiang, 2023).

In recent years, the incorporation of low molecular weight compounds into polymer matrices has garnered significant interest for enhancing membrane separation performance. Meshkat et al. (2019) introduced benzoic acid and isophthalic acid, both of which contain carboxylic acid groups, into the Pebax matrix. Their findings indicated that benzoic acid was more effective in enhancing the performance of Pebax, achieving improvements in CO_2/N_2 selectivity and CO_2 permeability of 55% and 120%, respectively, compared to the pure Pebax membrane. Sanaeipour et al. (2019) incorporated glycerol, a compound with hydroxyl groups, into the Pebax matrix. While the addition of glycerol led to a 172% increase in CO_2/N_2 selectivity, it also led to a 23% reduction in CO_2 permeability relative to the pure Pebax membrane. Elyasi et al. (2021a) utilized aniline, which contains an amino group, in the Pebax

matrix. The presence of aniline created a facilitated transport mechanism, resulting in increases of 101% in CO_2/N_2 selectivity and 76% in CO_2 permeability compared to the pure Pebax membrane. Hassanzadeh et al. (2022) added sorbitol, characterized by its six hydroxyl groups, to the Pebax matrix. This modification yielded a modest 0.5% increase in CO_2 permeability, while CO_2/N_2 selectivity improved by 29% compared to the pure Pebax membrane. Given these studies, researchers are actively seeking to identify an optimal compound that can further enhance the performance of Pebax. This compound should ideally feature appropriate functional groups to reinforce the interaction between the CO_2 molecules and polymer matrix, while also ensuring compatibility with the polymer matrix to prevent defects at the membrane structure, which could otherwise diminish selectivity. Choosing a compound that can interact with CO_2 faster and easier is essential. As mentioned, various compounds containing hydroxyl, carboxylic, amine, and ether groups have been used extensively as CO_2 carriers in recent years. The amino group necessitates the availability of water to engage in reactions with CO_2, thereby restricting its applicability. In contrast, ether, hydroxyl, and carboxyl groups can interact with CO_2 under various conditions, making them more versatile. Selecting a material that possesses at least two of these functional groups can prove advantageous. Ethylene glycol monophenyl ether (EGME) is a compound that contains both an ether group and a hydroxyl group.

In this research, EGME was identified to enhance the separation efficiency of Pebax. The study examined its influence on the chemical structure, morphology, physical and thermal characteristics, as well as the CO_2 separation capabilities of this polymer. EGME can interact with CO_2 by Lewis acid-base interactions via its hydroxyl group and can engage in dipole-quadrupole interactions with CO_2 through its ether group. Furthermore, the π electrons present in the aromatic ring of the EGME structure can facilitate π-quadrupole interactions with CO_2.

2. Experimental

2.1. Materials

CO_2 and N_2 gases with 99.9% purity were provided by Araz Oxygen Co. Pebax®1657 was purchased from Arkema. EGME and ethanol were obtained from Sigma-Aldrich.

2.2. Membrane Preparation

To prepare the membranes, first 0.58 g of Pebax was dissolved in 22.4 cc of a ethanol/water solution (70/30 wt%), which was refluxed at 85 °C for a duration of 2 hours, leading to a 3 wt% solution. Once the solution reached room temperature, 0.145 g of EGME (20 wt%) was added to the Pebax solution and stirred for 30 min. After that, the prepared solution was bath sonicated for 20 min and then was subsequently stirred for 2 hour. The resultant solution was then poured into a designated Teflon mold and placed in an oven set at 50°C for 24 hours. Following this period, during which membrane films were formed, the membranes were transferred to an oven at 110°C for an additional 6 hours to ensure complete drying.

2.3. Characterizations

The physical properties and thermal characteristics of the membranes were assessed through differential scanning calorimetry (DSC) using a Netzsch instrument (Netzsch DSC-200 F3, Germany). Fourier transform infrared spectroscopy (FTIR) was conducted utilizing an alpha-p spectrometer (Bruker, UK) to analyze the chemical composition of EGME and the prepared membranes. The morphology of the membranes was also investigated via field emission scanning electron microscopy (FESEM) with a TESCAN BRNO-Mira3 LMU apparatus, while the mechanical strength of the membranes was determined by a Zwick/Roell tensile testing machine (Z010, Germany).

3.4. Gas Permeation Tests

The gas separation performance of prepared membranes was examined under conditions of varying volume and constant pressure, which is shown schematically in (Figure 1). In this regard, The prepared membranes were cut into the round shape disc with the diameter of 6 cm. These experiments were carried out at a pressure of 7 bar and temperature of 25 °C. The gas permeability (P) was calculated using Eq. 1 (Amini & Asghari, 2018).

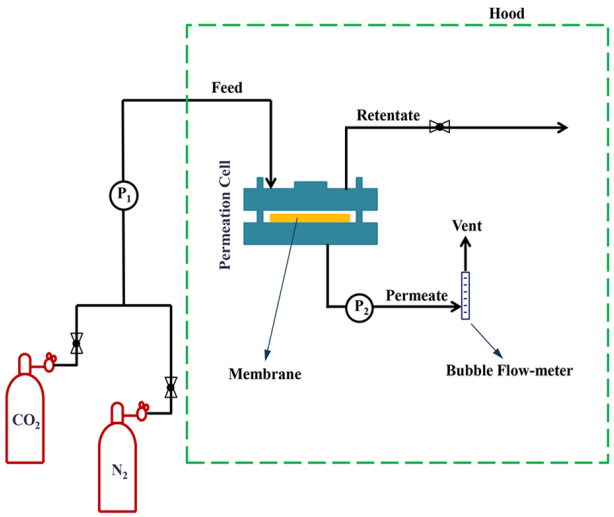

Figure 1. Schematic of the Experimental Setup for Gas Permeation Measurement

In this equation, Q denotes the volumetric flow rate of the gas flowing through, measured in cm^3/s. A represents the effective membrane area in cm^2, Δp signifies the pressure difference across the membrane in cmHg, and L indicates the thickness of the membrane in cm. The permeability derived from this equation is quantified in Barrer, where 1 Barrer is equivalent to 10^{-10} cm^3(STP) cm/(cm^2cmHg). Moreover, the selectivity ($\alpha_{i/j}$) for the gas pair i and j is determined by the ratio of their permeability, as outlined in Eq. 2 (Momeni et al., 2019).

$$\alpha_{i/j} = \frac{P_i}{P_j} \quad (1)$$

3. Experimental

3.1. Characterizations

(Figure 2) shows the findings from the FTIR analysis conducted on EGME and the prepared membranes. The FTIR spectrum of EGME reveals distinct peaks at 1230 cm^{-1} and 1088 cm^{-1}, which correspond to the C–O and C–O–C bonds, respectively. Furthermore, while C–H groups are identified at 2880 cm^{-1}, hydroxyl groups are observed in the region of 3500 cm^{-1}. The FTIR analysis of both the pure Pebax membrane and the Pebax/EGME membrane reveals distinct peaks associated with the N–H group of the polyamide component of Pebax at 3296 cm^{-1} (Kojabad et al., 2021b). Peaks at 2900 cm^{-1} and 1734 cm^{-1} correspond to the CH_2 group and the C = O ester bond, respectively, while the peak for the H-N-C = O bond is observed at 1650 cm^{-1}. Furthermore, the peak at 1090 cm^{-1} is attributed to the C–O–C bond present in the polyether segment of Pebax (Mahdavi et al., 2017). A comparison of the FTIR spectra between the pure membrane and the EGME contained membrane indicates that the addition of EGME does not result in any significant alterations to the FTIR spectrum of the Pebax polymer matrix. This suggests that the interactions between EGME and the polymer matrix are predominantly physical and hydrogen bonds.

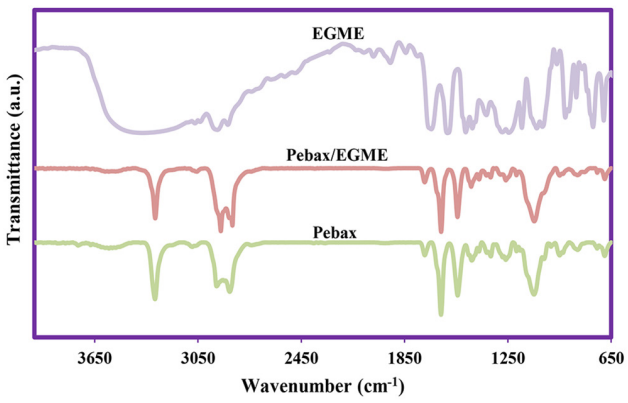

Figure 2. FTIR Spectra of EGME and the Prepared Membranes

To investigate the morphology of the prepared membranes, FESEM images was employed, with results presented at two distinct magnifications in (Figure 3). The figure indicates that the prepared membranes are devoid of any structural imperfections and exhibit a compact, non-porous configuration. It is evident that the incorporation of EGME into Pebax has resulted in a final membrane that is more brittle and textured. This change may be due to the formation of hydrogen bonds between the Pebax chains and the functional groups of EGME. In essence, as EGME molecules interpose between the polymer chains and establishing hydrogen bonds with various segments, the polymer matrix become brittle.

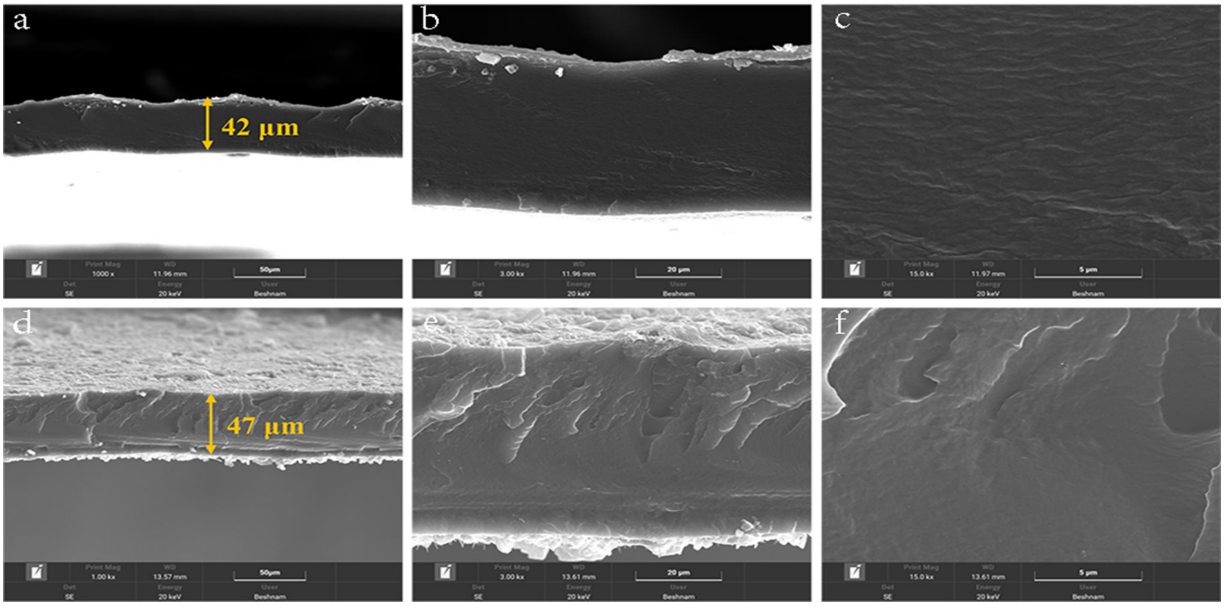

Figure 3. Cross-sectional FESEM Images of the Prepared Membranes with Two Different Magnifications: (a, b, and c) Pebax; (d, e, and f) Pebax/EGME

(Figure 4) and (Table 1) present the findings from the DSC analysis. The glass transition temperature (T_g) of the Pebax/EGME membrane is elevated compared to that of the Pebax membrane. This indicates that the Pebax/EGME mebrane become more glassy due to hydrogen bonds between EGME and polymer chins. The prepared membranes display two distinct melting points: one associated with the polyamide component ($T_{m,PA}$) and the other with the polyether component ($T_{m,PE}$) of the Pebax. A comparison of the melting point temperatures of Pebax/EGME, as opposed to the pure membrane, reveals that the addition of EGME has raised the $T_{m,PE}$ while lowering that of the $T_{m,PA}$. The presence of EGME molecules within the polymer chains facilitates the formation of hydrogen bonds with both the polyether and polyamide segments of the Pebax chain, leading to a partial loss of microphase separation between these two phases (Lotfi Mayan Sofla et al., 2019). This interaction results in the amide component melting at higher temperatures due to its integration within the polyether structure, while the polyether component freezes at lower temperatures as it is incorporated within the polyamide structure. As indicated in the table, the blending of the polyamide and polyether components, facilitated by EGME, has resulted in a reduction in the crystallinity of both components. The polyether segment of Pebax plays a crucial role in the transport of CO_2 molecules due to its inherent flexibility. Therefore, decreasing the crystallinity of polyether segment ($X_{c,PE}$) will enhance both its flexibility and CO_2 permeability. Furthermore, a reduction in the crystallinity of the polyamide segment ($X_{c,PA}$) may also create a synergistic effect, contributing to an increase in gas permeability.

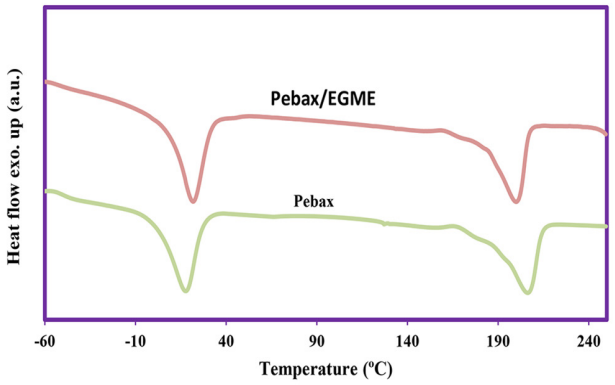

Figure 4. DSC Thermograms of the Prepared Membranes

Table 1. The Physical and Thermal Characteristics of the Prepared Membranes

Membranes	T_g (°C)	$T_{m,PE}$ (°C)	$T_{m,PA}$ (°C)	$\Delta H_{m,PE}$ (J/g)	$\Delta H_{m,PA}$ (J/g)	$X_{c,PE}$ (%)	$X_{c,PA}$ (%)
Pebax	-53.6	17.7	206.4	20.0	21.2	20.0	23.1
Pebax/EGME	-50.2	21.8	199.6	18.1	19.6	18.1	21.3

The mechanical characteristics of both Pebax and Pebax/EGME membranes were examined utilizing a tensile testing apparatus, with the findings presented in (Figure 5) and (Table 2). The results indicate that the Young's modulus of the membrane was enhanced twofold with the incorporation of EGME in comparison to the pure membrane. Furthermore, the tensile strength of the Pebax/EGME membrane exhibited a notable increase relative to that of the pure membrane. This substantial enhancement in tensile strength and Young's modulus attributed to the addition of EGME may be linked to the intercalation of its molecules within the Pebax chains, facilitating the creation of multiple hydrogen bonds. The molecules of EGME have contributed to the rigidity and strength of the membrane by creating hydrogen bonds with both the polyether and polyamide segments of Pebax. It is evident that the elongation at break of the Pebax/EGME has experienced a slight reduction compared to the pure membrane, likely due to the increased stiffness of the polymer matrix resulting from the aforementioned hydrogen bonding. This behavior suggests a trade-off between tensile strength and Young's modulus in relation to the elongation at break, which needs to be optimized based on the specific application. In membrane separation applications, a key characteristic of the membrane is its high mechanical strength and resistance to abrupt deformation. Therefore, both tensile strength and Young's modulus are critical; however, it is also essential for the membrane to possess sufficient elasticity to avoid brittleness.

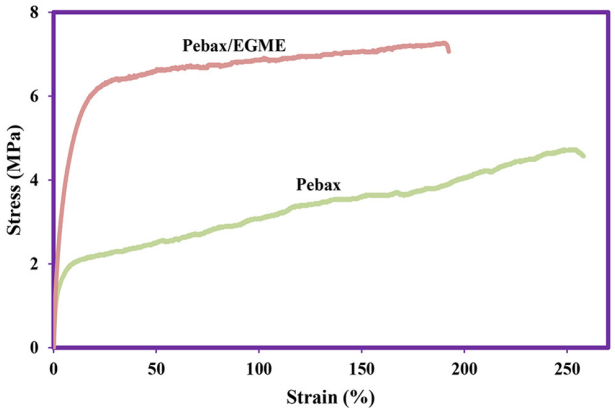

Figure 5. Stress-strain Curves of the Prepared Membranes

Table 2. Mechanical Properties of the Prepared Membranes

Membranes	Young's modulus (MPa)	Tensile strength (MPa)	Elongation at break (MPa)
Pebax	87.5	4.7	253.2
Pebax/EGME	174.6	7.2	191.2

3.2. Gas Permeation Properties

The CO_2 permeability of the Pebax and Pebax/EGME membranes is illustrated in (Figure 6). The results reveals a significant enhancement in CO_2 permeability by incorparation EGME to Pebax. Specifically, the incorporation of EGME to pebax matrix leads to increase in CO_2 permeability from 83 Barrer to 287 Barrer, representing an approximate increase of 3.5 times. (Figure 7) shows a schematic representation of the performance of

the Pebax incorporating EGME. In the pure Pebax membrane, a dipole-quadrupole interaction occurs between the CO_2 molecules and ether groups of the Pebax chain. EGME creates three distinct types of interactions, which significantly enhance CO_2 permeability. 1. A Lewis acid-base interaction between $CO_2$and the hydroxyl group of EGME; 2. A dipole-quadrupole interaction between the ether group in the structure of EGME and CO_2 molecules; 3. A π-quadrupole interaction involving the π electrons of the aromatic ring in EGME and CO_2 molecules (Meshkat et al., 2019; Sanaeepur et al., 2019). Due to the lower electronegativity of carbon atoms compared to oxygen, the CO_2 molecules exist as transient quadrupolar, allowing them to interact with dipolar ether groups. This transient quadrupole can also interact with the π bond present in the aromatic ring of EGME. Moreover, oxygen atoms of hydroxyl groups of EGME have negative charges, while the corresponding hydrogen atoms are positively charged and can act as acidic hydrogens. CO_2 has two couples of carbonyl groups with a positively charged center carbon that can be attracted by the electron withdrawing oxygen atoms of EGME. This Lewis acid-base interaction has the potential to help a better transport of CO_2 through the membranes. The addition of EGME into the polymer matrix leads to remarkable increase in CO_2 permeability by 247%, driven by the synergistic effects of these three interactions. As illustrated in (Figure 6), the permeability of N_2 exhibited a moderate increase with the incorporation of EGME. This enhancement in N_2 permeability can be attributed to the liquid state of EGME. Due to its liquid nature, this substance offers limited resistance to N_2 diffusion when situated between polymer chains, allowing N_2 gas to infiltrate the Pebax/EGME membrane more readily than in the pure membrane. Notably, the increase in CO_2 permeability was substantial in comparison to the reduction in N_2 permeability, resulting in an overall enhancement of CO_2/N_2 selectivity from 45.8 to 68.1 with the addition of EGME to the Pebax membrane, representing a 49% increase. (Figure 8) shows the long-term stability of Pebax/EGME separation performance. It is clear that the CO_2 permeability and CO_2/N_2 selectivity had a limited decline in the initial times, but subsequently had a relatively stable trend, which enhances the membrane's operability in industrial applications.

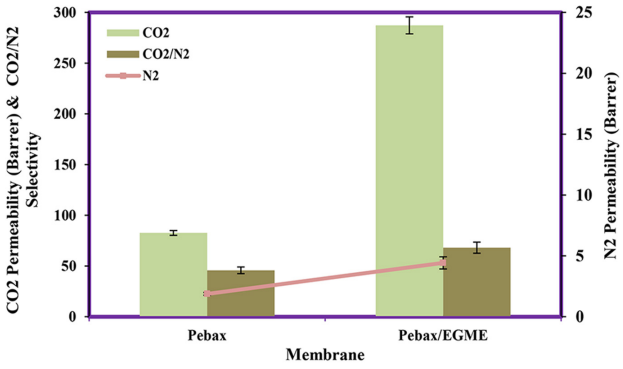

Figure 6. Effect of EGME on CO_2 Separation Properties

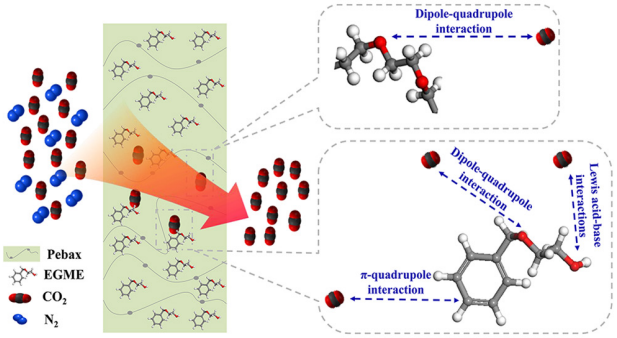

Figure 7. Schematic of CO_2 Separation Mechanism in Pebax/EGME Membrane

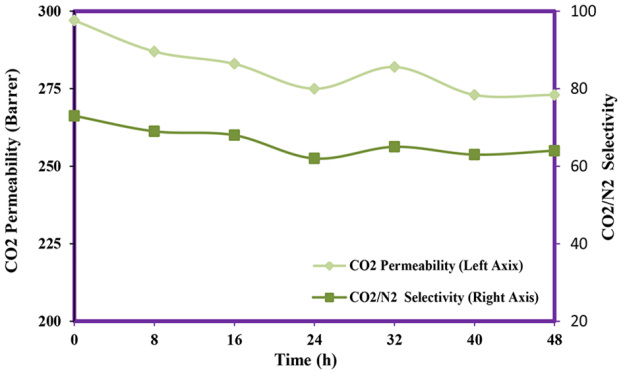

Figure 8. The Long-term Stability of Pebax/EGME Separation Performance

3.3. Comparison with other Works

(Figure 9) shows the positioning of the membrane developed in this study in comparison to the pure Pebax membrane, as well as several membranes created in recent years for CO_2 separation. The figure indicates that the separation performance of the pure membrane falls short of the Robeson upper bound line. However, the incorporation of EGME enhances the separation performance of the membranes, placing them above the Robeson upper bound line. This indicates that simultaneous increase in both CO_2/N_2 selectivity and CO_2 permeability created by addition of EGME, effectively surpassing the Trade-off limitation. Furthermore, when evaluating the performance of the membrane developed in this study against that of other membranes prepared in recent years, it can be concluded that the performance of the membranes produced here is comparable to that of the majority of membranes created by researchers. This suggests that EGME, as an easily obtainable compound, has significantly enhanced the separation efficiency of the Pebax polymer membrane.

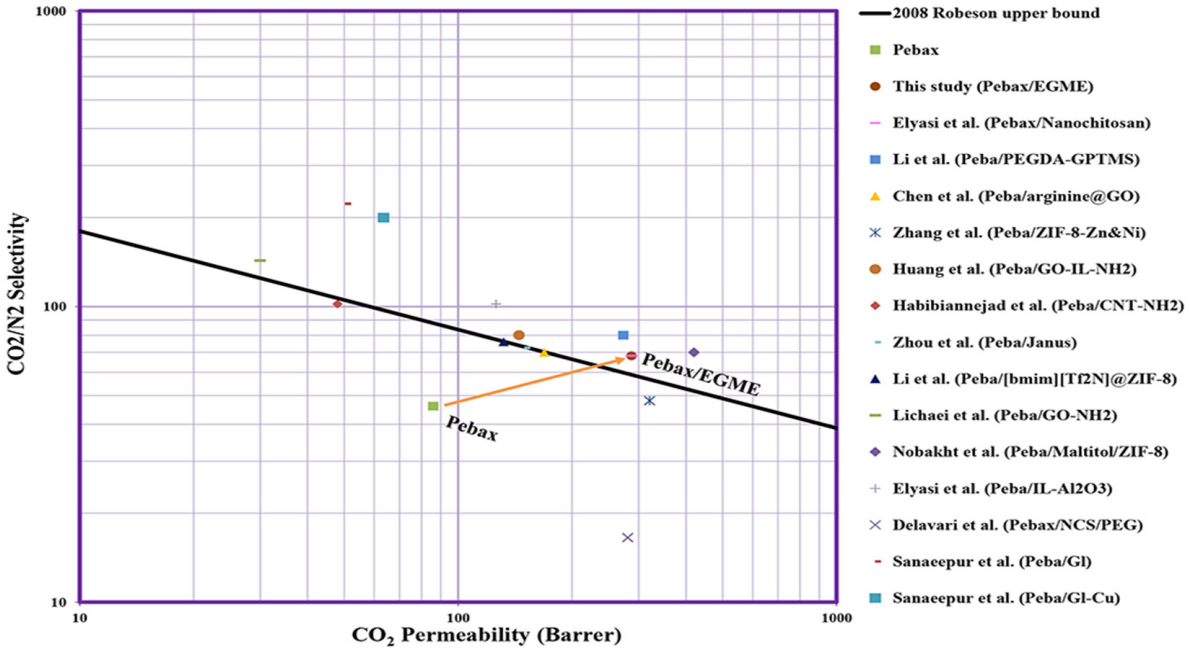

Figure 9. Separation Performance of Prepared Membranes Compared to Some Recent Studies (Chen et al., 2022; Delavari et al., 2024; Elyasi and Norouzi, 2025; Habibiannejad et al., 2016; Huang et al., 2018; Kojabad et al., 2021c; Li et al., 2016; Li et al., 2023; Lichaei et al., 2022; Nobakht and Abedini, 2023; Sanaeepur et al., 2019; Zhang et al., 2018; Zhou et al., 2015)

4. Conclusions

In this study, Pebax/EGME polymer membranes were prepared for CO_2/N_2 separation by incorporating EGME into the Pebax matrix. Following this, an examination of the chemical structure, morphology, physical and thermal properties, tensile strength, and separation performance of the resulting membrane was conducted, with the findings being thoroughly analyzed. The FTIR analysis revealed that the interactions between the Pebax and EGME polymer chains were predominantly of a physical type. The FESEM images of the membranes illustrated that the addition of EGME resulted in a rougher and more brittle membrane texture. The results of the DSC analysis showed that the crystallinity of the polyamide and polyether

components of Pebax was diminished due to the incorporation of EGME between the polymer chains, which facilitated the formation of multiple hydrogen bonds between these components. Furthermore, the EGME-modified membrane exhibited significantly increased Young's modulus and tensile strength compared to the pure Pebax membrane. The gas separation performance assessment of the prepared membranes demonstrated that the inclusion of EGME in the Pebax matrix resulted in 247% increase in CO_2 permeability, driven by interactions such as dipole-quadrupole, Lewis acid-base, and π-quadrupole interactions. Moreover, the CO_2/N_2 selectivity of the Pebax/EGME membrane improved by 49% compared to that of the pure membrane. This enhanced performance allowed the Pebax/EGME membrane to surpass the Robeson upper bound, demonstrating the significant potential of EGME for improving Pebax-based CO_2 separation. The elevated CO_2 permeability of the membranes developed in this research diminishes the surface area necessary for application in the CO_2 separation application, thereby offering membrane systems that are optimally sized and reasonably priced.

References

Afshoun, H. R., Chenar, M.P., & Ismail, A. F. 2017. Effect of Coating Method and Feed Pressure and Temperature on CO_2/CH_4 Gas Separation Performance of Pebax/PES Composite Membranes. Journal of Gas Technology, 3(1), 48-65.

Amini, Z., & Asghari, M. 2018. Preparation and characterization of ultra-thin poly ether block amide/nanoclay nanocomposite membrane for gas separation. Applied Clay Science, 166, 230-241.

Chen, Z., Zhang, P., Wu, H., Sun, S., You, X., Yuan, B., Hou, J., Duan, C., & Jiang, Z. 2022. Incorporating amino acids functionalized graphene oxide nanosheets into Pebax membranes for CO_2 separation. Separation and Purification Technology, 288, 120682. https://doi.org/10.1016/J.SEPPUR.2022.120682.

Delavari, M., Beyranvand, F., Jahangiri, M., & Abdipour, H. 2024. Increasing the Permeability of Carbon Dioxide and Nitrogen Gases Through a Polymer Membrane Consisting of a Modified Polyether Block Amide and Experimental Design. Journal of Polymers and the Environment, 32(10), 4822-4841. https://doi.org/10.1007/s10924-024-03247-z.

Elyasi, M., & Norouzi, A. 2025. Pebax / NC-PCL membrane containing well-distributed PCL grafted biodegradable nano-chitosan particles for CO_2 separation. Colloids and Surfaces A: Physicochemical and Engineering Aspects, 705, 135576. https://doi.org/10.1016/j.colsurfa.2024.135576.

Habibiannejad, S. A., Aroujalian, A., & Raisi, A. 2016. Pebax-1657 mixed matrix membrane containing surface modified multi-walled carbon nanotubes for gas separation. RSC Advances, 6(83), 79563-79577. https://doi.org/10.1039/c6ra14141b.

Hassanzadeh, H., Abedini, R., & Ghorbani, M. 2022. CO_2 Separation over N2 and CH4 Light Gases in Sorbitol-Modified Poly (ether- block -amide) (Pebax 2533) Membrane. Industrial & Engineering Chemistry Research, 61(36), 13669-13682.

Hosseinkhani, A., Omidkhah, M., & Ebadi Amooghin, A. 2024. Fine-tuning CO_2 separation of mixed matrix membranes by constructing efficient transport pathways through the addition of hybrid porous 2D nanosheets. Chemical Engineering Journal Advances, 20, 100685. https://doi.org/10.1016/j.ceja.2024.100685.

Huang, G., Pournaghshband, A., Muchtar, A., &

Sakurai, K. 2018. Pebax/ionic liquid modi fi ed graphene oxide mixed matrix membranes for enhanced CO_2 capture. Journal of Membrane Science, 565, 370-379.

Khosravi, T. 2021. Optimizing CO_2/CH_4 Separation Performance of Modified Thin Film Composite Pebax MH 1657 Membrane Using a Statistical Experimental Design Technique. Journal of Gas Technology, 6(1), 43-50.

Kojabad, M. E., Amirabedi, P., & Dorfeshan, M. 2024. A Two-Way Facilitated Transport Membrane for CO_2 Separation with Synergy of Nucleophilic Addition and Π-Complexing Reactions: Molecular Simulation and Experimental Study. Iranian Journal of Polymer Science and Technology, 36(6), 647-660. https://doi.org/10.22063/JIPST.2024.3470.2258.

Kojabad, M. E., Babaluo, A. A., Tavakoli, A., & Kahnamouei, H. G. 2021. A novel high-performance facilitated transport membrane by simultaneously using semi-mobile and fixed carriers for CO_2/N_2 separation. Process Safety and Environmental Protection, 156, 304-314. https://doi.org/10.1016/J.PSEP.2021.10.017.

Kojabad, M. E., Babaluo, A., & Tavakoli, A. 2021. A novel semi-mobile carrier facilitated transport membrane containing aniline/poly (ether-block-amide) for CO_2/N_2 separation: Molecular simulation and experimental study. Separation and Purification Technology, 118494. https://doi.org/10.1016/j.seppur.2021.118494.

Kojabad, M. E., Babaluo, A. A., Tavakoli, A., Sofla, R. L. M., & Kahnamouei, H. G. 2021. Comparison of acidic and basic ionic liquids effects on dispersion of alumina particles in Pebax composite membranes for CO_2/N_2 separation: Experimental study and molecular simulation. Journal of Environmental Chemical Engineering, 9(5), 106116. https://doi.org/10.1016/J.JECE.2021.106116.

Kojabad, M. E., Bekhradinassab, E., & Kahnamouei, H. G. 2024. Journal of Environmental Chemical Engineering Reinforced facilitated transport PEBA membrane by 2D Fe-doped TiO2 macroporous nanosheets for CO_2 separation : Utilizing cationic and non-ionic surfactants Ti Precursor Hydrolyzing agents Ethanol Mixing to f. Journal of Environmental Chemical Engineering, 12(5), 113963. https://doi.org/10.1016/j.jece.2024.113963.

Li, H., Tuo, L., Yang, K., Jeong, H., Dai, Y., He, G., & Zhao, W. 2016. Simultaneous enhancement of mechanical properties and CO_2 selectivity of ZIF-8 mixed matrix membranes : Interfacial toughening effect of ionic liquid. Journal of Membrane Science, 511, 130-142.

Li, S., Zhang, K., Liu, C., Feng, X., Wang, P., & Wang, S. 2023. Nanohybrid Pebax/PEGDA-GPTMS membrane with semi-interpenetrating network structure for enhanced CO_2 separations. Journal of Membrane Science, 674, 121516. https://doi.org/10.1016/j.memsci.2023.121516.

Lichaei, M. M., Pazani, F., Aroujalian, A., & Rodrigue, D. 2022. Two-step surface functionalization/alignment strategy to improve CO_2/N_2 separation from mixed matrix membranes based on PEBAX and graphene oxide. Process Safety and Environmental Protection, 163, 36-47. https://doi.org/10.1016/j.psep.2022.05.024.

Lotfi Mayan Sofla, R., Rezaei, M., & Babaie, A. 2019. Investigation of the effect of graphene oxide functionalization on the physical, mechanical and shape memory properties of polyurethane/reduced graphene oxide nanocomposites. Diamond and Related Materials, 95, 195-205. https://doi.org/10.1016/j.diamond.2019.04.012.

Mahdavi, H. R., Azizi, N., & Mohammadi, T. 2017. Performance evaluation of a synthesized and characterized Pebax1657/PEG1000/γ-Al_2O_3 membrane for CO_2/CH_4 separation using response surface methodology. Journal

of Polymer Research, 24(5). https://doi.org/10.1007/s10965-017-1228-1.

Meshkat, S., Kaliaguine, S., & Rodrigue, D. 2019. Enhancing CO_2 separation performance of Pebax® MH-1657 with aromatic carboxylic acids. Separation and Purification Technology, 212, 901-912.

Momeni, M., Kojabad, M. E., Khanmohammadi, S., Farhadi, Z., Ghalandarzadeh, R., Babaluo, A. A., & Zare, M. 2019. Impact of support on the fabrication of poly (ether-b-amide) composite membrane and economic evaluation for natural gas sweetening. Journal of Natural Gas Science and Engineering, 62, 236-246. https://doi.org/10.1016/j.jngse.2018.12.014.

Narkkun, T., Kraithong, W., Ruangdit, S., Klaysom, C., Faungnawakij, K., & Itthibenchapong, V. 2023. Pebax/Modified Cellulose Nanofiber Composite Membranes for Highly Enhanced CO_2/CH_4 Separation. ACS Omega, 8(48), 45428-45437. https://doi.org/10.1021/acsomega.3c04800.

Nobakht, D., & Abedini, R. 2023. A new ternary Pebax®1657/maltitol/ ZIF-8 mixed matrix membrane for efficient CO_2 separation. Process Safety and Environmental Protection, 170, 709-719. https://doi.org/10.1016/j.psep.2022.12.058.

Sanaeepur, H., Ahmadi, R., Ebadi, A., & Ghanbari, D. 2019. A novel ternary mixed matrix membrane containing glycerol-modified poly (ether- block -amide) (Pebax 1657)/copper nanoparticles for CO_2 separation. Journal of Membrane Science, 573, 234-246.

Setiawan, W. K., & Chiang, K. 2023. Enhancement strategies of poly (ether-block-amide) copolymer membranes for CO_2 separation : A review Balance degree. Chemosphere, 338, 1-45.

Sun, Q. Q., Zhu, M. C., Zhu, P. fei, OuYang, Y. X., Lu, Y. Z., Li, N., & Chen, S. W. 2024. Enhancement of CO_2 separation efficiency in mixed matrix membranes through zinc ion modified g-C_3N_4 nanosheets. Journal of Applied Polymer Science, 141(36), 1-14. https://doi.org/10.1002/app.55906.

Zhang, S., Geng, X., Niu, C., Zhang, J., & Shan, M. 2025. Novel mixed matrix membranes containing calixarene for enhanced CO_2/N_2 separation. Separation and Purification Technology, 356, 129792. https://doi.org/10.1016/j.seppur.2024.129792.

Zhang, X., Zhang, T., Wang, Y., Li, J., Liu, C., Li, N., & Liao, J. 2018. Mixed-matrix membranes based on Zn/Ni-ZIF-8-PEBA for high performance CO_2 separation. Journal of Membrane Science, 560, 38-46. https://doi.org/10.1016/j.memsci.2018.05.004.

Zhou, T., Luo, L., Hu, S., Wang, S., Zhang, R., & Wu, H. 2015. Janus composite nanoparticle-incorporated mixed matrix membranes for CO_2 separation. Journal of Membrane Science, 489, 1-10. https://doi.org/10.1016/j.memsci.2015.03.070..

JOURNAL OF GAS TECHNOLOGY

Volume 9 / Issue 2 / Winter 2024 / Pages 39-53

Journal Home page: http://jgt.irangi.org

Application of Ultrasonic Waves on the Demulsification (Dehydration) of Crude Oil

Asieh Hafezi[1], Amir Hossein Saeedi Dehaghani[2], Serveh Abdollahi[3], Mehdi Razavifar[4*]

1. Ph.D. student, Department of Chemistry and Chemical Engineering, Rasht Branch, Islamic Azad University, Rasht, Iran
2. Associate professor, Department of Petroleum Engineering, Faculty of Chemical Engineering, Tarbiat Modares University, Tehran, Iran
3. Assistant professor, Department of Chemistry and Chemical Engineering, Rasht Branch, Islamic Azad University, Rasht, Iran
4. Assistant professor, Faculty of Chemical and Petroleum Engineering, University of Tabriz, Tabriz, 5166616471, Iran

ARTICLE INFO

REVIEW ARTICLE

Article History:
Received: 09 November 2024
Revised: 12 December 2024
Accepted: 26 December 2024

Keywords:
Ultrasonic wave
Crude oil
Emulsion
Demulsification
Dehydration

ABSTRACT

Demulsification (dehydration) of crude oil plays a crucial role in reducing oil contamination within the porous media of soil and rock structures and preventing corrosion of pipelines and surface facilities. Over the past two decades, the application of ultrasonic wave irradiation for demulsification and desalting of crude oil has gained increasing attention due to its significant environmental and economic advantages. However, a research gap exists regarding the comparison of conventional demulsification methods with ultrasonic treatment (UST). In this study, a comprehensive review was conducted to evaluate the effects of UST on crude oil demulsification. UST decreases the stability of water-in-oil emulsions, particularly when low-frequency waves are applied. Based on the findings, UST emerges as a promising method for both demulsification and desalting of crude oil. Based on the results, UST causes salt removal rates surpassing 90% and residual water content consistently under 0.3% vol., even for high-viscosity heavy crude feedstocks. When deployed in refinery pre-treatment systems, this technology enhances desalter efficacy while slashing chemical demulsifier consumption by 40-60%. The results highlight a dual benefit: robust operational performance under extreme conditions and a significant reduction in chemical dependency. The primary mechanisms of UST-driven demulsification are cavitation and wave-induced vibrations. These mechanisms alter the interfacial tension (IFT) between crude oil and water, reduce oil viscosity, increase pressure and temperature, and crack heavy crude oil components, especially asphaltene clusters. Combining UST with conventional demulsification methods can enhance performance. For instance, the simultaneous application of UST and nanotechnology presents a practical approach for efficient demulsification. Additionally, the synergistic effects of UST and chemical additives should be comprehensively investigated to identify optimal operational conditions. The results of this research provide insights for the oil industry to improve demulsification efficiency and reduce environmental contamination associated with crude oil.

DOR: 20.1001.1/jgt.2025.2053635.1051

How to cite this article
A. Hafezi, A.H. Saeedi Dehaghani, S. Abdollahii, M. Razavifar, Application of Ultrasonic Waves on the Demulsification (Dehydration) of Crude Oil. Journal of Gas Technology. 2024; 9(2): 39-53. (https://www.jgt.irangi.org/article_723920.html)

* Corresponding author.
E-mail address: m.razavifar@tabrizu.ac.ir, (M. Razavifar).

Available online 30 December 2024

1. Introduction

UST has emerged as a groundbreaking technology revolutionizing multiple industries through its unique combination of operational efficiency and environmental benefits. In petroleum processing, UST significantly improves crude oil demulsification and desalting processes by generating controlled cavitation that effectively destabilizes water-oil emulsions [1], reduces IFT, and inhibits asphaltene aggregation in transportation pipelines [2]. The pharmaceutical and specialty chemical sectors utilize UST's precision energy delivery for critical applications, including nanomaterial dispersion, controlled drug crystallization, and clean extraction methodologies. The food industry has adopted ultrasonic technology for its ability to achieve microbial inactivation through non-thermal pasteurization [3] while simultaneously improving product homogeneity [4] and emulsion stability [5]. Environmental engineering applications demonstrate UST's versatility in advanced wastewater treatment systems, where it efficiently mineralizes organic contaminants and maintains membrane filtration efficiency, as well as in industrial precision cleaning operations for high-value components in aerospace and automotive manufacturing [6]. Perhaps most significantly, UST offers a sustainable alternative to conventional processes by dramatically reducing both energy consumption (replacing thermal methods) and chemical dependency, while maintaining cost competitiveness across industrial scales.

The application of ultrasonic waves in the petroleum industry traces its origins to the mid-20th century, when researchers began exploring non-invasive methods to enhance oil recovery and improve process efficiency [7-8]. Early studies in the 1950s-70s focused on using low-frequency ultrasound for well stimulation and permeability enhancement, leveraging its mechanical vibrations to dislodge trapped hydrocarbons in reservoir rock [9-10]. By the 1980s, advancements in transducer design enabled higher-frequency systems, expanding applications to emulsion breaking, desalination, and contaminant removal. Notably, ultrasonic cavitation, the formation and collapse of micro-bubbles, emerged as a key mechanism for destabilizing water-oil emulsions, offering a chemical-free alternative to traditional demulsifiers [11-12].

Crude oil produced from reservoirs typically contains saltwater (brine). This water dissolves in the oil due to the drag forces of oil flow and a reduction in the IFT between oil and water. Lowering IFT plays a significant role in the formation of water-in-oil emulsions. As IFT decreases, more water emulsions form within the oil. In other words, reduced IFT enhances water's tendency to mix with the oil [13-14].

Chemical additives such as surfactants can further reduce the IFT between oil and water. Additionally, reservoir conditions including pressure and temperature along with water properties (salinity and pH) and crude oil characteristics (density, viscosity, and composition) influence the quantity and size of water emulsions in crude oil [15-16].

The presence of water-in-oil emulsions significantly affects crude oil quality. These emulsions pose challenges such as accelerated corrosion in pipelines and surface equipment within petrochemical and refinery plants. From an environmental perspective, emulsions are concerning because they can contaminate porous media in soil and rock structures. Moreover, such contamination may spread to surface water and aquifers [17-18].

Mineral deposition from high-salinity water can clog pore throats in soil and rock, leading to reduced permeability and restricted fluid flow at the pore scale. These deposits also narrow the effective diameter of pipes, altering

fluid pressure. Furthermore, mineral scaling can damage surface facilities and reduce their efficiency. This process also promotes corrosion in pipelines and equipment due to changes in the system's electrical charge [18-19]. (Figure 1) illustrates the key benefits of demulsification in the oil industry.

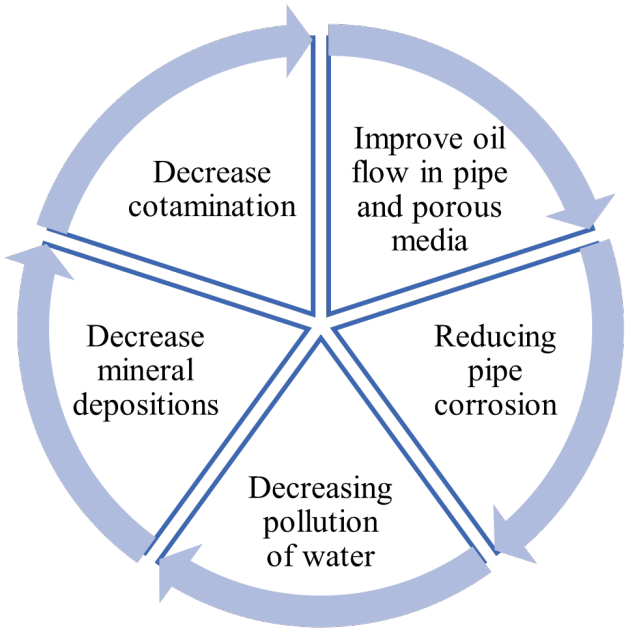

Figure 1. Advantage of Demulsification Operation in the Oil Industry

Various methods exist for demulsification and desalting of crude oil, including chemical and thermal approaches, but these conventional techniques have significant economic and environmental limitations. Recently, UST has attracted growing interest due to its lower operational costs and enhanced safety compared to traditional methods. However, a research gap remains regarding a systematic comparison between conventional demulsification methods and UST, as well as a detailed analysis of ultrasonic wave advantages.

In this study, we conducted a comprehensive review of UST's effects on crude oil demulsification. The findings of this research can be applied in the oil industry to optimize demulsification efficiency and minimize oil-related contamination.

2. Demulsification Methods

Demulsification refers to the process of separating a crude oil emulsion into distinct oil and water phases. This phase separation is crucial in petroleum processing. Three primary demulsification methods exist: physical, chemical, and biological approaches, with effectiveness determined by their ability to destabilize emulsions until complete phase separation occurs.

Common demulsification (dehydration) techniques encompass several approaches, including electromagnetic or electrical heating, which applies energy to separate emulsions; hot fluid injection, where heated fluids are introduced to reduce viscosity; solvent injection, particularly using surfactants to alter IFT; and fluid pressure control, which manipulates system pressure to facilitate phase separation [20-21]. In dehydration processes, warm dry air is typically circulated over oil to extract moisture, with efficiency enhanced by oil thinning. For natural gas, dehydration involves removing water molecules through absorption or adsorption. Modern crude oil separation often employs hot furnace systems [21-22].

The demulsification process serves as a critical step in crude oil purification by effectively separating water from oil. Commonly employed demulsifiers include acid/base-catalyzed phenol-formaldehyde resins, polyamines and polyols, and specialized surfactants, each selected based on their specific interaction properties with oil-water emulsions. Chemical desalting, an essential complementary process, follows three key stages: first, introducing water and surfactant demulsifiers to the crude oil; second, heating the mixture to facilitate impurity dissolution; and finally, allowing sufficient settling time in separation tanks for complete phase separation. As the predominant industrial method, chemical demulsification effectively treats both water-in-oil and oil-in-water emulsions by accelerating

emulsion breakdown. However, formulating emulsion-specific demulsifiers remains technically challenging. For desalination, the most prevalent methods are reverse osmosis (membrane-based) and multistage flash distillation (thermal-based) [23-24].

Conventional demulsification methods present several notable limitations that hinder their effectiveness. Chemical methods are often hampered by three primary constraints: prohibitively high operational costs, significant risks of environmental contamination, and limited applicability in industrial-scale operations. Similarly, thermal methods face substantial challenges, particularly their heavy dependence on electrical energy and economic impracticality when implemented in large-scale projects [24-25]. In light of these limitations, UST has gained prominence in recent years as a viable and promising alternative for crude oil demulsification. As visually summarized in (Figure 2), UST stands among various available demulsification techniques, offering distinct advantages over these conventional approaches.

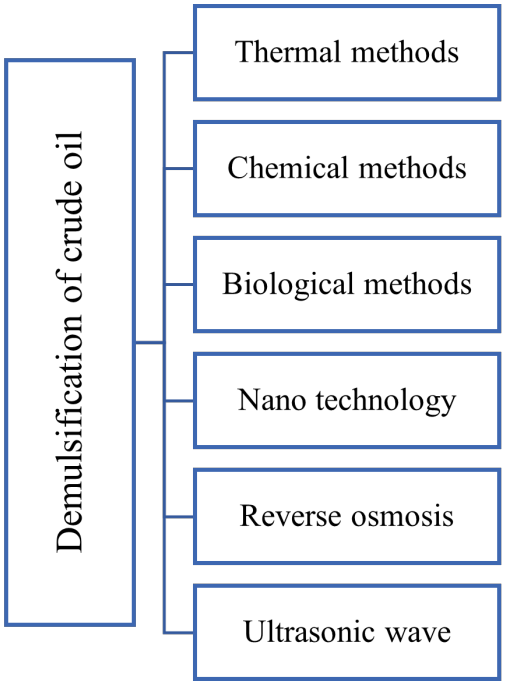

Figure 2. Various Methods for Demulsification of Crude Oil

3. Ultrasonic Treatment

Ultrasonic wave irradiation has emerged as an innovative and versatile technique for modifying key fluid properties in crude oil systems. This advanced approach effectively reduces IFT between oil and water phases, significantly decreases overall fluid viscosity, and facilitates the breakdown of heavy hydrocarbon components, particularly effective against stubborn asphaltene clusters. These simultaneous modifications work synergistically to enhance oil flow characteristics and improve separation efficiency, making UST a valuable tool for modern petroleum processing applications. Operating at frequencies above 20 kHz, ultrasonic wave power depends on the piezoelectric properties of the transducers employed [26-27]. When applied to crude oil, wave radiation generates internal bubbles due to pressure differentials. These bubbles collapse upon reaching critical size, triggering a sharp increase in oil temperature and pressure, a phenomenon known as cavitation.

Additionally, UST induces vibrational energy within the oil. Cavitation and vibration can alter the oil's molecular structure and composition. Specifically, UST breaks down heavy crude oil components through cavitation effects.

Research has identified the existence of an optimal UST condition characterized by minimized oil viscosity and significantly reduced asphaltene cluster formation [28-29], as visually demonstrated in (Figure 3), which illustrates the mechanistic impact of ultrasonic waves on asphaltene clusters within crude oil systems.

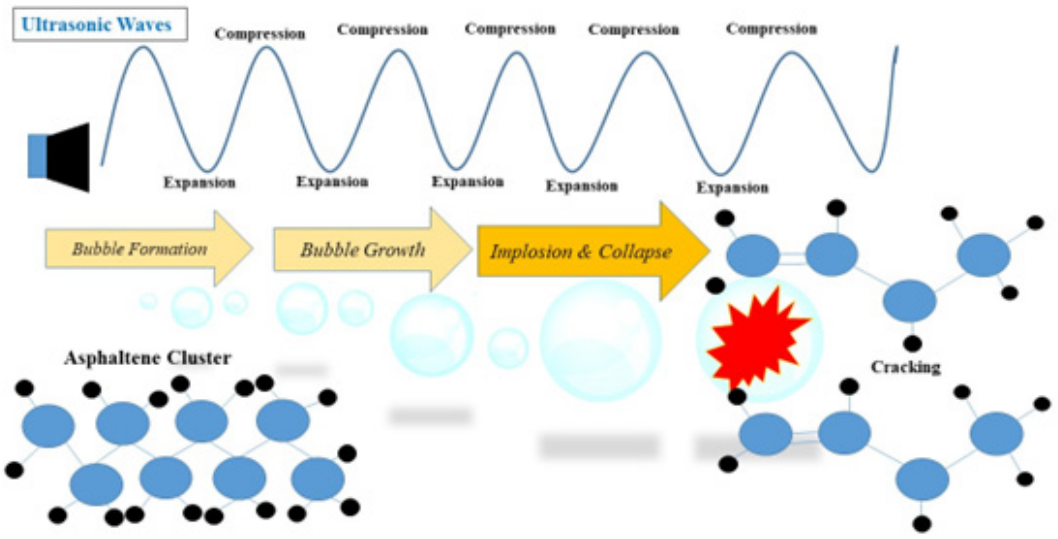

Figure 3. Schematic Image of the Ultrasonic Wave Effect on the Asphaltene Clusters in the Crude Oil

Recently, UST has been utilized for the demulsification and desalting of crude oil. During this process, cavitation and wave vibrations decrease the stability of water-in-oil emulsions and promote the aggregation of water droplets [29-30]. The primary mechanisms driving demulsification include: 1) A rise in fluid temperature resulting from cavitation, and 2) Energy distribution within the oil caused by wave vibrations. Additionally, increased oil temperature reduces IFT between oil and water and alters their interactions [31-32].

Experimental results demonstrate that UST significantly reduces both the quantity and size of water emulsions in crude oil. Furthermore, an optimal irradiation time exists, which depends on the properties of crude oil, reservoir rock, and irradiated wave parameters. Thus, identifying optimal ultrasonication conditions is critical for large-scale projects to enhance oil flow efficiency.

For surface facilities and transport pipelines facing challenges such as inorganic (mineral) deposition, these optimal UST conditions must be thoroughly investigated and precisely determined to ensure operational efficacy [33-35].

4. Advantages of UST

Compared to conventional methods such as chemical, mechanical, or biological approaches, UST offers significant economic and environmental advantages. Unlike these methods, UST avoids damage and pollution in pipelines, equipment, and porous rock media while eliminating the need to inject chemical additives (e.g., solvents or demulsifiers) into the system. Moreover, UST is inherently safer, posing no health hazards to personnel during operations [36-39].

Economically, UST requires no costly pumping systems, specialized materials, or advanced equipment. Instead, only a transducer powered by electricity is needed. Additionally, UST can target specific sections of pipelines or porous media (rock/soil) to mitigate damage and prevent organic/inorganic deposition. Critically, UST operates continuously during oil production, avoiding economic losses associated with shutdowns [40-42].

Mechanistically, UST reduces oil viscosity through cavitation phenomena, significantly improving oil flow rates post-treatment. Alterations in pressure and temperature during

UST modify fluid properties, including IFT and wettability. Experimental evidence confirms UST's efficacy in both demulsification and desalting of crude oil [43-45].

Synergistic integration of UST with conventional methods such as chemical solvent injection, thermal treatments, nanotechnology, or gas injection enhances outcomes while minimizing system damage. In summary, combining UST with other techniques optimizes demulsification efficiency [46-49]. (Figure 4) highlights the key benefits of UST.

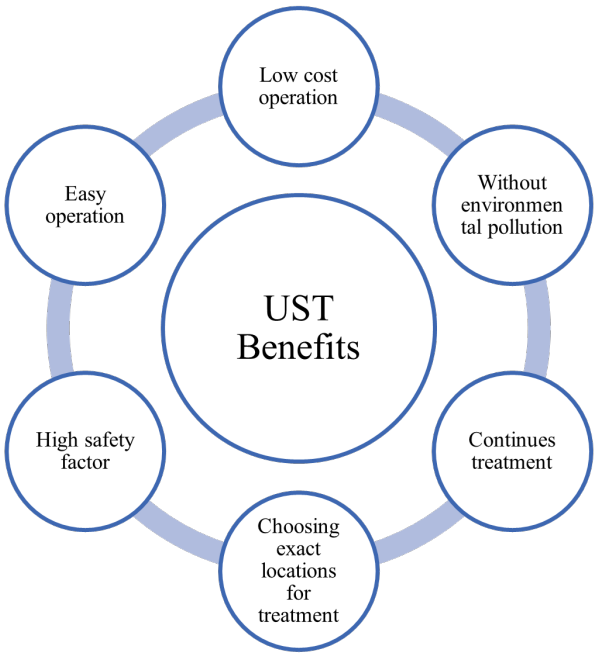

Figure 4. Benefits of Ultrasonic Technology as a Well-Stimulation Method

5. Challenges of UST

The primary limitation of UST is its limited penetration depth. Ultrasonic waves can only affect a small portion of a rock or pipe and cannot treat large-scale systems. Consequently, UST is unsuitable for addressing large-scale issues such as pipeline blockages. For high-production-rate crude oil demulsification, UST faces significant limitations and must be integrated with conventional methods like thermal or chemical treatments. Another key challenge involves identifying optimal operating conditions [50-53].

As noted earlier, determining the optimal irradiation duration is crucial and must be tailored to each crude oil's specific properties. This process requires extensive experimental analysis of the crude oil's physical and rheological characteristics. Such analyses can prolong operational timelines, posing practical constraints for industrial applications.

6. Summary of Experimental Results

Numerous studies have explored the demulsification and desalting of crude oil using UST. Researchers have demonstrated that ultrasound irradiation alters crude oil properties, reducing emulsion stability and promoting water droplet aggregation [54-56]. UST is an effective method for both desalting and demulsification, offering significant environmental benefits, such as minimizing oil pollution in soil porous media and preventing pipeline corrosion caused by brine. Economically, UST lowers costs associated with repairing or replacing surface and subsurface equipment through efficient demulsification. A summary of key studies on UST's impact on crude oil demulsification is provided in (Table 1).

Ultrasonic wave irradiation induces phase separation in water-oil emulsions by elevating fluid temperature and generating vibrational energy. This process relies on viscosity reduction in crude oil post-irradiation, enabling water droplets to coalesce and form distinct oil and water phases [42-45]. Low-frequency ultrasonic waves are highly effective for demulsification, whereas high frequencies prove ineffective due to induced emulsion instability [14-16].

Ultrasonic demulsification is critical in the oil industry as it rapidly separates water from crude oil without chemical additives and operates at relatively low temperatures. Furthermore, ultrasonic waves disrupt adhesion forces between particles by transferring energy, leading to their disintegration.

Table 1. A Summary of the Recent Studies on the Effect of Ultrasonic Waves on the Demulsification of Crude Oil

Authors/Year	Ultrasonic Waves Characteristics	Emulsion Blocking	Mixed Deposition
Yang et al (2009) [13]	20 kHz 100 W	Measure demulsifying velocity	• Result was a dehydrating ratio of 97.7% under the condition of 10 min of irradiating time, 50 mg/L of demulsifier, and 75℃ of water bath temperature..
Yi et al (2017) [14]	20-40 kHz 50-150 W	Microscopic imaging	• Combined method of UST and chemical demulsifier has the best demulsification effect, followed by chemical demulsifier. • UST without using a chemical demulsifier has the least demulsification effect. • Final demulsification rate increases with the increase of temperatures and wave power and almost does not change with the increase of wave irradiation time.
Pedrotti et al (2018) [15]	35 kHz 200 W	Particle size analysis and Droplet size distribution (DSD) analyzing	• Demulsification efficiency up to 93% was obtained with 15 min of UST (100% amplitude) using a few amounts of chemical demulsifier. • Reactors positioned in the most intense acoustic regions provided a much higher efficiency of demulsification in comparison with the ones positioned in the less intense acoustic field region.
Xu et al (2019) [16]	10 kHz, 15 kHz, 20 kHz, 25 kHz, 30 kHz 200 W	Imaging and record the total volumes of the dehydrated water and the whole mixed sample	• Demulsification rate increases with the increase of sound intensity, but the demulsification rate will decrease when wave intensity reaches a certain level; the demulsification rate decreases with the increase of wave frequency. • The demulsification rate increases with the increase of sedimentation time, but the increasing extent of the dehydration rate tends to be reduced with the increase of sedimentation time. • With the increase in temperature, the effect of UST on the demulsification of crude oil is decreased, or the advantages of UST can be fully displayed only at low temperatures.
Romanova et al (2022) [17]	40 kHz 1000 W	Microscopic imaging	• Destruction above 99% of all the studied emulsions is achieved by UST with 1.0 kW power together with the addition of nanopowder AlN suspension in acetone. • Application of this approach leads to a significant decrease in oily waste formation. • The exposure time was 0.5-3 min, and the additive amount was 4-8 %vol. • The proposed method applies to destroying regular and gel-containing emulsions.
Song et al (2024) [18]	40 kHz	Measuring the volume of separated oil and water	• The combined UST and pyrolysis of the crude oil shows a dehydration rate of 61 %, beneficial for the green transformation and utilization of subsequent demulsification products.
Gao et al (2024) [19]	20 kHz 650 W	Microscopic and particle size analyses	• Oil samples achieve demulsification and dehydration under UST, with a maximum dehydration rate of 98 %. • UST destabilizes the oil-water interfacial membrane and causes droplets of different sizes to collide, agglomerate, and settle.

To refine and desalt crude oil, salt removal is essential. A common desalting method involves electrical processes; however, research indicates that combining UST with electrical methods significantly enhances desalting and dewatering efficiency. For example, crude oil with high initial salt concentrations retained elevated salinity after two-stage electrical refining, but applying UST-electrical hybrid technology under optimal conditions reduced salt content from 68 mg/L to 4 mg/L in a single stage, with water content dropping below 0.3% by volume [54].

These results demonstrate that UST outperforms standalone electrical methods for desalting high-salinity crude oil. In a 2013 experimental study, UST achieved an 80% desalting rate under optimal parameters (10kHz frequency, 5-minute irradiation time) [55]. A summary of key studies on UST's desalting efficacy is provided in (Table 2).

Table 2. A Summary of the Recent Studies on the Effect of Ultrasonic Waves on the Desalting of Crude Oil

Authors/Year	Ultrasonic Waves Characteristics	Type of Experiments	Main Findings
Guoxiang et al (2008) [56]	20 kHz 100 W	Measuring TDS	• The salt content of crude oil can be reduced from 67.5 mg.L-1 to 3.97 mg.L-1 after UST and the water content falls below %0.3 (by volume). • Ultrasonic-electric united process is more effective than the electric process in high salt-contenting oil desalting. • This technology should be useful in the refinery process.
Ye et al (2010) [57]	10 kHz 0.38 W/cm	Measure of salt content	• The combined application of a standing wave field and demulsifier demonstrated superior performance compared to the use of demulsifier alone. Specifically, the desalting and dewatering rates were 11.5% and 4.3% higher, respectively, in the hybrid treatment.
Check et al (2014) [58]	30 kHz 75 and 50 W	Measure of salt content and depositions	• The dehydration rate was more than 95% and the final salt content was up to 2.5 PTB, which can meet the need for refineries. • This proposed technique managed to reduce the settling time to 5(×2) min after UST.
Hu et al (2014) [59]	75 W	Investigation of oil recovery and salt removal	• In general, ultrasonic irradiation could be an effective method in terms of oil recovery and salt removal from refinery oily sludge, but the separated wastewater still contains relatively high concentrations of PHCs and salt, which requires proper treatment.
Wang et al (2018) [60]	10 kHz, 15 kHz, 20 kHz, 25 kHz, 30 kHz	Sedimentation Analysis and Imaging	• Dehydration rate will decrease when sound intensity reaches a certain level. • Water ratio has a heavy and complex influence on ultrasonic dehydration rate. • The effect of ultrasonic dehydration becomes better with the increase of temperature.
Pedrotti et al (2018) [15]	35 kHz	Average droplet size distribution analysis	• Demulsification efficiency up to 93% was obtained with 15 min of sonication (100% amplitude) using few amount of chemical demulsifier.
Xu et al (2019) [16]	100 W and 250 mg/L	Comparison of demulsifying and dehydrating crude oil	• Sonochemical technique has the best effect for crude oil demulsification/dehydration. • The demulsification effect varies with the increase of ultrasonic radiation time. • Ultrasonic wave acts as demulsifying agents, and with the increase of power, the dehydration rate of the crude oil emulsion increases.
Sadatshojaie et al (2021) [61]	20 kHz 80 W to 1000 W	Microscopic imaging	• Water separation under UST was effective and occurred rapidly. • As the intensity of the ultrasonic waves increased, the amount of water segregated from crude oil also increased. • UST offers environmentally friendly alternatives to treatments using chemical demulsifiers as they reduce the desalination requirements of wastewater.
Ronchi et al (2021 [62]	35, 45, and 130 kHz	Imaging of water droplets	• Low-frequency UST is also a practical method for treating the produced water to remove oil. • Oil removal efficiency is about 77%.
Chen et al (2022) [63]	40 kHz 260 W	Imaging of water droplets	• The most effective operation parameters are temperature, followed by acoustic power intensity, ultrasonic irradiation time and demulsifier concentration. • Water droplets in heavy oil undergo less aggregation than those in light crude oil.
Bahmani et al (2024) [64]	40 kHz 100 W	Response surface methodology (RSM)	• Desalting of crude oil was achieved successfully in a remarkable number of experiments. • The maximum desalting of 80% was obtained when the flow rate and water content were 18 ml/s and 20%, respectively.

UST has emerged as an innovative and efficient technology for crude oil desalting and dehydration, leveraging unique physico-chemical mechanisms to overcome limitations of conventional methods. The technology operates through three synergistic effects: (1) intense cavitation generates localized microjets and shockwaves that rupture stabilizing films at oil-water interfaces, (2) high-frequency vibrations promote droplet coalescence through enhanced collision frequency, and (3) controlled thermal effects reduce viscosity while preserving heat-sensitive components. This multi-modal action achieves remarkable processing efficiencies, with field demonstrations showing salt reduction exceeding 90% and residual water content below 0.3% vol., even for challenging heavy crude applications. Modern implementations combine UST with electrostatic separation in refinery pre-treatment systems, where it significantly enhances desalter performance while reducing chemical demulsifier requirements by 40-60%. The technology's compact footprint and rapid processing (typically 5-15 minutes versus hours for conventional systems) make it particularly valuable for offshore platforms and pipeline terminals. Current research focuses on intelligent process optimization through machine learning algorithms that dynamically adjust ultrasonic parameters based on real-time crude quality monitoring, while nanotechnology integration shows promise for further efficiency gains. Despite its demonstrated advantages in energy efficiency (30-50% reduction versus thermal methods) and environmental benefits, scale-up challenges persist, particularly in maintaining uniform acoustic fields in large-volume processing vessels, an area where phased-array transducer configurations are showing potential solutions. These ongoing advancements position UST as a transformative technology in the petroleum industry's transition toward more sustainable and cost-effective processing solutions.

7. Future Direction and Suggestions

Based on the findings, we recommend integrating UST with conventional demulsification methods to enhance efficiency. For instance, combining UST with nanotechnology offers a practical approach. Specifically, Fe_2O_3 NPs or CDs exhibit enhanced demulsification efficiency in crude oil. Future studies should explore magnetic NPs, as a research gap exists regarding their synergy with UST.

Another viable strategy is coupling UST with chemical demulsification. Combining solvent injection (e.g., toluene) with chemical demulsifiers can alter IFT between oil and water, thereby destabilizing water-in-oil emulsions. We propose investigating the synergistic effects of UST and surfactants to identify optimal conditions for maximum demulsification efficiency.

Additionally, integrating UST with thermal methods (e.g., hot fluid injection) could improve water separation and desalting. Notable research gaps remain in exploring UST's synergies with chemical and thermal methods, urging researchers to rigorously evaluate these combinations for novel solutions. (Figure 5) summarizes proposed future research directions for UST hybrid methodologies.

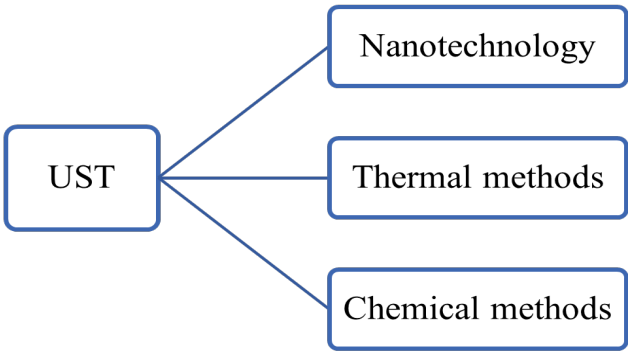

Figure 5. Combination of Ultrasonic Treatment with other Methods

8. Discussion

UST revolutionizes crude oil demulsification and desalting through three core mechanisms: cavitation, vibration, and thermal effects. Cavitation generates microbubbles that collapse violently, disrupting interfacial films between oil and water, while vibrational shear forces accelerate droplet coalescence. Simultaneously, localized heating reduces oil viscosity and fractures heavy components like asphaltene clusters, enhancing phase separation. These mechanisms collectively reduce IFT and improve salt dissociation, achieving >90% desalting efficiency and <0.5% residual water content in optimized systems. The technology's benefits include rapid processing (minutes vs. hours), reduced chemical dependency, and lower energy consumption compared to thermal methods, making it particularly effective for viscous or heavy crude oils. However, limitations persist: UST's limited penetration depth restricts scalability in large tanks, and optimal parameters (e.g., frequency, irradiation time) require crude-specific calibration. Additionally, high-frequency waves may destabilize emulsions unpredictably. Despite these challenges, UST's environmental and economic advantages drive its adoption in refineries and offshore platforms. Future advancements in hybrid systems (e.g., UST + nanotechnology) and AI-driven process optimization promise to overcome current constraints, positioning UST as a cornerstone of sustainable petroleum processing.

9. Conclusion

In this study, the impact of UST on crude oil demulsification and desalting was comprehensively investigated. Key findings from this review include:

1. UST offers significant advantages over conventional demulsification methods (e.g., thermal or chemical approaches). It is an environmentally friendly, high-safety, and cost-effective solution for dehydration projects.
2. UST destabilizes water-in-oil emulsions, particularly under low-frequency wave conditions. Experimental evidence confirms its efficacy for both demulsification and desalting of crude oil.
3. The primary mechanisms driving UST demulsification are cavitation and wave-induced vibrations. These physical phenomena modify the IFT between crude oil and water, while simultaneously reducing oil viscosity, elevating system pressure and temperature, and breaking down heavy hydrocarbon components - particularly asphaltene clusters.
4. One significant limitation of UST is its limited penetration depth, which restricts its effectiveness for crude oil demulsification. Furthermore, UST achieves optimal efficiency only under specific conditions that must be individually determined for each crude oil type. These ideal operating parameters are directly influenced by multiple factors, including ultrasonic wave power, the crude oil's density and viscosity, and the system's pressure and temperature.
5. The integration of UST with conventional demulsification methods can significantly enhance overall performance. Specifically, combining UST with nanotechnology represents a particularly promising approach for efficient demulsification. Moreover, a thorough investigation of the synergistic effects between UST and various chemical additives could help establish optimal operational parameters for maximum effectiveness.

Nomenclature

Abbreviation	Full Term
AI	Artificial Intelligence
CDs	Carbon dots
IFT	Interfacial Tension
kHz	kilohertz
NPs	Nanoparticles
UST	Ultrasonic wave treatment
W	Watt

References

1- Romanova, Y. N., Koroleva, M. Y., Musina, N. S., & Maryutina, T. A. (2025). Ultrasonic demulsification of water-in-crude oil emulsions: Influence of rheological properties. Chemical Engineering and Processing-Process Intensification, 211, 110242.

2- Razavifar, M., Yunusov, T., Mukhametdinova, A., Bakulin, D., Qajar, J., Cheremisin, A., & Riazi, M. (2025). Improving oil recovery with ultrasound: mitigating asphaltene-induced formation damage. Journal of Petroleum Exploration and Production Technology, 15(4), 78.

3-Wen, H., Cheng, D., Chen, Y., Yue, W., & Zhang, Z. (2024). Review on ultrasonic technology enhanced biological treatment of wastewater. Science of The Total Environment, 925, 171260.

4- Singla, M., & Sit, N. (2021). Application of ultrasound in combination with other technologies in food processing: A review. Ultrasonics Sonochemistry, 73, 105506.

5- Lü, Y., Zhu, S., Lin, G., Wang, M., & Wang, C. (2025). Research on Ultrasonic Demulsification Characteristics and Parameter Optimization of Condensate Oil Emulsion. Chemical Engineering and Processing-Process Intensification, 110185.

6- Lyu, F., Zhou, X., Ding, Z., Qiao, X., & Song, D. (2024). Application research of ultrasonic-guided wave technology in pipeline corrosion defect detection: A review. Coatings, 14(3), 358.

7- Nikolaevskii, V. N. (1992). Rock vibration and finite oil recovery. Fluid dynamics, 27(5), 689-696.

8- Huh, C. (2006, August). Improved oil recovery by seismic vibration: a preliminary assessment of possible mechanisms. In SPE International Oil Conference and Exhibition in Mexico (pp. SPE-103870). SPE.

9- Naderi, K., & Babadagli, T. (2008, October). Effect of ultrasonic intensity and frequency on oil/heavy-oil recovery from different wettability rocks. In SPE International Thermal Operations and Heavy Oil Symposium (pp. SPE-117324). SPE.

10- Westermark, R. V., Brett, J. F., & Maloney, D. R. (2001, March). Enhanced oil recovery with downhole vibration stimulation. In SPE Oklahoma City Oil and Gas Symposium/ Production and Operations Symposium (pp. SPE-67303). SPE.

11- Gunal, O. G., & Islam, M. R. (2000). Alteration of asphaltic crude rheology with electromagnetic and ultrasonic irradiation. Journal of Petroleum Science and Engineering, 26(1-4), 263-272.

12- Beresnev, I. A. (1993, June). Review of using acoustic and seismic waves for stimulation of oil reservoirs-Methods and results. In 55th EAEG Meeting (pp. cp-46). European Association of Geoscientists & Engineers.

13- Yang, X. G., Tan, W., & Tan, X. F. (2009). Demulsification of crude oil emulsion via ultrasonic chemical method. Petroleum Science and Technology, 27(17), 2010-2020.

14- Yi, M., Huang, J., & Wang, L. (2017). Research

on crude oil demulsification using the combined method of ultrasound and chemical demulsifier. Journal of Chemistry, 2017(1), 9147926.

15- Pedrotti, M. F., Enders, M. S., Pereira, L. S., Mesko, M. F., Flores, E. M., & Bizzi, C. A. (2018). Intensification of ultrasonic-assisted crude oil demulsification based on acoustic field distribution data. Ultrasonics sonochemistry, 40, 53-59.

16- Xu, X., Cao, D., Liu, J., Gao, J., & Wang, X. (2019). Research on ultrasound-assisted demulsification/dehydration for crude oil. Ultrasonics sonochemistry, 57, 185-192.

17- Romanova, Y. N., Maryutina, T. A., Musina, N. S., & Spivakov, B. Y. (2022). Application of ultrasonic treatment for demulsification of stable water-in-oil emulsions. Journal of Petroleum Science and Engineering, 209, 109977.

18- Song, Z., Ren, F., Wang, S., Pang, Y., Zhao, X., Sun, J., ... & Su, Y. (2024). Factors influencing demulsification of refinery oily sludge via ultrasonic treatment. Chemical Engineering and Processing-Process Intensification, 204, 109936.

19- Gao, J., Zhu, J., Gao, Q., Zhao, X., Yu, L., Zhao, J., ... & Guo, J. (2024). Mechanism study of aging oil demulsification and dehydration under ultrasonic irradiation. Ultrasonics Sonochemistry, 105, 106859.

20- Faizullayev, Saidulla, et al. "Recent demulsification methods of crude oil emulsions–Brief review." Journal of Petroleum Science and Engineering 215 (2022): 110643.

21- Shah Buddin, Meor Muhammad Hafiz, et al. "A review of demulsification technique and mechanism for emulsion liquid membrane applications." Journal of Dispersion Science and Technology 43.6 (2022): 910-927.

22- Saad, M. A., et al. "An overview of recent advances in state-of-the-art techniques in the demulsification of crude oil emulsions." Processes 7.7 (2019): 470.

23- Hadi, Ahmed Abdulrazzaq, and Ali Abdulkhabeer Ali. "A review of petroleum emulsification types, formation factors, and demulsification methods." Materials Today: Proceedings 53 (2022): 273-279.

24- Issaka, Souleyman A., Abdurahman H. Nour, and Rosli Mohd Yunus. "Review on the fundamental aspects of petroleum oil emulsions and techniques of demulsification." Journal of Petroleum & Environmental Biotechnology 6.2 (2015): 1.

25- Abdulredha, Murtada Mohammed, Hussain Siti Aslina, and Chuah Abdullah Luqman. "Overview on petroleum emulsions, formation, influence and demulsification treatment techniques." Arabian Journal of Chemistry 13.1 (2020): 3403-3428.

26- Hamidi, Hossein, et al. "Recent applications of ultrasonic waves in improved oil recovery: A review of techniques and results." Ultrasonics 110 (2021): 106288.

27- Ehsani, MohammadAmin, Mohammadreza Akbari, and Yasin Khalili. "A Comprehensive Review of Ultrasonic-Assisted Oil Recovery: Principles, Applications, and Future Prospects." Journal of Chemical and Petroleum Engineering (2025).

28- Zhang, Huan, et al. "Revisiting the Application of Ultrasonic Technology for Enhanced Oil Recovery: Mechanisms and Recent Advancements." Energies 17.14 (2024): 3517.

29- Wang, Zhenjun, and Yuanming Xu. "Review on application of the recent new high-power ultrasonic transducers in enhanced oil recovery field in China." Energy 89 (2015): 259-267.

30- Adeyemi, Idowu, Mahmoud Meribout, and Lyes Khezzar. "Recent developments, challenges, and prospects of ultrasound-assisted oil technologies." Ultrasonics Sonochemistry 82 (2022): 105902.

31- Shafiai, Siti Habibah, and Adel Gohari. "Conventional and electrical EOR review: the development trend of ultrasonic application in EOR." Journal of Petroleum Exploration and Production Technology 10.7 (2020): 2923-2945.

32- Luo, Xiaoming, et al. "Research on mechanism and characteristics of oil recovery from oily sludge in ultrasonic fields." Journal of Hazardous Materials 399 (2020): 123137.

33- Hafezi, Asieh, et al. "Experimental investigation on the synergetic effect of low salinity water and ultrasonic wave on crude oil flow in porous media." Petroleum Science and Technology (2024): 1-20.

34- Thilakarathna, R. C. N., et al. "A review on application of ultrasound and ultrasound assisted technology for seed oil extraction." Journal of Food Science and Technology 60.4 (2023): 1222-1236.

35- Taheri-Shakib J, H Naderi, Y Salimidelshad, A Teymouri, A Shekarifard. Using ultrasonic as a new approach for elimination of inorganic scales (NaCl): an experimental study. Journal of Petroleum Exploration and Production Technology. 8 (2018) 553-64.

36- Chunsheng P, S Daohan, Z Shushan, X Hongxing. Technology of removing near wellbore inorganic scale damage by high power ultrasonic treatment. Petroleum Exploration and Development. 38 (2011) 243-8.

37- Mousavi SM, A Ramazani, I Najafi, SM Davachi. Effect of ultrasonic irradiation on rheological properties of asphaltenic crude oils. Petroleum science. 9 (2012) 82-8.

38- Hamidi H, E Mohammadian, R Junin, R Rafati, M Manan, A Azdarpour, M Junid. A technique for evaluating the oil/heavy-oil viscosity changes under ultrasound in a simulated porous medium. Ultrasonics. 54 (2014) 655-62.

39- Hamidi H, E Mohammadian, M Asadullah, A Azdarpour, R Rafati. Effect of ultrasound radiation duration on emulsification and demulsification of paraffin oil and surfactant solution/brine using Hele-shaw models. Ultrasonics sonochemistry. 26 (2015) 428-36.

40- Mullakaev M, G Volkova, O Gradov. Effect of ultrasound on the viscosity-temperature properties of crude oils of various compositions. Theoretical Foundations of Chemical Engineering. 49 (2015) 287-96.

41- Wang Z, Y Xu, Y Gu. Lithium niobate ultrasonic transducer design for enhanced oil recovery. Ultrasonics Sonochemistry. 27 (2015) 171-7.

42- Aliev F, I Mukhamatdinov, A Kemalov. The influences of ultrasound waves on rheological and physico-chemical properties of extra heavy oil from Ashalcha field. International Multidisciplinary Scientific GeoConference Surveying Geology and Mining Ecology Management, SGEM. (2017) 941-8.

43- Dehshibi RR, A Mohebbi, M Riazi, F Danafar. Visualization study of the effects of oil type and model geometry on oil recovery under ultrasonic irradiation in a glass micro-model. Fuel. 239 (2019) 709-16.

44- He S, X Tan, X Hu, Y Gao. Effect of ultrasound on oil recovery from crude oil containing sludge. Environmental technology. 40 (2019) 1401-7.

45- Karami S, AHS Dehaghani, SAHS Mousavi. Condensate blockage removal using microwave and ultrasonic waves: Discussion on rock mechanical and electrical properties. Journal of Petroleum Science and Engineering. 193 (2020) 107309.

46- Razavifar, Mehdi, and Jafar Qajar. "Synergistic effects of ultrasonic irradiation and α-Fe_2O_3 nanoparticles on the viscosity and thermal properties of an asphaltenic crude oil and their application to in-situ combustion EOR." Ultrasonics 120 (2022): 106655.

47- Nguele R, H Okawa. Effect of ultrasound irradiation on asphaltene aggregation and implications to rheological behavior of bitumen. Ultrasonics Sonochemistry. 80 (2021) 105811.

48- Razavifar, Mehdi, and Jafar Qajar. "Experimental investigation of the ultrasonic wave effects on the viscosity and thermal behaviour of an asphaltenic crude oil." Chemical Engineering and Processing-Process Intensification 153 (2020): 107964.

49- Otumudia E, H Hamidi, P Jadhawar, K Wu. Effects of reservoir rock pore geometries and ultrasonic parameters on the removal of asphaltene deposition under ultrasonic waves. Ultrasonics sonochemistry. 83 (2022) 105949.

50- Nguele R, AO Saheed, H Okawa, K Sasaki. Insights Into Bitumen Viscosity Reduction Using Ultrasound-Assisted EOR. SPE Western Regional Meeting. SPE2023. pp. D021S01R03.

51- Qajar J, M Razavifar, M Riazi. A mechanistic study of the synergistic and counter effects of ultrasonic and solvent treatment on the rheology and asphaltene structure of heavy crude oil. Chemical Engineering and Processing-Process Intensification. 195 (2024) 109619.

52- Galimzyanova AR, RN Gataullin, YS Stepanova, EA Marfin, MA Khelkhal, AV Vakhin. Elucidating the impact of ultrasonic treatment on bituminous oil properties: A comprehensive study of viscosity modification. Geoenergy Science and Engineering. 233 (2024) 212487.

53- Razavifar, Mehdi, Jafar Qajar, and Masoud Riazi. "Experimental study on pore-scale mechanisms of ultrasonic-assisted heavy oil recovery with solvent effects." Journal of Petroleum Science and Engineering 214 (2022): 110553.

54- Ye, Guoxiang, et al. "Application of ultrasound on crude oil pretreatment." Chemical Engineering and Processing: Process Intensification 47.12 (2008): 2346-2350.

55- GR. Check, D. Mowla. "Theoretical and experimental investigation of desalting and dehydration of crude oil by assistance of ultrasonic irradiation". Ultrasonics sonochemistry (2013) 20(1):378-85.

56- Guoxiang, Y., Xiaoping, L. Ü., Fei, P., Pingfang, H., & Xuan, S. H. E. N. (2008). Pretreatment of crude oil by ultrasonic-electric united desalting and dewatering. Chinese Journal of Chemical Engineering, 16(4), 564-569.

57- Ye, G., Lu, X., Han, P., & Shen, X. (2010). Desalting and dewatering of crude oil in ultrasonic standing wave field. Journal of Petroleum Science and Engineering, 70(1-2), 140-144.

58- Check, G. R. (2014). Two-stage ultrasonic irradiation for dehydration and desalting of crude oil: a novel method. Chemical Engineering and Processing: Process Intensification, 81, 72-78.

59- Hu, G., Li, J., Thring, R. W., & Arocena, J. (2014). Ultrasonic oil recovery and salt removal from refinery tank bottom sludge. Journal of Environmental Science and Health, Part A, 49(12), 1425-1435.

60- Wang, Z., Gu, S., & Zhou, L. (2018). Research on the static experiment of super heavy crude oil demulsification and dehydration using ultrasonic wave and audible sound wave at high temperatures. Ultrasonics Sonochemistry, 40, 1014-1020.

61- Sadatshojaie, A., Wood, D. A., Jokar, S. M., &

Rahimpour, M. R. (2021). Applying ultrasonic fields to separate water contained in medium-gravity crude oil emulsions and determining crude oil adhesion coefficients. Ultrasonics Sonochemistry, 70, 105303.

62- Ronchi, R. P., Negris, L., Melo, B. N., Pereira, L. S., Vicente, M. A., Flores, E. M., & Santos, M. D. F. P. (2021). Removal of oil from synthetic heavy crude oil-in-water emulsions by the association of glass raschig rings and ultrasound. Journal of Dispersion Science and Technology, 43(1), 22-32.

63- Chen, W. S., Chen, Z. Y., Chang, J. Y., Chen, C. Y., & Zeng, Y. P. (2022). Ultrasound-assisted desalination of crude oil: The influence of mixing extent, crude oil species, chemical demulsifier and operation variables. Ultrasonics Sonochemistry, 83, 105947.

64- Bahmani, H., Hojjat, Y., Yazdian, A., & Shirkosh, M. (2024). Ultrasonic-assisted dewatering of crude oil under various transient flow regimes: an experimental and simulation study. Petroleum Science and Technology, 1-17.

JOURNAL OF GAS TECHNOLOGY

Volume 9 / Issue 2 / Winter 2024 / Pages 54-69

Journal Home page: http://jgt.irangi.org

Optimisation of Steel Pipe-Rack Structures in the Oil Industry Using Metaheuristic Algorithms

Ruholamin Chatrazar[1], Hamed Ghohani Arab[2*], Mahmoud Miri[3]

1. Master's student, Department of Civil Engineering, Faculty of Engineering, University of Sistan and Baluchestan, Zahedan, Iran
2. Associate Professor, Department of Civil Engineering, Faculty of Engineering, University of Sistan and Baluchestan, Zahedan, Iran
3. Professor, Department of Civil Engineering, Faculty of Engineering, University of Sistan and Baluchestan, Zahedan, Iran

ARTICLE INFO

ORIGINAL RESEARCH ARTICLE

Article History:
Received: 14 November 2024
Revised: 19 December 2024
Accepted: 30 December 2024

Keywords:
Steel pipe rack structure
Optimisation
Metaheuristic algorithms
Grey Wolf Optimiser (GWO) algorithm
Whale Optimisation Algorithm (WOA)

ABSTRACT

Steel pipe racks are among the most critical structures in various industries, including oil and petrochemical sectors. They are used for transporting fluids, gases, and chemicals. Given the extensive application of these structures in the oil and gas industry, their optimisation is of paramount importance. This research aims to reduce the construction costs of steel pipe racks via practical weight optimisation using the Grey Wolf Optimiser (GWO) and Whale Optimisation Algorithm (WOA) metaheuristic algorithms, as well as comparing their responses. In this study, the aforementioned algorithms are developed automatically through MATLAB, and by interfacing with ETABS, enable the optimal design of steel pipe racks while adhering to design code requirements. Leveraging metaheuristic algorithms and complying with design code requirements, this research seeks to provide a practical solution for the safe and optimised design of steel pipe rack structures, thereby reducing construction costs in the oil and gas industry. The proposed framework is evaluated on two steel pipe racks, incorporating key design considerations. The results demonstrate that both GWO and WOA metaheuristic optimisation methods can serve as effective tools for engineers in achieving cost-efficient designs.

DOR: 20.1001.1/jgt.2025.2057791.1055

How to cite this article
R. Chatrazar, H. Ghohani Arab, M. Miri, Comparative Study of Biotreated Leachate before and After Using AOPs Treatment for Removing COD, BOD and Color. Journal of Gas Technology. 2024; 9(2): 54-69. (https://www.jgt.irangi.org/article_725004.html)

* Corresponding author.
E-mail address: ghohani@eng.usb.ac.ir, (H. Ghohani Arab).

Available online 30 December 2024

1. Introduction

Given the growing global demand for energy, the oil and gas industry continues to play a pivotal role in meeting this need. According to forecasts by the International Energy Agency (IEA), oil consumption in Middle Eastern continues to constitute the majority of energy use. China, recognised as the world's largest petrochemical consumer, continues to exhibit rising demand. The expansion of petrochemical production in China has been a key driver of recent oil market shifts, altering the distribution of petrochemical outputs in other regions. Moreover, this trend has partially offset declining demand in other sectors. Between 2019 and 2023, China's oil consumption as petrochemical feedstock increased by over 1.5 million barrels per day. Over the next decade, oil demand growth in the country is expected to remain primarily driven by petrochemical industry development.

Meanwhile, in emerging and developing economies—home to the majority of the global population—energy demand has grown at an average annual rate of 2.6% over the past decade. This surge stems from factors such as population growth, a 50% expansion in economic output, and a 40% increase in industrial production. Additionally, built-up area has grown by 40,000 square kilometres, equivalent to the total land area of the Netherlands. Given this rapid development, clean energy in these economies must expend considerably more effort to replace fossil fuels—including oil, gas, and coal—compared to advanced economies(Agency International Energy, 2024). This high demand level underscores that oil and gas infrastructure in emerging economies requires urgent development.

Despite the development of renewable energy, oil will remain one of the world's primary energy sources, particularly in the Middle East, China, and India, which play a pivotal role in global production and consumption markets. The optimisation of pipe rack structures can be economically and environmentally justified under these circumstances. It may significantly enhance the productivity of the oil and gas industry. In this context, research on pipe rack structures can improve system performance and reduce operational costs. A key objective of this study is to identify and implement optimisation methods for designing pipe racks to reduce costs while maintaining the efficiency and safety of oil and gas condensate transportation. In recent years, limited research has been conducted on the optimisation of pipe rack structures. In 2010, Richard Drake and Robert Walter summarised design load codes and other design considerations for piperacks(M. DRAKE & J. WALTER, 2010). Karimi et al. (2011) evaluated the seismic performance of existing pipe racks in Iranian petrochemical plants(Karimi et al., 2011). In 2019, Kaval and Naval studied three bracing patterns in pipe racks to achieve an optimised configuration through positional adjustments(Kawade & Navale, 2019). Nitish J. Singh and Mohammad Eshtiaghi (2016) conducted an optimised design and analysis of steel pipe racks for gas industry in compliance with international codes and standards(J Singh & Ishtiyaque, 2016). Shahidtabar and Mirghaderi (2013) proposed a novel method to account for pipe-rack interaction, reducing material usage by 29%(Shahiditabat & Mirghaderi, 2013). Pooya Zakian et al. (2021) optimised steel pipe racks using Particle Swarm Optimisation (PSO), Grey Wolf Optimiser (GWO), and an enhanced GWO algorithm(Zakian et al., 2021). The Industrial Revolution marked a turning point in engineering history, as advancements in mathematics and physics gave rise to disciplines such as civil and mechanical engineering(HOFFECKER, 2005). Post-Industrial Revolution, the growing

demand for rapid construction and increased resource consumption led to challenges such as economic constraints, unsustainable use of non-renewable resources, excessive hazardous waste, and greenhouse gas emissions. These issues not only impact the environment but also jeopardise future generations(HOFFECKER, 2005). In response, advances in science and technology have led to the development of metaheuristic algorithms, which have become essential engineering tools for optimising large-scale, complex problems due to their problem-solving capabilities (Kaveh, 2017).

These algorithms combine stochastic methods with search strategies to identify optimal solutions for diverse problems. Nature-inspired metaheuristic algorithms have gained significant popularity in engineering applications in recent years and are classified into four main categories: evolutionary-based, physics-based, swarm-based, and human behaviour-based. Despite their diverse inspirations, they all share two fundamental components: exploration and exploitation(Mirjalili & Lewis, 2016). Exploration refers to the algorithm's ability to conduct a global search of the solution space, offering advantages such as avoiding local optima and increasing the likelihood of finding global optima. However, it may also lead to slower convergence rates and higher computational resource consumption(Talbi, 2009). Previous years have seen numerous studies on conventional frame structure optimisation, with various metaheuristic algorithms being developed. The Genetic Algorithm has been employed by researchers such as Rajeev and Krishnamoorthy(Rajeev & Krishnamoorthy, 1992), Pezeshk et al(Pezeshk et al., 2000), and Kaveh and Rahami(Kaveh & Rahami, 2006)for steel frame optimisation problems. Other metaheuristic algorithms including improved Ant Colony Optimisation(Kaveh & Talatahari, 2010a), Imperialist Competitive Algorithm(Kaveh & Talatahari, 2010b), Big Bang-Big Crunch(HasançEbi, & Kazemzadeh Azad, 2012), Bat Algorithm(Hasançebi & Carbas, 2014), and Artificial Bee Colony(Aydoğdu et al., 2016) have been investigated by various scholars. TalaTaheri et al.(Talatahari et al., 2015) proposed a hybrid Eagle Strategy with Differential Evolution, implemented through SAP2000 and MATLAB interfaces for optimal structural frame design. Khajeh et al.(Khajeh et al., 2017) developed a hybrid method combining Particle Swarm Optimisation with Grid Search to reduce computational time. Mirjalili et al. introduced the Grey Wolf Optimiser in 2014(Mirjalili et al., 2014) and the Whale Optimisation Algorithm in 2016(Mirjalili & Lewis, 2016).

In this paper, the grey wolf optimisation and whale optimisation methods have been developed for weight optimisation of steel pipe rack structures while complying with the seismic design code for oil industry facilities and structures(Seismology, International Institute of Earthquake Engineering and structures Edition 4, 2023) and design constraints. This research presents a method for designing steel pipe racks through the connection of computational software MATLAB and ETABS2016, which enables the use of optimisation algorithms. The connection between these two software programs is established through the ETABS API. The connection process operates as follows: MATLAB sends the required information such as geometric specifications and analysis settings to ETABS through API functions. Subsequently, ETABS conducts the analysis and design and returns the desired results such as stresses and displacements to MATLAB. MATLAB uses this data to execute the optimisation algorithm and optimises the structural sections. This process is repeated until an optimal design is achieved. In this method, the pipe rack structure is modelled in ETABS2016 in full compliance with the seismic design code for

oil industry facilities and structures and AISC-LRFD(AISC, 2010), after which the optimisation process is carried out. The Auto Select List feature in ETABS is designed to select optimal sections based on load-to-capacity ratios. This method typically does not consider important structural constraints such as drift limitations in the section selection process. Consequently, sections selected solely based on strength criteria may exhibit undesirable structural drift and violate code limits. In the present research, in addition to observing member strength requirements, drift control has also been incorporated into the design process. This approach ensures that the obtained results are not only theoretically reliable but also directly applicable to the design of pipe rack structures.

2. Design of Pipe Rack Structures

In a large portion of petrochemical facilities, pipe rack structures are used. As shown in (Figure 1), these structures are designed as open frameworks to facilitate the passage and placement of components such as pipes, mechanical and electrical equipment, and due to their application in transporting fluids and petroleum condensates, they are constructed on a large scale.

Figure 1. Steel Pipe-Rack

Among the characteristics of pipe racks are geometric irregularities in height and length, as well as multiple dead and live loads from the equipment and pipes supported by these structures, along with seismic and thermal loads. This results in complex geometries for this type of industrial structure, making the process of achieving an optimal design challenging(Hsu & Jean, 2003). In the design of these structures, moment frames are used in one direction to provide access to operational equipment and installation of main pipes. Moment frames, while providing accessibility for equipment and pipe installation, can be vulnerable to excessive lateral deformations under seismic loads. In the other direction of the structure, braced frames are typically used due to less need for access to equipment installed on the pipe rack. These frames provide an efficient structural system for delivering stiffness and can reduce their ductility against lateral loads(Hsu & Jean, 2003).

Structural design begins with defining the applied loads. These loads include dead loads, live loads, wind loads, seismic loads, and other operational loads that are determined based on the type of structure and its application. The loading process ensures that all influencing factors are considered in the design. After defining the loads, structural modelling is completed in ETABS2016. This software uses the finite element method to analyse the structure's behaviour under the defined loads. The outputs of this analysis include stresses, displacements, and internal member forces that form the basis for design. The design of structural members is performed according to the relevant codes to ensure the structure can withstand the applied loads and safety criteria are met. It is essential to note that in the design process, the main objective is not only to ensure structural safety and performance but also to consider its economic optimisation. In the design of pipe rack structures, various loads including dead, live, operational, and seismic loads are applied, with explanations for each provided in (Table 1) (M. DRAKE & J. WALTER, 2010; Shahiditabat & Mirghaderi, 2013).

Table 1. Applied Loads on Pipe Rack Structure

Load Type	Symbol	Description
Dead Load	D	Self-weight of structure and permanent equipment (access platforms, fire-fighting equipment) supported by the structure.
Thermal Load	T	Includes environmental thermal effects.
Structural Seismic Load	EQx, EQy	Seismic forces generated by the structure itself.
Large-Diameter Pipe Seismic Load	EQx-P, EQy-P	Seismic forces from large-diameter pipes, calculated by piping engineers.
Empty Pipe Load	EMP, EMP-Frx, EMP-Fry	Load caused by the weight of empty pipes.
Operating Pipe Load	OP, OP-Frx, OP-Fry	Load from pipe weight, fluid acceleration, and thermal effects of internal fluid.
Fabrication Imperfection Load	Notional	Accounts for potential member out-of-plumb condition and initial imperfections.
Wind Load	Wind	Loads resulting from wind pressure.
Hydrotest Load	HYD	Load generated by pipe weight and water mass during pipeline testing.

The main loads acting on the structure include operational loads, seismic loads, and thermal loads. Pipes with diameters greater than 12 inches are considered large-diameter pipes. After determining the pipe routing path and calculating the forces exerted on the structure by the pipes, along with performing the related calculations, the pipe rack loading diagrams (SLD[1]) are prepared. Based on these diagrams, the design engineer carries out the design process and determines the section sizes.

3. Pipe Rack Design Criteria

The objective of structural optimisation is to reduce member sizes while considering applied loads to decrease weight and required construction materials, thereby reducing overall costs(Togˇan, 2012).

In most structural optimisation studies, the objective function is defined as Eq. (1):

$$f(x) = \sum_{i=1}^{n} (\gamma l A)_i \tag{1}$$

In Eq. (1), l represents element length, A denotes member cross-sectional area, γ is the specific weight of steel, $f(x)$ is the objective function, n indicates the number of members, and i represents the current frame member(Mahallati et al., 2018).

The AISC-LRFD code(AISC, 2010) has been employed for the design and capacity verification of structural members. The optimisation constraints for frame design include: (1) the member capacity constraint (V_i^{σ}), and (2) the inter-storey drift constraint as defined in Eq. (2) and (3).

$$V_i^{\sigma} = \left|\frac{\sigma_i}{\sigma_{\alpha}^{i}}\right| - 1 \leq 0 \qquad i = 1,2,\ldots n \tag{2}$$

$$\frac{\delta_{max}}{\bar{\delta}} - 1 \leq 0 \tag{3}$$

1. Structure Loading Diagram or Single Load Diagram

In Eq. (2) and (3), σi is the internal force in member i, $\sigma_{\alpha}^{\ i}$ is the load-bearing capacity of member i, δ_{max} is the relative displacement of each storey level, and $\bar{\delta}$ is the allowable relative displacement.

The design constraints (v_i^I) for frame members according to AISC-LRFD(AISC, 2010)are based on Eq. (4), (5) and (6):

$$v_i^I = \frac{P_u}{2\emptyset_c p_n} + \left(\frac{M_{ux}}{\emptyset_b M_{nx}} + \frac{M_{uy}}{\emptyset_b M_{ny}}\right) \ldots \leq 1 \quad \text{for } \frac{P_u}{\emptyset_c p_n} < 0.2 \quad (4)$$

$$v_i^I = \frac{P_u}{\emptyset_c p_n} + \frac{8}{9}\left(\frac{M_{ux}}{\emptyset_b M_{nx}} + \frac{M_{uy}}{\emptyset_b M_{ny}}\right) \ldots \leq 1 \quad \text{for } \frac{P_u}{\emptyset_c p_n} \geq 0.2 \quad (5)$$

In Eq. (4) and (5), φ_b is the resistance reduction factor for bending with a value of 0.9, φ_c is the resistance reduction factor in compression equal to 0.9 and in tension equal to 0.85, P_u is the existing compressive force, P_n is the nominal tensile or compressive resistance, M_{uy} is the existing (amplified) bending moment about the y-axis (weak axis), M_{ny} is the nominal bending resistance about the y-axis (weak axis), M_{ux} is the existing (amplified) bending moment about the x-axis (strong axis), and M_{nx} is the nominal bending resistance about the x-axis (strong axis).

For shear capacity, Eq. (6) has been applied as a constraint:

$$\frac{V_u}{\varphi_v V_n} \leq 1 \quad (6)$$

In Eq. (6), V_u is the existing shear force and V_n is the nominal shear resistance of each member, and φ_v is the shear resistance reduction factor equal to 1.

The stability of frame members has been verified according to Eq. (7) and (8):

$$\gamma_m = \frac{Kl_m}{r_m} \leq 200 \quad \textit{For Compressive Members} \quad (7)$$

$$\gamma_m = \frac{l_m}{r_m} \leq 300 \quad \textit{For Tensile Member} \quad (8)$$

In Eq. (7) and (8), l_m is the unbraced length of the member, r_m is the radius of gyration of the member, and K is the effective length factor. Frame structures are controlled by displacement limits, which are determined according to the seismic design code for oil industry facilities and structures.

For calculating compressive and Euler stresses, the effective length factor (K) is required. The value of K for beams is equal to one, and for columns it is obtained from Eq. (9).

$$K = \sqrt{\frac{1.6G_AG_B + 4G_AG_B + 7.5}{G_A + G_B + 7.5}} \geq 1 \quad (9)$$

The value of K for braces is calculated from Eq. (10):

$$K = \frac{3G_AG_B + 1.4(G_A + G_B) + 0.64}{3G_AG_B + 2(G_A + G_B) + 1.28} \quad (10)$$

In Eq. (9) and (10), G_A and G_B represent the boundary conditions at both ends of the compressive member(Salama, 2013).

4. Grey Wolf Optimisation Algorithm

The general form of the optimisation problem is shown in Eq. (11).

$$\textit{Minimize } f(x)$$

$$\textit{Subject to: } \begin{cases} h_i(x) = 0 & i = 1, 2 \ldots, m_1 \\ g_j(x) < 0 & j = 1, 2 \ldots, m_2 \\ L_n < x_n < U_n & n = 1, 2 \ldots, m_3 \end{cases} \quad (11)$$

In Eq. (11), x represents an n-dimensional vector that denotes the design variables. g and h represent inequality and equality constraints, respectively. L and U indicate the lower and upper bounds of the design variables. m_1, m_2, and m_3 specify the number of equality constraints, inequality constraints, and the dimensions of the search space, respectively. The space where all constraints are satisfied is called the decision space, which determines the number of decision variables(Mahallati et al., 2018).

The Grey Wolf Optimiser (GWO) algorithm was introduced by Mirjalili et al. in 2014. This metaheuristic algorithm is inspired by the hunting behaviour of grey wolves and belongs to the category of swarm intelligence and population-based algorithms(Mirjalili et al., 2014).

The algorithm is developed and mathematically modelled based on the social hierarchy and cooperative hunting behaviour of grey wolves. Grey wolves are known as apex predators at the top of the food chain.

They typically live in packs averaging 5-12 wolves. A distinctive characteristic of grey wolves is their strict social hierarchy. The pack leader, which can be male or female, is called the alpha wolf; this wolf is not necessarily the strongest in the pack but is the best in terms of pack management. The alpha wolf is primarily responsible for making important decisions regarding hunting, sleeping locations, and wake-up times, and other wolves must follow its orders(Mech, 1999).

The second level in the hierarchy consists of beta wolves, which serve as advisors to the alpha. These wolves follow the alpha's commands, reinforce its decisions, and also give orders to other wolves. The lowest ranking wolves are called omega wolves. These wolves help maintain the pack structure and are the last to eat. Wolves that don't belong to any of the above three categories are called delta wolves. These wolves follow the commands of alphas and betas but give orders to omega wolves. Delta wolves warn the pack when they sense danger and help ensure the pack's safety. Elderly and caretaker wolves belong to this group(Mirjalili et al., 2014).

In the GWO algorithm, the prey represents the best-known solution at the current moment, which the search agents follow to improve their positions. The hunting process represents finding the best possible solution to the problem. To model the social hierarchy in the GWO algorithm, the best position or solution is called alpha, the second-best solution is called beta, the third-best solution is called delta, and other solutions are called omega. For modelling the encircling behaviour of prey, Eq. (12) to (15) have been proposed:

$$\vec{X}(\mathrm{t}+1) = \overrightarrow{X_p}(t) - \vec{A}.\vec{D} \tag{12}$$

$$\vec{D}(t) = \left|\vec{C}.\overrightarrow{X_p}(t) - \vec{X}(t)\right| \tag{13}$$

$$\vec{A} = \vec{a}(2.\overrightarrow{r_1} - 1) \tag{14}$$

$$\vec{C} = 2.\overrightarrow{r_2} \tag{15}$$

In Eq. (12) to (15), $\vec{X}(t)$ represents the position of the grey wolf at iteration t, $\overrightarrow{X_p}(t)$ represents the position of the prey (the best known solution at that moment) at iteration t, and $\vec{D}(t)$ represents the distance between the grey wolf's position and the prey's position at iteration t. The component $\vec{a}$ decreases linearly from 2 to zero, while r_1 and r_2 are random numbers between zero and one. The grey wolf algorithm has two parameters, $\vec{C}$ and $\vec{A}$, which control the exploration and exploitation processes. During the search for the optimal solution, the actual position of the hunt is unknown. Therefore, the best position obtained up to that point is considered as the hypothetical position of the prey, which is typically the position of the alpha wolf representing the current best solution. The second and third best solutions, belonging to the beta and delta wolves respectively, are also considered as potential prey positions. Thus, the three best solutions found are stored, and other search agents (omega wolves) are required to update their positions according to the positions of alpha, beta, and delta. Eq. (16) to (19) represent these relationships:

$$\overrightarrow{X_1}(t) = \overrightarrow{X_\alpha}(t) - \overrightarrow{A_1}.\overrightarrow{D_\alpha}(t) \quad \& \quad \overrightarrow{D_\alpha}(t) = \left|\overrightarrow{C_1}.\overrightarrow{X_\alpha}(t) - \vec{X}(t)\right| \tag{16}$$

$$\overrightarrow{X_2}(t) = \overrightarrow{X_\beta}(t) - \overrightarrow{A_2}.\overrightarrow{D_\beta}(t) \quad \& \quad \overrightarrow{D_\beta}(t) = \left|\overrightarrow{C_2}.\overrightarrow{X_\beta}(t) - \vec{X}(t)\right| \tag{17}$$

$$\overrightarrow{X_3}(t) = \overrightarrow{X_\delta}(t) - \overrightarrow{A_3}.\overrightarrow{D_\delta}(t) \quad \& \quad \overrightarrow{D_\delta}(t) = \left|\overrightarrow{C_3}.\overrightarrow{X_\delta}(t) - \vec{X}(t)\right| \tag{18}$$

$$\vec{X}(\mathrm{t}+1) = \frac{\overrightarrow{X_1}(t) + \overrightarrow{X_2}(t) + \overrightarrow{X_3}(t)\big)}{3} \tag{19}$$

Optimisation involves two opposing processes: exploration and exploitation(Črepinšek et al., 2013). The exploration process aims to discover new areas of the search space by introducing sudden changes in solutions, preventing potential solutions from becoming trapped in local optima. The exploitation process works to improve existing solutions by examining their neighbourhoods more thoroughly and applying gradual changes to reach the optimal solution. Since exploration and exploitation are opposing processes, the algorithm must maintain a balance between them. The parameter C generates random values in the interval [0,2], influencing the prey's next position. When C >1, the algorithm moves to explore new areas, attempting to move away from the current position to potentially find better solutions and avoid local optima. In this case, the exploration process becomes more prominent than exploitation. When $\vec{C}$ becomes greater than one, according to Eq. (13), $\vec{D}$ generally increases, meaning the wolves' position changes occur over a larger range, expanding the search space. Conversely, when $\vec{C}$ is less than one, the focus shifts more toward exploiting existing areas. The other variable is parameter $\vec{A}$, which is defined based on the value of $\vec{a}$ in Eq. (20), decreasing linearly from 2 to 0:

$$\vec{a} = 2 - \mathrm{t}\left(\frac{2}{\mathrm{T}}\right) \tag{20}$$

When $\vec{A}$ is greater than 1 or less than -1, the value of $\vec{A}.\vec{D}$ increases, resulting in larger changes in the wolves' new positions. This means the search range and movement toward unknown and new areas increase, making the exploration process more prominent. On the other hand, when $\vec{A}$ falls within the interval [-1,1], the changes in new positions are smaller, aiding the exploitation process by allowing the algorithm to focus more on areas close to its current position(Mirjalili et al., 2014).

The pseudocode of the Grey Wolf Optimisation algorithm is presented in (Figure 2).

Initialize the grey wolf population X_i (i = 1, 2, ..., n)
Initialize a, A, and C
Calculate the fitness of each search agent
X_α=the best search agent
X_β=the second best search agent
X_δ=the third best search agent
while *(t < Max number of iterations)*
  for *each search agent*
    Update the position of the current search agent by equation (19)
  end for
  Update a, A, and C
  Calculate the fitness of all search agents
  Update X_α, X_β, and X_δ
  t=t+1
end while
return X_α

Figure 2. Pseudocode of the Grey Wolf Optimisation Algorithm(Mirjalili et al., 2014)

5. Whale Optimisation Algorithm

The Whale Optimisation Algorithm (WOA) is inspired by the hunting behaviour of a specific species of whales and was introduced by Mirjalili and Lewis in 2016(Mirjalili & Lewis, 2016). Whales are the largest mammals on Earth. Among the seven main species, we can mention killer whales, minke whales, sei whales, humpback whales, right whales, fin whales, and blue whales. These mammals possess unique characteristics including thinking ability, judgment, communication skills, and emotional capacity. A notable species is the humpback whale, which employs a distinctive hunting method called bubble-net feeding. In this method, whales create bubbles in a spiral path to trap their prey. It should be noted that this hunting technique is unique to humpback whales. The mathematical

modelling of this behaviour is explained below(Mirjalili & Lewis, 2016).

5.1. Encircling Prey

In the optimisation process, as mentioned in Section 4, the prey represents the best-known solution at the current moment, which the whales (search agents) follow to improve their positions, while the hunt represents the best possible solution to the problem that the algorithm seeks to find. Humpback whales identify the prey's location and encircle it. Since the exact location of the optimal solution is unknown, the algorithm assumes that the current best solution is close to the optimal point. Other search agents update their positions to move closer to the best solution. Eq. (21) and (22) represent this behaviour.

$$\vec{D} = \left|\vec{C}.\overrightarrow{X^*}(t) - \vec{X}(t)\right| \quad (21)$$

$$\vec{X}(t+1) = \overrightarrow{X^*}(t) - \vec{A}.\vec{D} \quad (22)$$

In Eq. (21) and (22), $\vec{A}$ and $\vec{D}$ are coefficients that change dynamically, and t represents the iteration number. $\overrightarrow{X^*}(t)$ denotes the current best solution found, while $\vec{X}$ represents the position of the search agent. The vectors $\vec{A}$ and $\vec{C}$ are defined in Eq. (23) and (24).

$$\vec{A} = 2\vec{a}.\vec{r} - \vec{a} \quad (23)$$

$$\vec{C} = 2.\vec{r} \quad (24)$$

The component $\vec{a}$ decreases linearly from 2 to 0, and r represents a random vector between 0 and 1. The combination of Eq. (21) to (24) helps the algorithm simulate the prey encirclement process.

5.2. Position Update with Spiral Motion

In this method, first the distance between the whale's position and the prey is calculated, and then Eq. (25) is used to simulate the whale's spiral movement toward the prey.

$$\vec{X}(t+1) = \overrightarrow{D'}.e^{bl}.\cos(2\pi l) + \overrightarrow{X^*}(t) \quad (25)$$

The value D' is obtained from Eq. (26).

$$\overrightarrow{D'} = \left|\overrightarrow{X^*}(t) - \vec{X}(t)\right| \quad (26)$$

In Eq. (25), b is a constant value that determines the shape of the spiral movement, and l is a random number in the interval [-1,1]. Humpback whales move in a gradually shrinking circular path that forms a spiral around their prey. To model this dual behaviour, the algorithm is assumed to select either the shrinking encircling method or the spiral model with a 50% probability to update the whales' positions. The mathematical model of this process is shown in Eq. (27) and (28) (Mirjalili & Lewis, 2016).

$$\vec{X}(t+1) = \overrightarrow{X^*}(t) - \vec{A}.\vec{D} \quad for\ p < 0.5 \quad (27)$$

$$\vec{X}(t+1) = \overrightarrow{D'}.e^{bl}.cos(2\pi l) \ldots + \overrightarrow{X^*}(t) \quad for\ p \geq 0.5 \quad (28)$$

Where p is a random number in the interval [0,1].

5.3. Exploration Phase

In the exploration phase, changes in the vector $\vec{A}$ are used. Whales search for prey randomly based on each other's positions. To ensure effective exploration of the search space, the value of $\vec{A}$ must be greater than 1 or less than -1. During this phase, whale positions are updated based on a randomly selected search agent, which is exactly opposite to the exploitation phase where the best-known solution is used for position updates. This approach, when $|\vec{A}|>1$, focusses on the exploration process, allowing the algorithm to search more extensively throughout the solution space for the optimal answer. The mathematical model of this process is shown in Eq. (29) and (30).

$$\vec{D} = \left|\vec{C}.\overrightarrow{X_{rand}} - \vec{X}(t)\right| \quad (29)$$

$$\vec{X}(t+1) = \overrightarrow{X_{rand}} - \vec{A}.\vec{D} \quad (30)$$

The whale algorithm begins with a random set of solutions. In each iteration, search agents update their positions either based on a random operation or the best solution found so far. Parameter a gradually decreases from 2 to 0 to enable both exploration and exploitation. When $|\vec{A}|>1$, a random search operation is selected, while when $|\vec{A}|<1$, the best solution is used to update whale positions. Depending on the value of p, the algorithm can switch between circular or spiral movement patterns(Mirjalili & Lewis, 2016). Throughout the algorithm's execution, the prey position is continuously updated as whales attempt to reach the optimal solution. This process continues until the algorithm converges and extracts the optimal solution.

The pseudocode of the Whale Optimisation Algorithm is shown in (Figure 3).

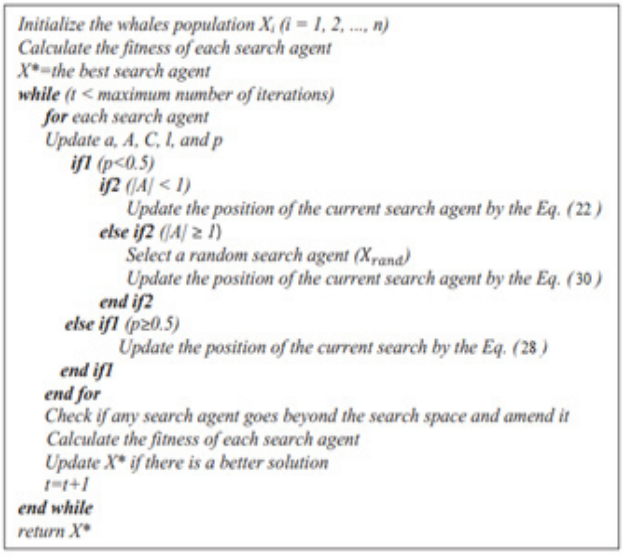

Figure 3. Pseudocode of the Whale Optimisation Algorithm(Mirjalili & Lewis, 2016)

6. Constraint Handling

In constrained optimisation problems, adhering to problem constraints is of utmost importance. In the studied optimisation algorithms, the penalty method is employed to guide solutions toward the feasible region. In this method, if a solution violates any constraints, its objective function value is modified by adding a penalty term. This penalty term is calculated as the product of a penalty coefficient and the degree of constraint violation.

7. Numerical Examples

Two steel pipe rack examples are presented to evaluate the performance of grey wolf and whale optimisation algorithms for this type of structure. The modelling was performed using the seismic design code for oil industry facilities and structures(Seismology, International Institute of Earthquake Engineering and structures Edition 4, 2023) along with AISC-LRFD(AISC, 2010) provisions. The structures feature ordinary concentric braced frames in the longitudinal direction and intermediate moment frames in the transverse direction. Due to the absence of rigid floor diaphragms, horizontal bracing is employed to enhance seismic performance and structural integrity.

For these structures, the steel density equals 7850 kg/m^3 with an elastic modulus of 200 GPa. The steel has a yield stress of 240 MPa and ultimate stress of 370 MPa. As standard practice for seismic calculations, equivalent static analysis and response spectrum analysis based on design codes are performed for structural evaluation and design. This analysis aims to determine seismic forces acting on the structure and verify design compliance with code requirements.

The design wind speed of 125 km/h (hourly average) has been applied to the structure according to ASCE7-10 code(Engineers American Society of Civil, 2010).

The lateral displacement of pipe rack structures is calculated using Eq. (31) based on the seismic design code for oil industry facilities and structures(Seismology, International Institute of Earthquake Engineering and structures Edition 4, 2023).

$$\delta_{DE} = \frac{C_d \times \delta_e}{I} \tag{31}$$

In Eq. (31), C_d represents the displacement amplification factor (4 for intermediate moment frames and 3.25 for ordinary concentric braced frames), δ_e denotes the elastic lateral displacement at each level due to lateral loads, I is the importance factor (1.25), and δ_{DE} indicates the design (inelastic) lateral displacement.

According to the relevant code, the allowable inter-storey drift ratio for pipe rack structures is considered as 0.01 of the storey height(Seismology, International Institute of Earthquake Engineering and structures Edition 4, 2023). P-Δ effects have been included, and load combinations follow AISC-LRFD(AISC, 2010) provisions.

The structural finite element model analysis is performed using ETABS2016, after which the optimisation algorithm coded in MATLAB environment gradually updates the design parameters. In this study, a termination criterion based on the number of iterations was employed to conclude the execution of the algorithm. This means that the algorithm automatically stops after completing a predefined number of iterations. This method was chosen due to its simplicity and high efficiency.

7.1. Steel Pipe Rack Example 1

The first example (Figure 4) shows a three-storey steel pipe rack with 99 members. The studied structure has three main spans in the longitudinal direction (x) with a length of 5 metres and one main span in the transverse direction (y) with a length of 6 metres, located at three elevation levels (z) with height codes of 4, 7, and 9.5 metres above ground level. Due to the absence of a roof and rigid diaphragm, horizontal bracing is used for better and more integrated performance against earthquakes. (Figure 4) provides an overall view of the structure.

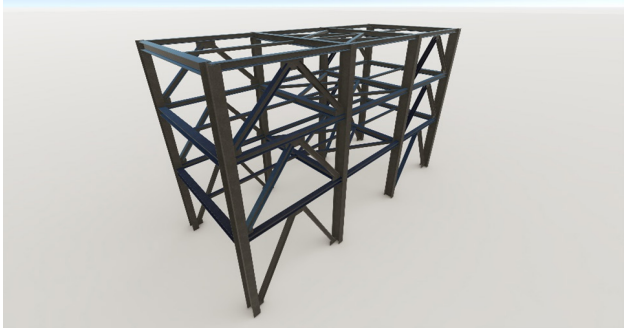

Figure 4. Steel Pipe-Rack Example 1

(Table 2) shows the seismic coefficient applied to the structure.

Table 2. Earthquake Coefficients Applied to the Structure of Steel Pipe-Rack Example 1

Type of Applied Load	Direction of Load Application	Value of Coefficient C	Value of Coefficient K
Earthquake	Direction X	0.461	1
	Direction Y	0.393	1

The number of analyses for the grey wolf and whale optimisation algorithms has been set to 7,500. The population size is set to 150, and the number of algorithm iterations is set to 50.

(Figure 5) and (Table 3) show the grouping of pipe rack sections and their corresponding colours. The structural members are categorised into 10 groups:

Table 3. Grouping and Number of Sections in Steel Pipe-Rack Example 1

Groups										
Section Type	Column				Beam			Lateral Brace		Floor bracing
Group Number	1	2	3	4	5	6	7	8	9	10
Number of Elements in Each Group	8	8	8	4	8	6	12	8	16	21
Colour										

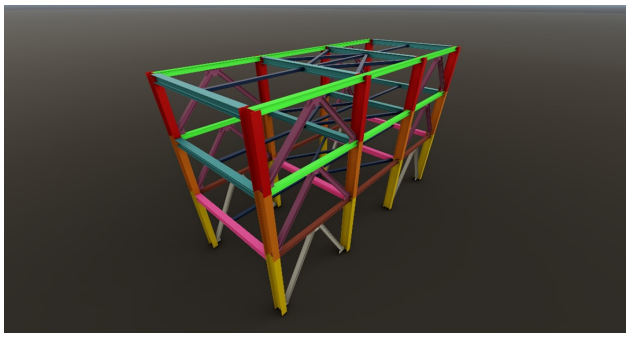

Figure 5. Display of Section Grouping in Steel Pipe-Rack Example 1

HEA and HEB sections are used for columns, beams, and lateral bracing, while box sections are used for floor bracing according to (Tables 4 and 5).

Table 4. HE Sections Used in Steel Pipe-Rack Example 1

HE100A	HE100B	HE120A	HE140A	HE160A	HE180A	HE200A
HE200B	HE220A	HE220B	HE240A	HE240B	HE260A	HE260B
HE280A	HE280B	HE300A	HE300B	HE320A	HE320B	HE340A
HE340B	HE360A	HE360B	HE400A	HE400B	HE450A	HE450B
HE500A	HE500B	HE550B	HE600B	HE650B	HE700B	

Table 5. BOX Sections Used in Steel Pipe-Rack Example 1

BOX140×70×3.6	BOX140×70×4	BOX140×70×4.5	BOX140×70×5	BOX140×70×5.4
BOX140×70×5.9	BOX140×70×7.1	BOX140×70×8	BOX140×70×10	BOX140×70×12.5
BOX140×98×5	BOX140×98×5.4	BOX140×98×5.9	BOX140×98×7.1	BOX140×98×8
BOX140×98×10	BOX140×98×12.5	BOX140×98×14.2	BOX140×98×16	BOX140×98×17.5

Thus, the 99 elements are divided into 10 groups, with groups 1 to 9 including 34 sections and group 10 including 20 sections for selection, creating a complex optimisation problem.

(Table 6) and (Figure 6) show the results obtained from the grey wolf and whale optimisation algorithms for the discussed pipe rack.

Table 6. Comparison of Results for the Whale and Grey Wolf Algorithms in Steel Pipe-Rack Example 1

Group Number of Member	GWO	WOA
1	HE450A	HE450A
2	HE450A	HE450A
3	HE360A	HE280A
4	HE450A	HE400A
5	HE320A	HE360A
6	HE220A	HE220A
7	HE180A	HE160A
8	HE200A	HE180A
9	HE140A	HE140A
10	TUBO140X98X5.4	TUBO140X98X5
Weight (KN)	264.79	264.1
Number of Analyses	7500	7500

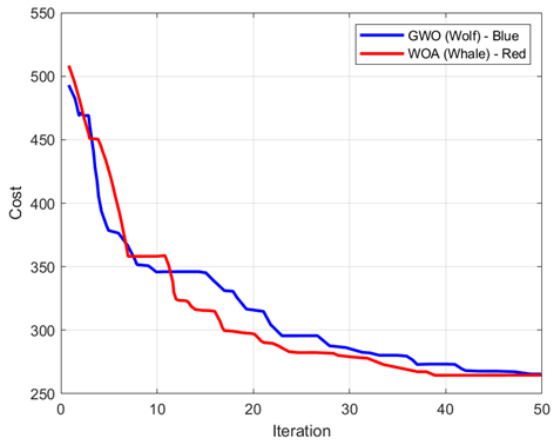

Figure 6. Optimisation Process in Steel Pipe Rack Example 1 Using the Grey Wolf and Whale Optimisation Algorithms

7.2. Steel Pipe Rack Example 2

The second example examines a two-storey steel pipe rack structure consisting of 138 members. The structure under investigation contains four main spans measuring 5 metres in the longitudinal (x) direction and two main spans of 6 metres in the transverse (y) direction. The structure is positioned at two elevation levels: 6.85 metres and 8.35 metres above ground level. (Figure 7) provides an overall illustration of the structure. (Table 7) presents the seismic coefficients applied to the structure.

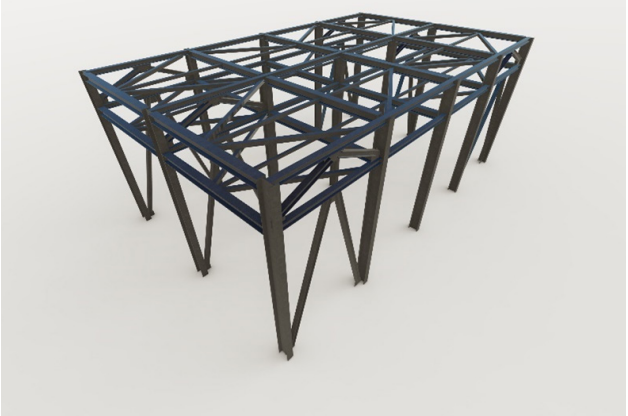

Figure 7. Steel Pipe-Rack Example 2

Table 7. Earthquake Coefficients Applied to the Structure of Steel Pipe-Rack Example 2

Type of Applied Load	Direction of Load Application	Value of Coefficient C	Value of Coefficient K
Earthquake	Direction X	0.461	1
	Direction Y	0.428	1

The whale optimisation algorithm was configured to perform 7,500 analyses. The population size is set to 150, and the number of algorithm iterations is set to 50.

(Figure 8) and (Table 8) display the pipe rack section groupings and their corresponding colour coding. The structural members are categorised into nine groups:

Table 8. Grouping and Number of Sections in Steel Pipe-Rack Example 2

Groups									
Section Type	Column	Beam				Lateral Brace		Floor bracing	
Group Number	1	2	3	4	5	6	7	8	9
Number of Elements in Each Group	30	10	10	12	12	12	12	20	20
Colour									

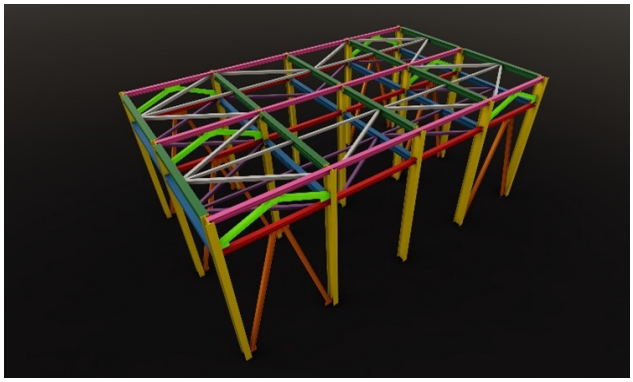

Fig. 8. Display of Section Grouping in Steel Pipe-Rack Example 2

columns, beams, and lateral bracing utilise HEA and HEB sections, while floor bracing employs box sections as detailed in (Tables 9 and 10).

Table 9. HE Sections Used in Steel Pipe-Rack Example 2

HE100A	HE100B	HE120A	HE140A	HE160A	HE180A	HE200A
HE200B	HE220A	HE220B	HE240A	HE240B	HE260A	HE260B
HE280A	HE280B	HE300A	HE300B	HE320A	HE320B	HE340A
HE340B	HE360A	HE360B	HE400A	HE400B	HE450A	HE450B
HE500A	HE500B	HE550B	HE600B	HE650B	HE700B	

Table 10. BOX Sections Used in Steel Pipe-Rack Example 2

BOX140×98×5	BOX140×98×5.4	BOX140×98×5.9	BOX140×98×7.1	BOX140×98×8
BOX140×98×10	BOX140×98×12.5	BOX140×98×14.2	BOX140×98×16	BOX140×98×17.5
BOX140×140×7.1	BOX140×140×8	BOX140×140×10	BOX140×140×12.5	BOX140×140×14.2
BOX140×140×16	BOX140×140×17.5	BOX140×140×20	BOX140×140×22.2	BOX140×140×25

Consequently, the 138 elements are divided into nine groups, with groups 1 through 7 offering 34 section options each, and groups 8 and 9 providing 20 section options each, creating a complex optimisation challenge.

(Table 11) and (Figure 9) present the results obtained from applying the grey wolf and whale optimisation algorithms to the pipe rack under consideration.

Table 11. Comparison of Results for the Whale and Grey Wolf Algorithms in Steel Pipe-Rack Example 2

Group Number of Member	GWO	WOA
1	HE450B	HE450B
2	HE400A	HE400A
3	HE450A	HE400A
4	HE280A	HE280A
5	HE180A	HE180A
6	HE260A	HE260A
7	HE180A	HE100A
8	TUBO140X140X7.1	BOX140×140×7.1
9	TUBO140X140X7.1	BOX140×140×7.1
Weight (KN)	565.907	550.65
Number of Analyses	7500	7500

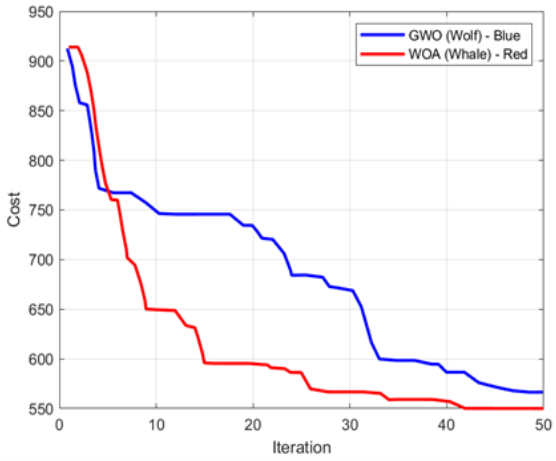

Figure 9. Optimisation Process in Steel Pipe-Rack Example 2 Using the Grey Wolf and Whale Optimisation Algorithms

8. Conclusions

In this research, the grey wolf and whale metaheuristic algorithms were used to optimise steel pipe rack structures. The performance of these methods was evaluated on two steel pipe racks. Establishing a connection between MATLAB and ETABS2016 enabled automated management of design inputs and outputs, which led to weight reduction of structures while complying with code requirements. The results show that both algorithms have high capability in optimising this type of steel structure. Using these methods in industrial structure design, especially in oil and gas projects, can help reduce costs and increase productivity. Furthermore, the high optimisation capability of the studied algorithms makes them applicable to other industrial structures as well. Finally, this research shows that the mentioned methods can be effective and practical tools for structural engineers and, by optimising pipe racks, can play an important role in reducing costs of civil engineering projects. For future research, it is recommended to explore the use of alternative optimisation algorithms with faster convergence rates. Additionally, the optimisation of concrete pipe-rack structures could be investigated.

References

Agency International Energy. (2024). World Energy Outlook 2024. International Energy Agency.

AISC. (2010). Specifications for structural steel buildings. IL: AISC.

Aydoğdu, i, Akın, A., & Saka, M. P. (2016). Design optimization of real world steel space frames using artificial bee colony algorithm with Levy flight distribution. Advances in Engineering Software, 92, 1-14. https://doi.org/10.1016/j.advengsoft.2015.10.013.

Črepinšek, M., Liu, S., & Mernik, M. (2013). Exploration and Exploitation in Evolutionary Algorithms: A Survey. ACM Computing Surveys, 45(3). https://doi.org/10.1145/2480741.2480752.

Engineers American Society of Civil. (2010). Minimum Design Loads for Buildings and Other Structures (ASCE/SEI 7-10). American Society of Civil Engineers.

Hasançebi, O., & Carbas, S. (2014). Bat inspired algorithm for discrete size optimization of steel frames. Advances in Engineering Software, 67, 173-185. https://doi.org/10.1016/j.advengsoft.2013.10.003.

HasançEbi, O., & Kazemzadeh Azad, S. (2012). An exponential big bang-big crunch algorithm for discrete design optimization of steel frames. Computers and Structures, 110-111, 167-179. https://doi.org/10.1016/j.compstruc.2012.07.014.

HOFFECKER, J. F. (2005). Innovation and Technological Knowledge in the Upper Paleolithic of Northern Eurasia. Evolutionary Anthropology, 14, 186-198. https://doi.org/10.1002/evan.20066.

Hsu, H. L., & Jean, S. Y. (2003). Improving seismic design efficiency of petrochemical facilities. Practice Periodical on Structural Design and Construction, 8(2), 107-117. https://doi.org/10.1061/(ASCE)1084-0680(2003)8:2(107).

J Singh, N., & Ishtiyaque, M. (2016). Optimized Design & Analysis of Steel Pipe Racks for Oil

& Gas Industries as per International Codes & Standards. International Journal of Research in Engineering and Technology, 5(10).

Karimi, M., Hosseinzadeh, N., Hosseini, F., & Kazem, N. (2011). Seismic Evaluation of Pipe Rack Supporting Structures in a Petrochemical Complex in Iran. International Journal of Advanced Structural Engineering, 3(1), 111-120.

Kaveh, A., & Rahami, H. (2006). Nonlinear analysis and optimal design of structures via force method and genetic algorithm. Computers & Structures, 84(12), 770-778. https://doi.org/10.1016/j.compstruc.2006.02.004.

Kaveh, A., & Talatahari, S. (2010a). An improved ant colony optimization for the design of planar steel frames. Engineering Structures, 32(3), 864-873. https://doi.org/10.1016/j.engstruct.2009.12.012

Kaveh, A., & Talatahari, S. (2010b). Optimum design of skeletal structures using imperialist competitive algorithm. Computers and Structures, 88(21-22), 1220-1229. https://doi.org/10.1016/j.compstruc.2010.06.011.

Kawade, M. G., & Navale, A. V. (2019). Optimization of Pipe Rack by Study of Braced Bay. International Journal of Research in Engineering, Science and Management, 2(2).

Khajeh, A., Ghasemi, M. R., & Ghohani Arab, H. (2017). Hybrid Particle Swarm Optimization, Grid Search. International Journal of Optimization in Civil Engineering, 7(2), 171-189.

M. DRAKE, R., & J. WALTER, R. (2010). Design of Structural Steel Pipe Racks. Engineering Journal, 47, 241-252.

Mahallati, A., Ghasemi, M. R., & Ghohani Arab, H. (2018). OPTIMIZATION OF STEEL MOMENT FRAME BY A PROPOSED EVOLUTIONARY ALGORITHM. INTERNATIONAL JOURNAL OF OPTIMIZATION IN CIVIL ENGINEERING, 8(4), 511-524.

Mech, L. D. (1999). Alpha status, dominance, and division of labor in wolf packs. Canadian Journal of Zoology, 77, 1196-1203. https://doi.org/10.1139/z99-099.

Mirjalili, S., & Lewis, A. (2016). The Whale Optimization Algorithm. Advances in Engineering Software, 95, 51-67. https://doi.org/10.1016/j.advengsoft.2016.01.008.

Mirjalili, S., Mirjalili, S. M., & Lewis, A. (2014). Grey Wolf Optimizer. Advances in Engineering Software, 69, 46-61. https://doi.org/10.1016/j.advengsoft.2013.12.007.

Pezeshk, S., V. Camp, C., & Chen, D. (2000). Design of Nonlinear Framed Structures Using Genetic Optimization. Journal of Structural Engineering, 126(3), 382-388. https://doi.org/10.1061/(ASCE)0733-9445(2000)126:3(382)

Rajeev, S., & Krishnamoorthy, C. S. (1992). Discrete Optimization of Structures Using Genetic Algorithms. Journal of Structural Engineering, 118(5), 1233-1250. https://doi.org/10.1061/(ASCE)0733-9445(1992)118:5(1233).

Salama, M. I. (2013). New simple equations for effective length factors. HBRC Journal, 10(2), 156-159. https://doi.org/10.1016/j.hbrcj.2013.10.003.

Seismology, International Institute of Earthquake Engineering and structures Edition 4. (2023). Seismic Design Regulations Oil industry facilities and structures Edition 4. Vice President of Engineering, Research and Technology.

Shahiditabat, A., & Mirghaderi, R. (2013). Pipe and Pipe Rack Interaction. International Journal of Applied Science and Technology, 3(5), 39-44.

Talatahari, S., Gandomi, A. H., Yang, X.-S., & Deb, S. (2015). Optimum design of frame structures using the Eagle Strategy with Differential Evolution. Engineering Structures, 91, 16-25. https://doi.org/10.1016/j.engstruct.2015.02.026.

Talbi, E. G. (2009). Metaheuristics: From Design to Implementation. Wiley.

Togˇan, V. (2012). Design of planar steel frames using Teaching-Learning Based Optimization. Engineering Structures, 34, 225-232. https://doi.org/10.1016/j.engstruct.2011.08.035.

Zakian, P., Ordoubadi, B., & Alavi, E. (2021). Optimal Design of Steel Pipe Rack Structures Using PSO, GWO, and IGWO Algorithms. Advances in Structural Engineering, 24(11), 1-13. https://doi.org/10.1177/13694332211004116.

JOURNAL OF GAS TECHNOLOGY

Volume 9 / Issue 2 / Winter 2024 / Pages 70-87

Journal Home page: http://jgt.irangi.org

The Impression of Roughness on Flow Pattern and Performance of Axial Gas Cyclone Along with Erosion Rate

Masoud Dorfeshan[1*], Sattar Moghaddam[2], Farzad Parvaz[3]

1. Assistant Professor, Department of Mechanical Engineering, Faculty of Engineering, Behbahan Khatam Alanbia University of Technology, Behbahan, Iran
2. M.Sc. Student, Department of Mechanical Engineering, Faculty of Engineering, Behbahan Khatam Alanbia University of Technology, Behbahan, Iran
3. M.Sc., Department of Mechanical Engineering, Semnan University, P.O. Box 35131-191, Semnan, Irann

ARTICLE INFO

ORIGINAL RESEARCH ARTICLE

Article History:
Received: 14 November 2024
Revised: 19 December 2024
Accepted: 30 December 2024

Keywords:
Axial gas cyclone
Wall roughness
Pressure drop
Wall erosion
Discrete phase model

ABSTRACT

In this study, the effect of wall roughness on flow pattern, performance, and erosion rate in an axial gas cyclone is investigated. Gas cyclones are widely used in various industries such as food processing, dryers, and the cement industry for separating solid particles from gas flow due to their flexibility, low maintenance costs, and efficiency in air pollution control. Numerical modeling is conducted using turbulence models, surface roughness models, the discrete phase model (DPM), and the erosion model to analyze key parameters such as pressure drop, tangential velocity, axial velocity, separation efficiency, and wall erosion rate. The results indicate that increasing wall roughness reduces tangential velocity, thereby decreasing centrifugal force, which negatively affects particle separation efficiency. On the other hand, increasing wall roughness leads to a reduction in pressure drop, which is considered an advantage in cyclone design. Erosion rate analysis also shows that the highest erosion occurs in the lower conical section of the cyclone, and increasing wall roughness can reduce erosion. Overall, this study reveals that wall roughness has conflicting effects on cyclone performance—reducing pressure drop on one hand while decreasing separation efficiency on the other. Therefore, optimizing surface roughness is essential to achieve a balance between these two factors in the design of axial gas cyclones. The results showed that increasing wall roughness reduced tangential velocity by up to 18%, cyclone collection efficiency dropped by approximately 12% for particles larger than 25 μm, while pressure drop decreased by around 9%, which can be considered beneficial in energy-sensitive applications. The highest erosion rate was observed at the cone tip of the cyclone, and wall roughness helped reduce average erosion by nearly 15%.

DOR: 20.1001.1/jgt.2025.2057137.1054

How to cite this article
M. Dorfeshan, S. Moghaddam, F. Parvaz, The Impression of Roughness on Flow Pattern and Performance of Axial Gas Cyclone Along with Erosion Rate. Journal of Gas Technology. 2024; 9(2): 70 -87. (https://www.jgt.irangi.org/article_726453.html)

* Corresponding author.
E-mail address: dorfeshan@bkatu.ac.ir, (M. Dorfeshan).

Available online 30 December 2024

1. Introduction

Gas cyclones are widely utilized across various industries to separate solid particles from airflow. Due to their flexibility, low maintenance costs, and effectiveness in air pollution control, these devices have gained significant attention from researchers and engineers. They are extensively applied in industries such as food processing, drying, and cement production. Gas cyclones operate based on centrifugal force, classifying solid particles according to their size or density. With advancements in computational technologies, commercial software has become instrumental in modeling complex flow patterns. Numerous studies have adopted numerical approaches to analyze gas cyclone performance (Vahedi et al., 2020; Parvaz et al., 2017; Vahedi et al., 2018; Vahedi et al., 2017; Parvaz et al., 2018; Parvaz et al., 2023; Dehdarinejad et al., 2023; Foroozesh et al., 2021; Babaoğlu et al., 2021; Elsayed et al., 2020; Babaoğlu et al., 2018; Parvaz et al., 2020; Parvaz et al., 2023). Among different types of gas cyclones, conventional gas cyclones and axial gas cyclones (AGCs) are commonly used for particle separation. The primary distinction between these two types lies in the direction of the gas stream, which is categorized into tangential inlets and guide vanes (Mao et al., 2019; Zhang et al., 2021). Both configurations facilitate gas flow within the cyclone. AGCs, as well as conventional gas cyclones, are widely employed in industrial applications to achieve high separation efficiency with minimal cost. Additionally, axial gas cyclones can be further classified into subcategories such as one-through gas cyclones, uniflow separators, and swirl flow separators (Austrheim, 2006). Compared to axial gas cyclones, these variants are generally smaller in size. While certain designs can reduce pressure drop, they often result in lower collection efficiency compared to axial gas cyclones (Austrheim, 2006; Deng et al., 2020). Notably, in AGCs, both gas flow and solid particles follow the same trajectory (Hsiao et al., 2011; Li et al., 2020), and the outlet for both the duty gas and clean gas is located at the same end. Extensive research has been conducted on the operation, design, and optimization of axial gas cyclones (Li et al., 2023; Elsayed and Lacor, 2010). Studies have focused on improving AGC performance by investigating geometric parameters, including the shape of guide vanes (Austrheim, 2006; Brar and Elsayed, 2018), the separator body (Elsayed et al., 2020; Brar and Elsayed, 2017), and the dimensions of the outlet tube (Brar et al., 2015). Ogawa et al. (1997) conducted both experimental and numerical studies on axial gas cyclones, evaluating axial velocity, tangential velocity, pressure drop, and cut-off diameter. However, their simulations exhibited slight deviations, particularly in total collection efficiency. In an effort to enhance AGC performance, Hsu et al. (2005) designed a novel guide vane for an axial separator dust collector operating under low-pressure conditions. Furthermore, they introduced three outlet tubes in an axial gas cyclone to compare AGC performance with conventional gas cyclones. Their findings indicated that a funnel-shaped outlet tube could enhance AGC performance, although pressure drop did not exhibit a direct correlation with funnel diameter. Similarly, Hsiao et al. (2011) investigated various geometric modifications, such as vortex finder length and an inverted cup structure, to predict AGC performance relative to conventional gas cyclones. Their results demonstrated that incorporating an inverted cup in AGCs could improve collection efficiency while reducing pressure drop. Further optimizations have been explored by Xiong et al. (2014), who analyzed the shape of the vortex finder, revealing that incorporating a helical gap and a reflex cone could enhance collection efficiency. Zhang et al. (2021) proposed a novel approach for determining the empirical constant introduced by Hsu et al. (2005), achieving strong agreement with experimental data. Additionally, Huang et

al. (2018) numerically examined the influence of geometric parameters on AGC performance. Their findings indicated that the torsion angle and exit angle of the vanes significantly impact both pressure drop and collection efficiency. Moreover, they investigated body diameter variations to determine the relationship between axial and tangential velocity and pressure drop. Gopalakrishnan et al. conducted numerical studies on pressure drop and collection efficiency in axial gas cyclones with axial inlets. They examined the influence of guide vane configurations on AGC performance, identifying that the number and angle of blades play a crucial role in enhancing collection efficiency. In this study, a simulation-based approach is employed to investigate the complex physical flow within an axial gas cyclone with high accuracy. Initially, the continuity phase is simulated using the k-ε turbulence model to establish preliminary convergence. Once all equations converge, the Reynolds Stress Model (RSM) is selected due to its capability of capturing detailed flow behavior within the gas cyclone, despite its relatively slow convergence compared to other turbulence models. Furthermore, the one-way coupling method is utilized to track suspended particles inside the axial gas cyclone. This study also examines the flow pattern and performance of gas cyclones, emphasizing the impact of wall roughness and erosion phenomena. Notably, the guide vanes, a crucial component of axial gas cyclones, play a significant role in enhancing collection efficiency.This revision improves the clarity, formality, and coherence of the text, making it more suitable for a scientific article. Recent works have emphasized the role of surface treatments and material engineering in enhancing cyclone performance. For instance, Li et al. (2024) demonstrated that surface coatings significantly influence wall erosion and flow stability. Similarly, Rahimi and Singh (2025) introduced a geometry-based optimization approach to improve both separation efficiency and mechanical durability in axial gas cyclones.

2. Governing Equations

2.1. Turbulent Model

Previous studies on gas cyclones have demonstrated that selecting an appropriate turbulence model is crucial for achieving high accuracy, as the airflow into gas cyclones exhibits significant swirl and strain. This suggests that the RSM model is more effective than the two-stage model (Dehdarinejad et al., 2023; Babaoğlu et al., 2021; Elsayed et al., 2020).

$$\frac{\partial \overline{u_i}}{\partial x_i} = 0 \tag{1}$$

$$\frac{\partial \overline{u_i}}{\partial t} + \overline{u_j}\frac{\partial \overline{u_i}}{\partial x_j} = -\frac{1}{\rho}\frac{\partial \overline{P}}{\partial x_i} + \nu\frac{\partial^2 \overline{u_i}}{\partial x_i \partial x_j} - \frac{\partial}{\partial x_j}R_{ij} \tag{2}$$

Where $\overline{u_i}$ is the mean velocity vector, xi is the position vector, $\overline{P}$ is the mean pressure, ρ is the gas density, ν is the gas kinematic velocity, and $R_{ij} = \overline{u_i' u_j'}$ is the Reynolds stress tensor. Here $u_i' = u_i - \overline{u_j}$ is the ith fluctuating velocity component. The RSM turbulence model provides the transport equations for the evaluation of turbulence stresses. That is,

$$\frac{\partial}{\partial t}R_{ij} + \overline{u_k}\frac{\partial}{\partial x_k}R_{ij} = \frac{\partial}{\partial x_k}\left(\frac{\nu_t}{\sigma^k}\frac{\partial}{\partial x_k}R_{ij}\right) + \left[R_{ik}\frac{\partial \overline{u_j}}{\partial x_i} + R_{jk}\frac{\partial \overline{u_i}}{\partial x_k}\right] - C_1\frac{\varepsilon}{k}\left[R_{ij} - \frac{2}{3}\delta_{ij}K\right] - C_2\left[P_{ij} - \frac{2}{3}\delta_{ij}P\right] - \frac{2}{3}\delta_{ij}\varepsilon \tag{3}$$

Where the turbulence production term P_{ij} is given as,

$$P_{ij} = -\left[R_{ik}\frac{\partial \overline{u_j}}{\partial x_k} + R_{jk}\frac{\partial \overline{u_i}}{\partial x_k}\right], \quad P = \frac{1}{2}P_{ij} \tag{4}$$

Here P stands for the fluctuating kinetic energy production, ν_t stands for the turbulence (eddy) kinematic viscosity, and the empirical constants are $\sigma^k = 1, C_1 = 1.8, C_2 = 0.8$. The transport equation for the turbulence dissipation rate, ε, is given as,

$$\frac{\partial \varepsilon}{\partial t} + \overline{u_j}\frac{\partial \varepsilon}{\partial x_j} = \frac{\partial}{\partial x_j}\left[\left(\nu + \frac{\nu_t}{\sigma^\varepsilon}\right)\frac{\partial \varepsilon}{\partial x_j}\right] - C^{\varepsilon 1}\frac{\varepsilon}{K}R_{ij}\frac{\partial \overline{u_i}}{\partial x_j} - C^{\varepsilon 2}\frac{\varepsilon^2}{K} \tag{5}$$

where $K = \frac{1}{2}\overline{u_i' u_j'}$ is the fluctuating kinetic energy. The values of constants are $\sigma^{\varepsilon} = 1.3$, $\sigma^{\varepsilon 1} = 1.44$, $\sigma^{\varepsilon 2} = 1.92$.

2.2. Surface Roughness Model (SRM)

The factor that affects the airflow resistance and the momentum transmission is the wall roughness of the cyclone. The law of the wall velocity profile near a rough surface is given by (Kaya et al., 2011).

$$\frac{\bar{u}}{u^*} = \frac{1}{k}\ln\left(\frac{yu^*}{\nu}\right) + B - \Delta B\left(k_S^+\right) \quad (6)$$

Where $\bar{u}_i$ is the mean velocity, y is the distance from the wall, u^* the friction velocity, v is the kinematic viscosity, and k_s^+ is the non-dimensional surface roughness height. In Equation (6) $k = 0.41$ is the von Karman constant, and B is an empirical constant for smooth walls. The friction velocity is defined by:

$$u^* = \left(\frac{\tau_w}{\rho}\right)^{0.5} \quad (7)$$

Where τ_w is the wall shear stress and ρ is the fluid density. The roughness function, ΔB, depends on the dimensionless surface roughness, k_s^+, which is calculated as,

$$k_S^+ = \frac{k_s u^*}{\nu} \quad (8)$$

In the case of hydro-dynamically smooth flows with $k_s^+ < 2.25$ the roughness function $\Delta B = 0$ The roughness function is given as,

$$\Delta B = \frac{1}{k}\ln\left(1 + C_s k_s^+\right) \quad (9)$$

If the flow is in a fully rough regime ($k_s^+ > 90$),

$$\Delta B = \frac{1}{k}\ln\left(\left(k_S^+ - 2.25\right)/87.75 + C_S k_S^+\right) \times \sin\left[0.4258\ln\left(k_s^+ - 0.811\right)\right] \quad (10)$$

Otherwise, the values of $B = 5.56$ and $C_S = 0.5$ are used.

2.3. Discrete Phase Modeling (DPM)

To simulate solid particles in gas cyclones, the solid particles are used in gas cyclone to name discrete phase modeling (DPM) (Liu et al., 2022). So, the interaction of particles was neglected, which would satisfy the statistical model of Euler-Lagrangian. According to Newton's second law, in Lagrangian model can obtain the particle trajectories. All particles are spherical and the gravity and drag force are extracted from the calculation. Therefore, the equation of movement of particles is written as:

$$\frac{d\vec{u}_p}{dt} = \frac{\vec{u} - \vec{u}_p}{\tau_r} + \frac{\vec{g}\left(\rho_p - \rho\right)}{\rho_p} \quad (11)$$

Particle relaxation time τ_r is written as:

$$\tau_r = \frac{\rho_p d_p^2}{18\mu}\frac{24}{\mathrm{Re}C_D} \quad (12)$$

Where $\overrightarrow{u_p}$ is the particle velocity, $\vec{u}$ is the gas velocity, d_p is particle diameter, ρ_p is the density of the particle, and relative Reynolds is defined as :

$$\mathrm{Re} = \frac{\rho_p d_p \left|\overrightarrow{u_p} - \vec{u}\right|}{\mu} \quad (13)$$

The drag coefficient, C_D for spherical solid particles can be written as :

$$C_D = a_1 + \frac{a_2}{\mathrm{Re}} + \frac{a_3}{\mathrm{Re}^2} \quad (14)$$

Where a_1, a_2, and a_3 are constant that employ several different range of Re given by Morsi and Alexander (Morsi and Alexander, 1972).

2.4. Model of Erosion

Erosion on cyclone walls owing to solid particle impact that was developed by Oka et al. (2005) is employed here to predict erosion rate on walls inside gas cyclones.

$$E_R = \sum_{n=1}^{N_P}\frac{E^{(i)}}{A_{face}^{\ i}} \quad (15)$$

Where E_R is the removed mass flux (kg/m²s). To

obtain the erosion rate (kg/s), E_R is integrated over the total area of the cyclone. In Equation (15) erosion rate, $E^{(i)}$, is determined by:

$$E^{(i)} = 1\times10^{-9} E_V \rho_w \dot{m}_P$$
$$E_V = f(a) E_{90} \quad (16)$$
$$E_{90} = L(H_v)^{k_1}\left(\frac{V_P^{(i)}}{V'}\right)^{k_2}\left(\frac{d_P}{d'}\right)^{k_3}$$

where E_V is volumetric erosion, ρ_w is wall density, $\dot{m}_p$ is mass flow rate of particle, H_v is Vickers hardness, V_P is particle impact velocity, V' is velocity fluctuation, d' is standard diameter, L and k are constant, and $f(\alpha)$ is a function of the impact angle that is given by:

$$f(a) = (\sin a)^{n_1}\left[1 + H_v(1-\sin a)\right]^{n_2} \quad (17)$$

The coefficients of Equations (16) and (17) are presented in (Table 1).

Table 1: Oka Erosion Model Coefficient

n_1	n_2	$H_V(GP)$	L	a	b
0.62	5.68	0.4	65	0.109	1.58
k_1	k_2	k_3	$V'(m/s)$	$d'(\mu m)$	
-0.12	2.22	0.19	104	326	

3. Solver Setting

3.1. Numerical Schemes

In this study, the numerical outlines for the gas stream were extracted by Karagoz and Kaya (2007). They studied the achievement of varied discretization outlines to select the best way to be more accurate in high swirls in the simulation of gas cyclones. (Table 2) shows the best setting, which is used in current work. One of the more accurate outlines was the PRESTO pressure interpolation. To couple velocity and Pressure, the SIMPELC is applied in the simulation of the airflow inside an axial gas cyclone and the numerical result is close to experimental results. Many researchers highly recommended that the QUICK scheme should be employed for momentum equations. The second order upwind outline was selected for the turbulent dissipation rate and turbulent kinetic energy. Also, the first order upwind was determined by the Reynolds stress.

Table 2: Detail of Numerical Schemes for the Present Study

Numerical setting	Scheme
Pressure discretization	PRESTO!
Pressure velocity couple	SIMPLEC
Momentum discretization	QUICK
Turbulent kinetic energy	Second Order Upwind
Turbulent dissipation rate	Second Order Upwind
Reynolds Stress	First Order Upwind

3.2. Geometry & Boundary Condition

Here, three boundary conditions are used to simulate two-phase flow inside an axial gas cyclone: inlet velocity, outlet, and walls. Airflow is incompressible and isothermal and moves 300 m^3/h uniformly. Solid particles inject independently and are carried by a gas flow. The physical characteristics of particles are followed by the concentration and the density of 300 mg/m^3 and 2710 kg/m^3 respectively. The boundary condition of "reflect" is chosen at all walls of the cylindrical part. Moreover, all walls of axial gas cyclone and collision between solid particles are supposed to be utterly elastic ($\epsilon = 1$) (Gimbun et al., 2005). Also, the boundary condition of " Trap " is chosen at the bottom of the conical part, where all trajectory calculations are completed and the destiny of particles are made according to "Trapping". Furthermore, the exit tube called the vortex finder chooses the outlet, where solid particles can easily escape and the end can calculate collection efficiency and cut of size diameter.

3.3. Grid Generation

In the present investigation, gas-particle flow is injected inside a usual axial gas cyclone. In general, the process of separation is related to centrifugal force, namely fine particles separate from coarse particles. Coarse particles move to walls owing to their density more than fine particles and these particles with the help of the gas boundary layer and gravity acceleration slide along the wall to reach the dustbin and trap, however, fine particles with the assistance of lift force escape through the exit tube. (Figure 1) shows different sections of the axial gas cyclone.

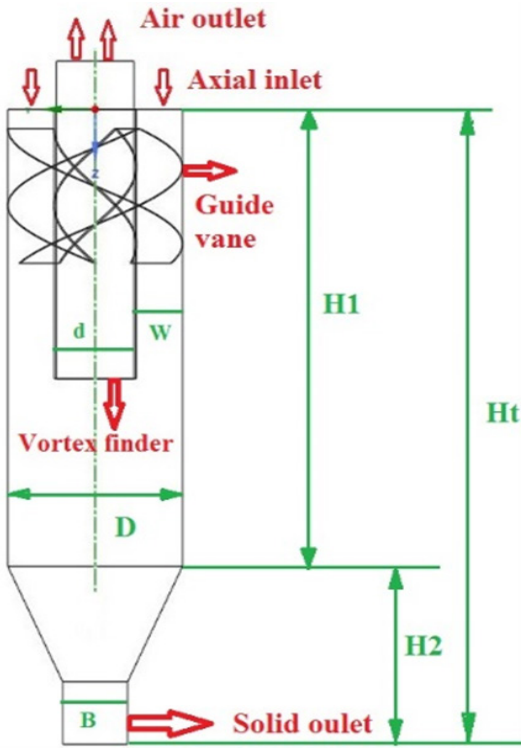

Figure 1. Different Components of the Axial Gas Cyclone

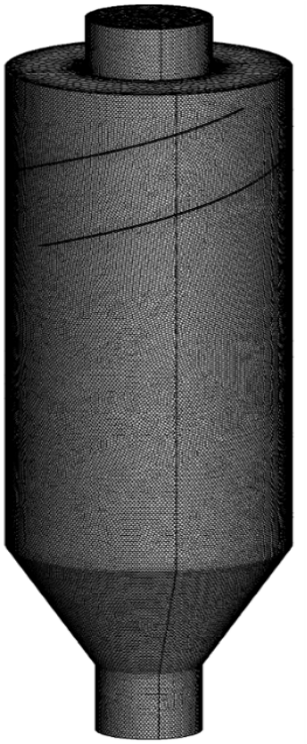

Figure 2. Structure of the Grids Generated and Used in this Simulation

Before simulation, meshes are the most significant factor that should be located in the suitable placement of the computational domain. In current numerical simulations, octagonal grids were generated the full domain of axial gas cyclone. (Figure 2) illustrates the shape of the generated grids that are employed in this simulation. For the current axial gas cyclone, the grid independence is investigated by comparing the results of different numbers of cells. (Table 3) shows the variation of cut of size diameter and pressure drop alongside the number of various grids. By comparing their percentage, the best grid was obtained to follow the rest of the simulations.

Table 3: Details of Grid Independence

Cell	Pressure Drop (Pa)	Cut Diameter (micron)
827932	498250	0.5
956657	496496	0.6
1234456	497765	0.5
Error %	5.4	1.4

3.4. Validation

In order to validate the present section, the numerical results are first compared with experimental data (Morsi and Alexander, 1972). The numerical results show that with an increase in

velocity for the continuous phase, the air-gas flow inside the axial cyclone experiences an increase in pressure drop. This indicates that this type of cyclone, similar to other gas cyclones, is highly dependent on the velocity or volumetric flow rate of the gas. For the discrete phase, particles ranging from 1 to 40 microns are injected, and the cyclone efficiency is calculated as the ratio of the number of particles released from the cyclone to the total number of particles injected. The results show that as the mass density of the injected particles increases, the efficiency of the cyclone increases, and more particles, compared to smaller ones, are trapped. This is illustrated in (Figure 3).

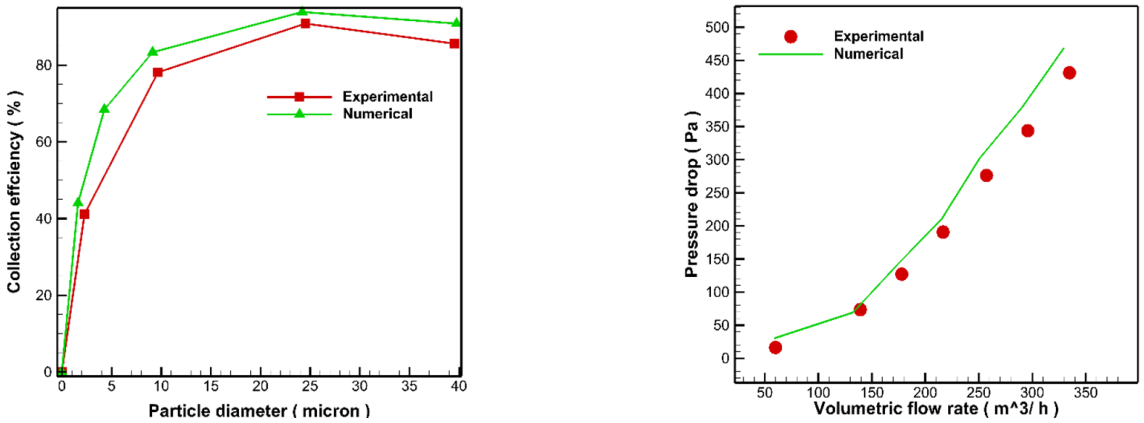

Figure 3. Validation of the Present Problem

For validation in the particle erosion section, which is a very important part of the simulation, data from Vera (Oka et al., 2005) for a 90-degree elbow, based on the Okafor model, have been simulated. The numerical results for particle sizes of 150 microns and 300 microns at different velocities, with averaging over the surface of the 90-degree elbow, have been evaluated and are shown in (Figure 4). The graph illustrates the relationship between inlet velocity and maximum erosion rate for two particle sizes (150 µm and 300 µm), based on both experimental and numerical data. As shown, the erosion rate increases with inlet velocity for both particle sizes, with the 300 µm particles exhibiting significantly higher erosion rates compared to the 150 µm particles. Furthermore, the numerical results align well with the experimental data, demonstrating the reliability of the simulation model in predicting erosion behavior under varying flow conditions.

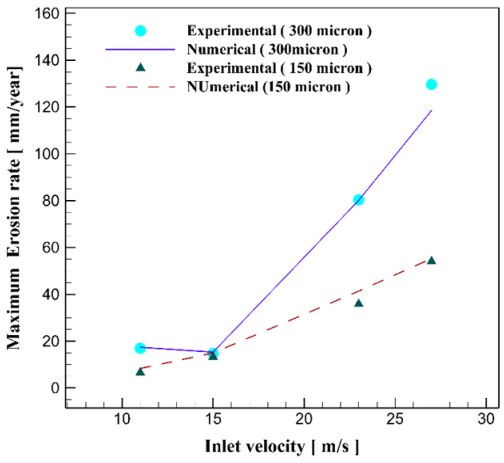

Figure 4. Validation of the Particle Erosion Section in a 90-Degree Elbow

As shown in (Figure 5), the highest erosion occurs at the critical angle, approximately 45 degrees, of the 90-degree elbow. The reason for this increase in particle erosion on the 90-degree elbow is that the farther the particles are from the center of curvature, the higher their acceleration and angular velocity. Consequently, the centrifugal force increases, leading to more frequent contact of the particles with the wall, especially at the 45-degree angle, which experiences the highest erosion.

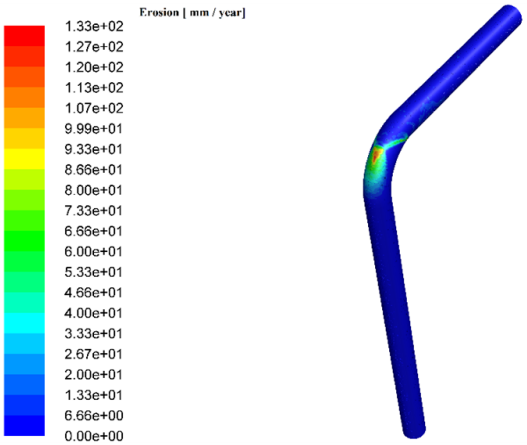

Figure 5. Particle Erosion Behavior in a 90-Degree Elbow

4. Results

4.1. Pressure Drop

When gas enters a cyclone, it forms a boundary layer along the inner wall due to rotational motion. This interaction between the gas and wall surface is the primary source of pressure loss. (Figure 6) shows that wall roughness influences this boundary layer by reducing momentum near the walls, thereby decreasing the pressure drop. As shown in (Figure 7), higher surface roughness consistently lowers the pressure differential between the inlet and outlet.

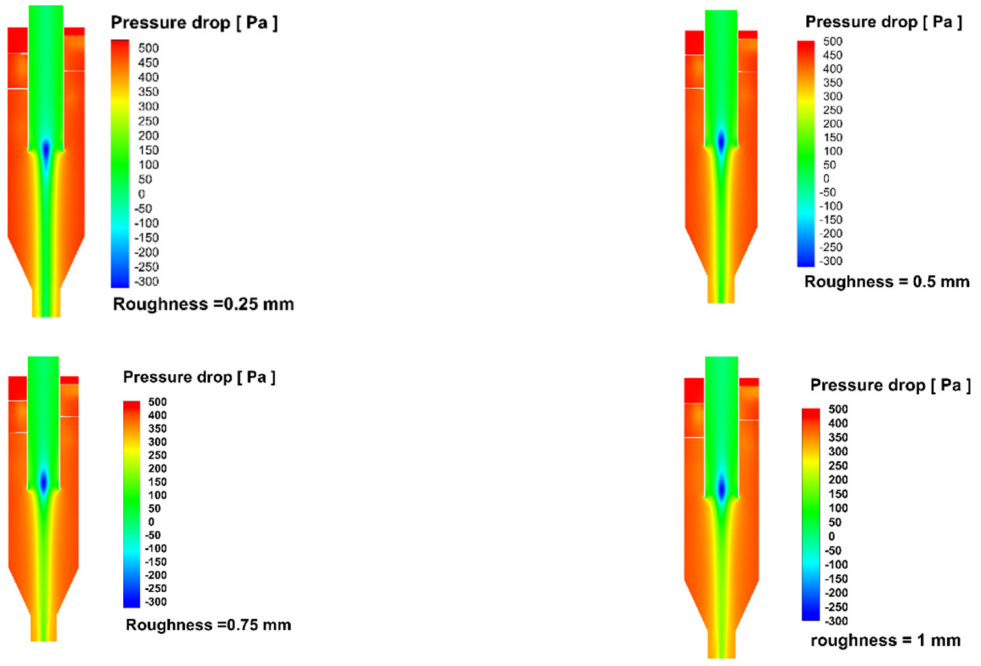

Figure 6. Pressure Drop Contours with Different Roughness at a Volumetric Flow Rate of 58.95 m²/s

This effect is particularly valuable in energy-sensitive applications where minimizing pressure loss is critical. In this section, we focus solely on the aerodynamic implications of surface texture, while its influence on efficiency and erosion is discussed in relevant sections.

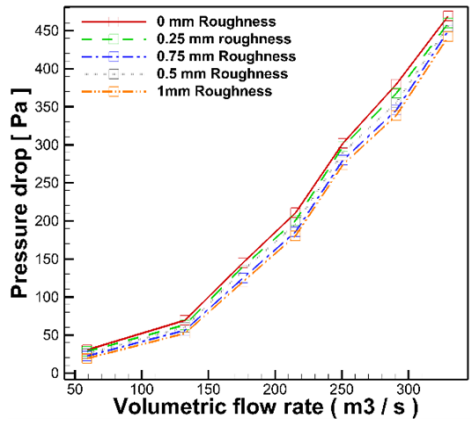

Figure 7. Effects of Varying Volumetric Flow Rate Under Different Roughness Conditions on Pressure Drop

4.2. Tangential Velocity

In general, internal flows in pipes or cyclonic flows, once the fluid flow transitions from laminar and transitional to turbulent flow, their velocity profiles within the pipe or gas cyclones no longer change, and they continue their path with essentially constant velocity. In the gas flow inside gas cyclones, the hydrodynamic flow behaves such that the flow, using either the tangential or axial channel, gains initial acceleration through centrifugal force, causing the flow to adopt a sweeping and tangential pattern along the walls. In fluids, there are generally two types of vortices that are important in internal flows. The primary vortex is a free vortex that usually forms along the walls. However, as the flow approaches the cyclone wall, the intensity of the gas's rotational flow decreases. This is primarily due to the gas boundary layer at the wall, where the viscous forces dominate over the diffusion forces, reducing and dissipating the fluid momentum. As a result, due to the no-slip condition at the cyclone walls, the velocity tends to approach zero, and the relationship can be expressed as follows:

$$V_t = \frac{C}{r} \tag{18}$$

However, in a forced vortex, due to the high rotation of the flow, the diffusion forces are able to overcome the viscous forces of the fluid. The relationship is linear, and the tangential velocity increases from the center of the cyclone toward the direction of the exit pipe. However, after reaching a maximum point, this value starts to decrease. The relationship for the free vortex is expressed as follows:

$$V_t = Cr \tag{19}$$

By combining both the forced vortex and the free vortex, a region is formed, which is referred to as the Rankine vortex. This is shown in (Figure 8).

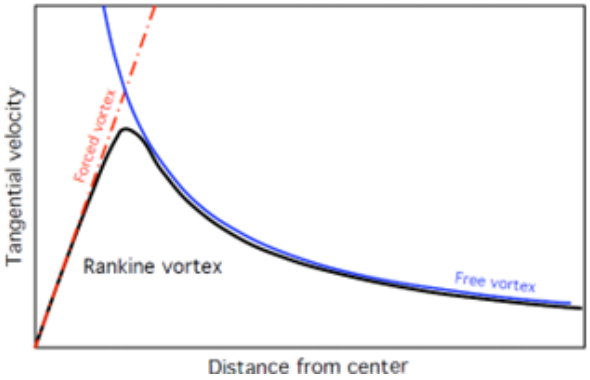

Figure 8. Introduction of Vortex Regions in Tangential Velocity

Considering the introduction of the hydrodynamic structure of tangential velocity in gas cyclones and inside pipes, this section discusses and examines the effects of wall roughness, which is crucial in the design, maintenance, and installation of gas cyclones. To investigate the effects of local roughness and observe the changes in tangential velocity along the radial direction, the entire computational domain of the axial gas cyclone is defined with four lines, as shown in the (Table 4).

Table 4: Radial Positions in the Axial Cyclone Relative to the Coordinate System Center

Z_1	Z_2	Z_3	Z_4
0 [mm]	33 [mm]	66 [mm]	99 [mm]

As shown in (Figure 9), the tangential velocities exhibit an M-shaped distribution, indicating the effects of different wall roughness conditions. It can be observed that the tangential velocity decreases with increasing wall roughness. This decrease is due to the reduction in fluid momentum and its impact on the formation of small eddies near the wall, which in turn affects the larger eddies in the center of the axial gas cyclone. As seen, with increased wall roughness, the maximum tangential velocity, represented by the peaks in each of the graphs, decreases at specific positions. This reduction hinders the centrifugal force generated by the tangential velocity from effectively transferring or pushing the particles toward the cyclone wall, thereby disrupting the separation process. As a result, the efficiency of axial gas cyclones decreases with increased wall roughness. It is worth mentioning that the most critical section of a gas cyclone is the cylindrical section, as this is where the separation process primarily occurs, assuming there are no inhibiting factors. The conical section, on the other hand, plays a role in providing gravitational acceleration, which pushes the particles toward the lower section for accumulation.

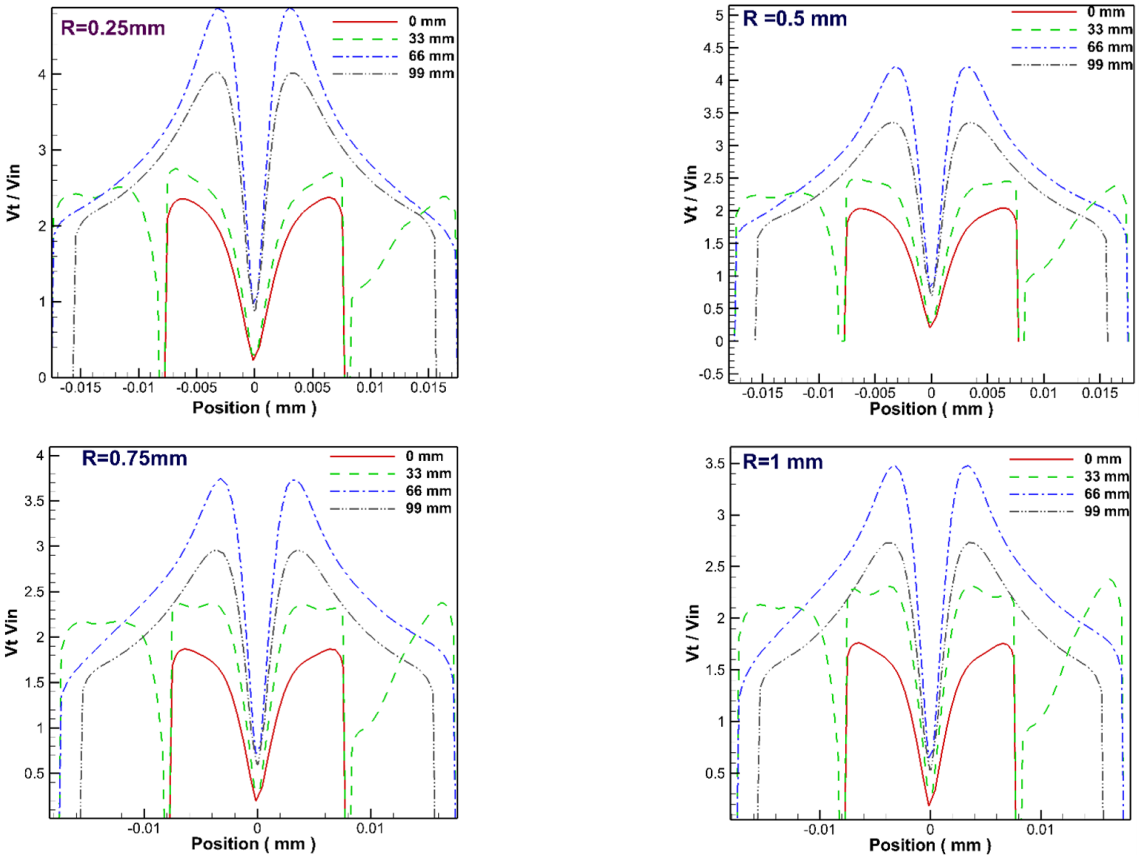

Figure 9. Radial Distribution of Tangential Velocity with Different Roughness Conditions

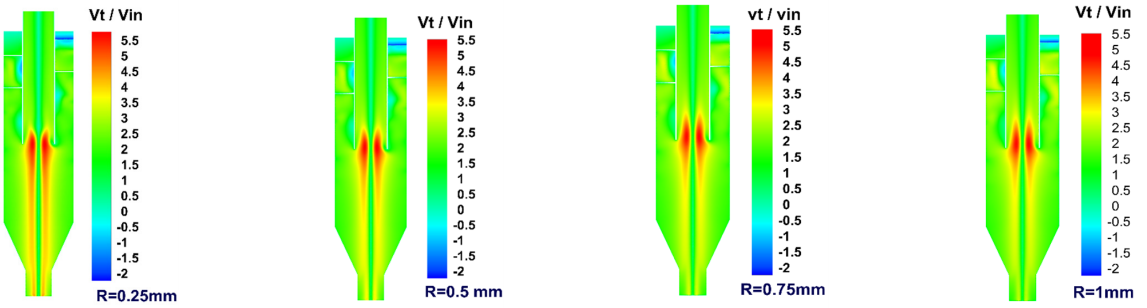

Figure 10. Contours of Tangential Velocity at X=1 with a Velocity of 3.56 m^2/s

As observed from the contours of tangential velocity shown in (Figure 10), the velocity increases in the baffle area due to the turbulence generated in the fluid. However, the roughness has a negative effect on the velocity in this region. On the other hand, the highest tangential velocity is found at the inlet of the exit pipe, as the flow undergoes a converging state, and the diameter of the exit pipe becomes smaller compared to the cyclone diameter, which leads to an increase in tangential velocity in this area. Up to this point, we have discussed the average tangential velocity, which plays a crucial role in the performance of the cyclone. However, in this section, the turbulent kinetic energy, which is related to the oscillatory velocities that lead to the transfer of momentum to the particles, will be discussed. As observed in (Figure 11), turbulent kinetic energy is directly related to the oscillatory velocities, as shown in Equation (20).

$$k = \frac{1}{2}\overline{u_i \acute{u}_j} \tag{20}$$

In (Figure 11), it can be observed that the location with the highest local velocity triggers oscillatory velocities in the turbulent gas flow, which in turn transfers additional momentum to the particles. As seen, at the inlet of the exit pipe, where the velocity is highest, the local turbulent kinetic energy is greater in this region compared to other areas. Therefore, with an increase in roughness, the momentum decreases, resulting in an inverse effect on the turbulent kinetic energy, which leads to the scattering of particles.

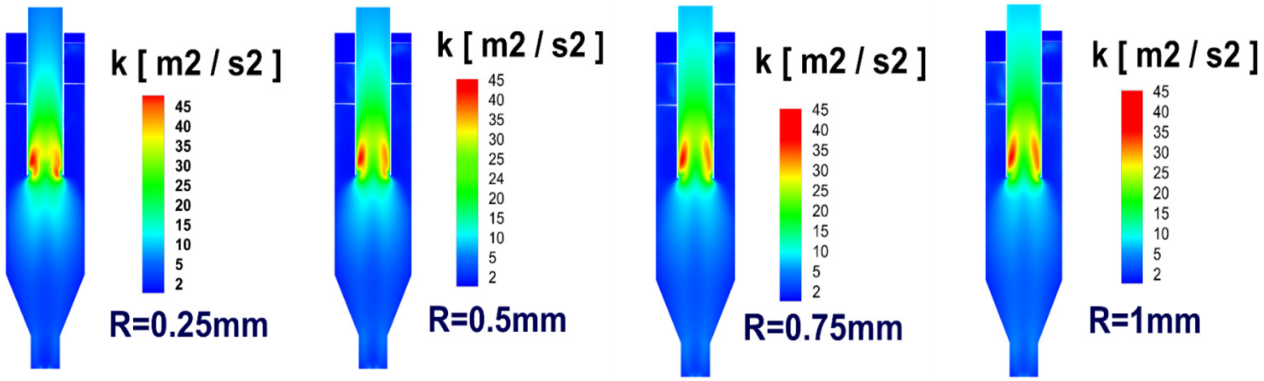

Figure 11. Contours of Turbulent Kinetic Energy with Different Roughness Conditions at an Inlet Velocity of 3.56 m/s at Position X=1

4.3. Axial Velocity

Particles vertically within the cyclone. It consists of two primary components: the downward axial flow, which carries gas and larger particles toward the conical section, and the upward flow through the central vortex, which guides finer particles toward the exhaust. Wall roughness influences axial velocity by altering near-wall momentum, particularly in the downward region where heavier particles tend to accumulate. Increased roughness reduces axial velocity near the walls due to added resistance, weakening the downward transport of coarse particles and potentially increasing their residence time. While the upward core flow is less directly impacted, the reduced tangential momentum and altered vortex strength (linked to roughness effects discussed in earlier sections) can disrupt the coherence of the upward flow as well. This, in turn, affects the evacuation of fine particles through the outlet. As shown in velocity contours (Figure 13), rougher walls lead to a noticeable decrease in axial flow near boundaries while maintaining relatively higher velocity in the vortex finder due to geometric convergence.

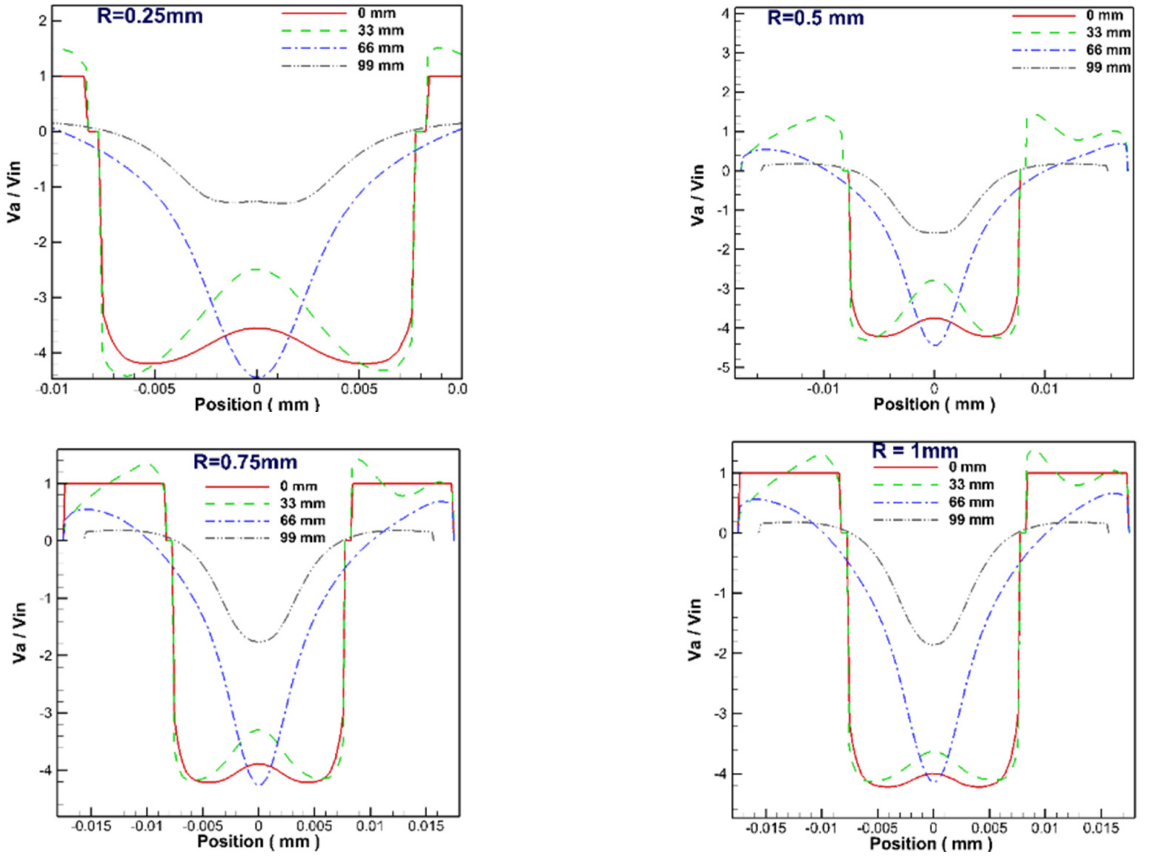

Figure 12. Radial Positions of Axial Velocity

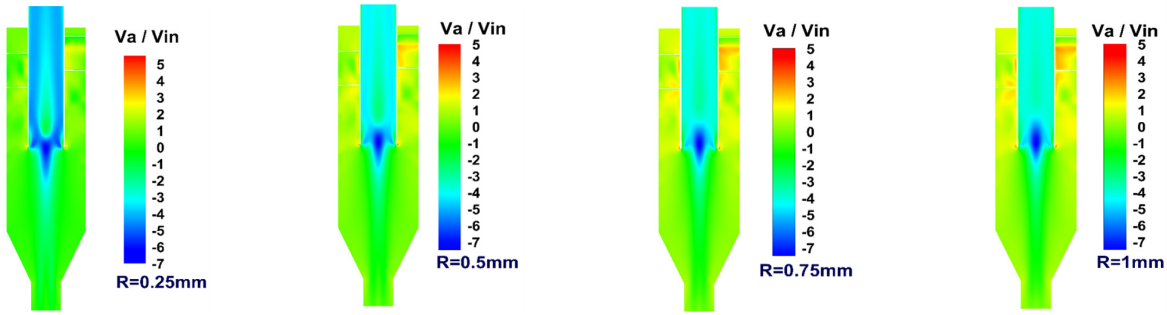

Figure 13. Axial Velocity Contours with Different Roughness Conditions at a Velocity of 3.56 m/s (X=1)

Overall, while axial velocity is not as dominant as tangential velocity in particle separation, its modulation by wall roughness significantly impacts flow stability, particle movement paths, and the balance between downward settling and upward escape, thereby influencing cyclone performance.

4.4. Efficiency of Axial Gas Cyclone

In general, for two-phase gas and particle flows in gas cyclones, the particle efficiency is obtained using the following relation:

$$\eta = \left(1 - \frac{n_{out}}{n_{total}}\right) \times 100 \quad (21)$$

In the above relation, n_{out} represents the number of particles exiting the gas cyclone, and n_{total} represents the total number of particles injected. The inlet velocity and even the configuration of the channel ends, gas inlet, and other geometric parameters such as cyclone diameter and inlet curvature angle are

interdependent in gas cyclones. Additionally, the particle material and even the material of the gas cyclone itself influence the cyclone's efficiency. Based on the hydrodynamic explanations provided in the sections on axial and tangential velocity, it can be observed that the effects of surface roughness and inlet velocity significantly influence this cyclone parameter, which is crucial in its design. Therefore, considering the results obtained from the effects of cyclone wall roughness along with variations in inlet velocity, as shown in (Figure 14), it can be concluded that increasing the inlet velocity improves the efficiency of the gas cyclone. As the inlet velocity increases, the tangential velocity and, consequently, the centrifugal force also increase, leading to higher efficiency and a reduction in the residence time of particles. This demonstrates that even the residence time of particles, which is related to their leakage, impacts the cyclone efficiency parameter.

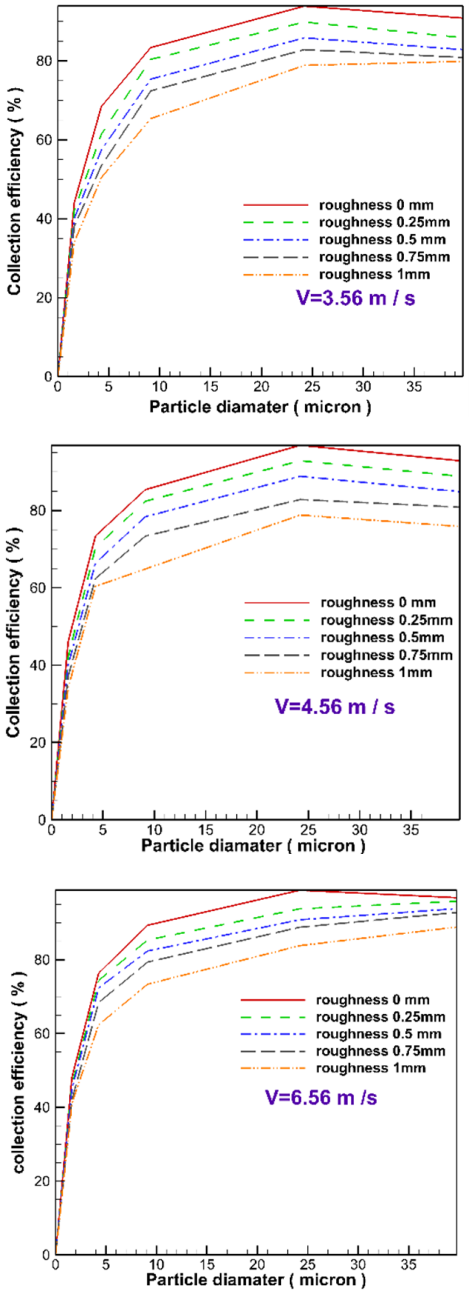

Figure 14. Efficiency of the Axial Gas Cyclone under Different Roughness Conditions with Varying Inlet velocities

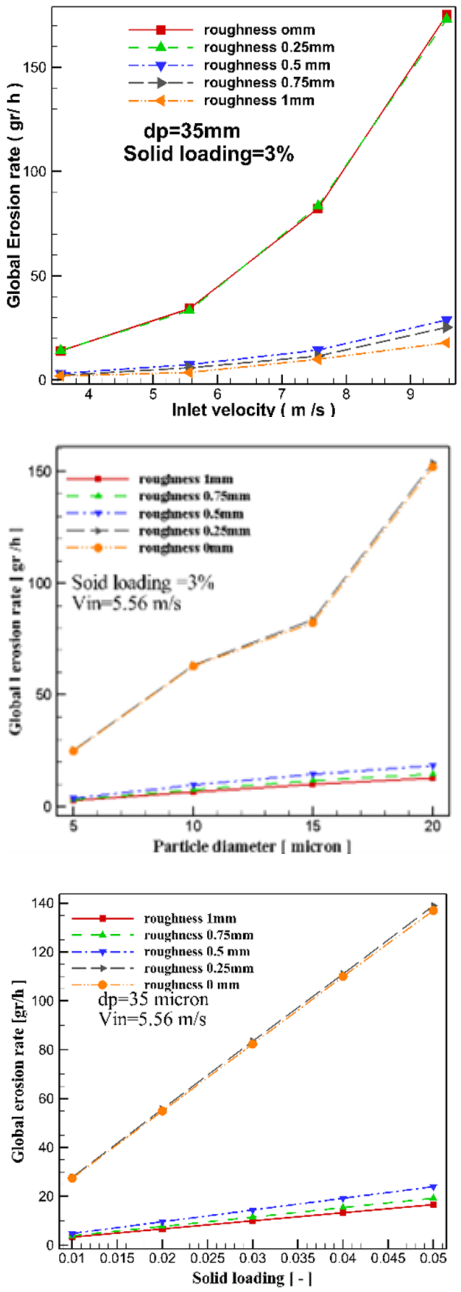

Figure 15. Effects of Different Hydrodynamic Conditions with Applied Wall Roughness on Gas Cyclone Wall Erosion

4.5. Gas Cyclone Wall Erosion

Wall erosion in gas cyclones is a critical durability concern, primarily caused by repeated impacts of solid particles on internal surfaces, particularly in high-velocity zones and at sharp directional changes in the flow. The erosion intensity depends on several factors, including particle size and concentration, gas velocity, impact angle, and the material properties of the cyclone wall. In this study, erosion is modeled using the Oka et al. (2005) approach to quantify material loss over time, with a specific focus on how wall roughness alters erosion behavior.

As demonstrated in (Figures 15 and 16), increased wall roughness leads to a measurable reduction in erosion rate. This occurs because rough surfaces disrupt high-speed particle trajectories, decreasing the frequency and severity of direct impacts—especially in critical regions such as the cone tip, where particle convergence is highest due to the flow's spiral and gravitational patterns. While high inlet velocities and large particle sizes still contribute to some degree of erosion, rough walls tend to diffuse particle motion and reduce radial pressure buildup near the surface, which collectively lowers localized stress. Moreover, the reduction in tangential and axial velocities observed in roughened configurations (as previously discussed) also translates to lower kinetic energy transfer during collisions, thereby enhancing mechanical durability. Although roughness may slightly compromise separation efficiency, its benefits in prolonging cyclone lifespan—by mitigating wall thinning and structural fatigue—make it a key factor in long-term cyclone design optimization. This trade-off underscores the importance of balancing aerodynamic performance with physical wear resistance when evaluating modifications such as surface treatments, coatings, or structural reinforcements in industrial cyclone applications.

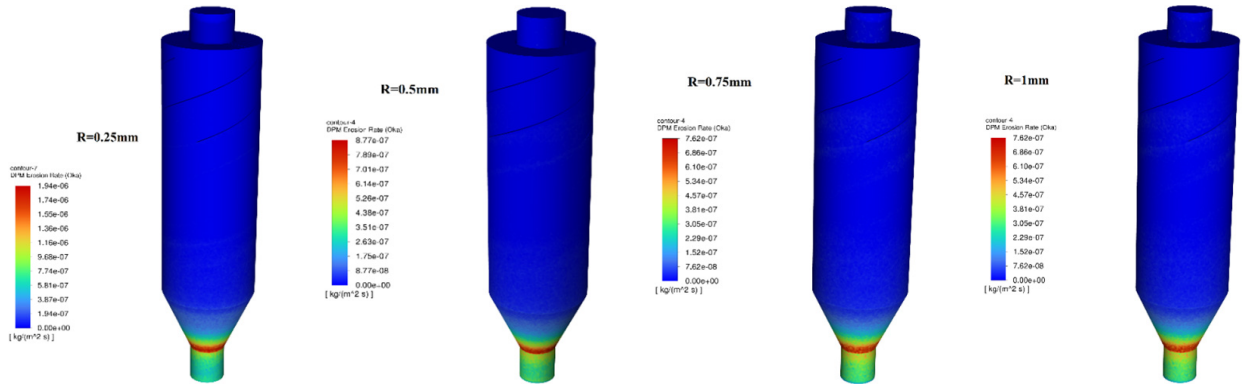

Figure 16. 3D Contours of Particle Erosion Rate at a Velocity of 3.56 m/s

To further validate the findings of this study, a comparison with relevant recent research is provided in (Table 5) The comparative analysis focuses on pressure drop, separation efficiency, and wall erosion behavior under varying wall roughness conditions and operating parameters.

Table 5: Comparison this Study with Other Studies

Study	Year	Focus	Pressure Drop	Collection Efficiency	Erosion Modeling	Notable Features
This study	2025	Axial cyclone with wall roughness	↓ 9% (with increased roughness)	↓ up to 12% (for >25 µm)	Included	Full CFD + RSM + erosion + DPM
Li et al.	2023	Outlet tube optimization	↓ 6%	↑ 5-8%	Not included	Geometric tuning only
Babaoğlu et al.	2023	Geometry + acoustic control	Not reported	↑ 10%	Not included	Focus on noise & shape
Foroozesh et al.	2021	Surface roughness impact	↓ 8%	↓ 10%	Included	Similar setup, limited velocity range
Kumar & Hassanpour	2024	Review on wall erosion	--	--	Included	Comprehensive review
Rahimi & Singh	2025	Axial cyclone geometry optimization	↓ %7.5	↑ %9-6	Not included	Applied response surface modeling

5. Conclusions

This study presents a comprehensive numerical investigation into the impact of wall roughness on flow behavior, pressure drop, separation efficiency, and erosion rate in axial gas cyclones. Using an integrated modeling approach—combining Reynolds Stress Model (RSM), Discrete Phase Modeling (DPM), and advanced erosion modeling—this work offers a detailed understanding of fluid-particle interactions under various roughness conditions. One of the key innovative aspects of this study is the simultaneous evaluation of aerodynamic performance and mechanical durability, which is often neglected in prior research. While previous works have primarily focused on geometric optimizations or performance metrics in isolation, this research highlights the trade-off between reduced pressure drop (≈9%) and lower separation efficiency (≈12% for particles >25 µm), while also showing a significant reduction in wall erosion (≈15%) due to increased roughness. Unlike many existing studies that do not incorporate erosion modeling or high-resolution turbulence approaches, our work provides a more holistic and realistic perspective on cyclone design. By emphasizing the dual role of wall roughness and validating results against experimental and literature data, this study contributes a valuable framework for optimizing axial cyclone designs. It bridges a critical gap in the literature by addressing not only flow performance but also long-term durability, offering practical insights for industrial applications where both efficiency and equipment lifespan are crucial.

References

Austrheim, T. (2006). Experimental characterization of high-pressure natural gas scrubbers, PhD thesis, University of Bergen.

Brar, L. S., Sharma, R. P., & Elsayed, K., 2015. The effect of the cyclone length on the performance of Stairmand high-efficiency cyclone. Powder Technology, 286, 668-677. https://doi.org/10.1016/j.powtec.2015.09.003.

Brar, L. S., & Elsayed, K., 2017. Analysis and optimization of multi-inlet gas cyclones using large eddy simulation and artificial neural network. Powder Technology, 311, 465-483. https://doi.org/10.1016/j.powtec.2017.02.004.

Brar, L. S., & Elsayed, K., 2018. Analysis and optimization of cyclone separators with eccentric vortex finders using large eddy simulation and artificial neural network. Separation and Purification Technology, 207, 269-283. https://doi.org/10.1016/j.seppur.2018.06.013

Babaoğlu, N. U., Parvaz, F., Hosseini, S. H., Elsayed, K., & Ahmadi, G., 2021. Influence of the inlet cross-sectional shape on the performance of a multi-inlet gas cyclone. Powder Technology, 384, 82-99. https://doi.org/10.1016/j.powtec.2021.02.008

Babaoğlu, N. U., Parvaz, F., Foroozesh, J., Hosseini, S. H., Ahmadi, G., & Elsayed, K., 2023. Geometry optimization of axial cyclone for high performance and low acoustic noise. Powder Technology, 427, 118738. https://doi.org/ 10.1016/j.powtec.2023.118738

Deng, Y., Yu, B., & Sun, D., 2020. Multi-objective optimization of guide vanes for axial flow cyclone using CFD, SVM, and NSGA II algorithm. Powder Technology, 373, 637-646. https://doi.org/10.1016/j.powtec.2020.06.078

Dehdarinejad, E., Bayareh, M., Parvaz, F., Hosseini, S. H., & Ahmadi, G., 2023. Performance analysis of a gas cyclone with a converging-diverging vortex finder. Chemical Engineering Research and Design, 193, 587-599. https://doi.org/10.1016/j.cherd.2023.04.012

Elsayed, K., & Lacor, C., 2010. Optimization of the cyclone separator geometry for minimum pressure drop using mathematical models and CFD simulations. Chemical Engineering Science, 65(22), 6048-6058. https://doi.org/10.1016/j.ces.2010.08.042

Elsayed, K., Parvaz, F., Hosseini, S. H., & Ahmadi, G., 2020. Influence of the dipleg and dustbin dimensions on performance of gas cyclones: An optimization study. Separation and Purification Technology, 239, 116553. https://doi.org/10.1016/j.seppur.2020.116553

Foroozesh, J., Parvaz, F., Hosseini, S. H., Ahmadi, G., Elsayed, K., & Babaoğlu, N. U., 2021. Computational fluid dynamics study of the impact of surface roughness on cyclone performance and erosion. Powder Technology, 389, 339-354. https://doi.org/10.1016/j.powtec.2021.05.041

Gimbun, J., Chuah, T. G., Choong, T. S., & Fakhru'l-Razi, A., 2005. Prediction of the effects of cone tip diameter on the cyclone performance. Journal of Aerosol Science, 36(8), 1056-1065. https://doi.org/10.1016/j.jaerosci.2004.10.014

Hsiao, T. C., Chen, D., Greenberg, P. S., & Street, K. W., 2011. Effect of geometric configuration on the collection efficiency of axial flow cyclones. Journal of Aerosol Science, 42(2), 78-86. https://doi.org/10.1016/j.jaerosci.2010.11.004

Hsu, Y. D., Chein, H. M., Chen, T. M., & Tsai, C. J., 2005. Axial flow cyclone for segregation and collection of ultrafine particles: theoretical and experimental study. Environmental science & technology, 39(5), 1299-1308. https://doi.org/10.1021/es0491735

Huang, L., Deng, S., Chen, Z., Guan, J., & Chen, M. (2018). Numerical analysis of a novel gas-liquid pre-separation cyclone. Separation and Purification Technology, 194, 470-479. https://doi.org/10.1016/j.seppur.2017.11.050

Karagoz, I., & Kaya, F. (2007). CFD investigation of the flow and heat transfer characteristics in a tangential inlet cyclone. International Communications in Heat and Mass Transfer, 34(9-10), 1119-1126. https://doi.org/10.1016/j.icheatmasstransfer.2007.05.017

Kaya, F., Karagoz, I., & Avci, A. (2011). Effects of

surface roughness on the performance of tangential inlet cyclone separators. Aerosol science and technology, 45(8), 988-995. https://doi.org/10.1080/02786826.2011.574174

Kumar, D., & Hassanpour, A. (2024). Recent advances in cyclone separator modeling: A review on wall roughness and erosion. Powder Technology, 432, 118945. https://doi.org/10.1016/j.powtec.2023.118945

Li, J., Wang, T., Zhang, L., Chang, J., Song, Z., & Ma, C. (2020). Multi-objective optimization of axial-flow-type gas-particle cyclone separator using response surface methodology and computational fluid dynamics. Atmospheric Pollution Research, 11(9), 1487-1499. https://doi.org/10.1016/j.apr.2020.06.002

Li, W., Huang, Z., & Li, G. (2023). Improvement of the cyclone separator performance by the wedge-shaped roof: A multi-objective optimization study. Chemical Engineering Science, 268, 118404. https://doi.org/10.1016/j.ces.2023.118404

Li, M., Zhao, Y., & Chen, W. (2024). A comparative study on the effect of wall surface coatings on erosion in industrial cyclones. Chemical Engineering Journal, 465, 142387. https://doi.org/10.1016/j.cej.2023.142387

Liu, G., Wang, W., Yu, J., & Li, X. (2022). Effect of extra inlets structure on cyclone wall erosion. Powder Technology, 411, 117926. https://doi.org/10.1016/j.powtec.2022.117926

Mao, Y., Pu, W., Zhang, H., Zhang, Q., Song, Z., Chen, K., & Han, D. (2019). Orthogonal experimental design of an axial flow cyclone separator. Chemical Engineering and Processing-Process Intensification, 144, 107645. https://doi.org/10.1016/j.cep.2019.107645

Morsi, S. A. J., & Alexander, A. J. (1972). An investigation of particle trajectories in two-phase flow systems. Journal of Fluid mechanics, 55(2), 193-208. https://doi.org/10.1017/S0022112072001806

Ogawa, A., Iwanami, T., & Shono, H. (1997). Estimation of the collection efficiency of the axial flow cyclone dust collector with the fixed guide vanes. Journal of Thermal Science, 6, 58-65. https://doi.org/10.1007/s11630-997-0017-2

Oka, Y. I., Okamura, K., & Yoshida, T. (2005). Practical estimation of erosion damage caused by solid particle impact: Part 1: Effects of impact parameters on a predictive equation. Wear, 259(1-6), 95-101. https://doi.org/10.1016/j.wear.2005.01.039

Oka, Y. I., & Yoshida, T. (2005). Practical estimation of erosion damage caused by solid particle impact: Part 2: Mechanical properties of materials directly associated with erosion damage. Wear, 259(1-6), 102-109. https://doi.org/10.1016/j.wear.2005.01.040

Parvaz, F., Hosseini, S. H., Ahmadi, G., & Elsayed, K. (2017). Impacts of the vortex finder eccentricity on the flow pattern and performance of a gas cyclone. Separation and Purification Technology, 187, 1-13. https://doi.org/10.1016/j.seppur.2017.06.045

Parvaz, F., Vahedi, S. M., & Khandan, M. (2018). Numerical investigation of the effects of geometry variation on the flow pattern and performance of Gas-Particle cyclones. Iranian Journal of Mechanical Engineering Transactions of ISME, 19(4), 101-122. https://doi.org/10.22060/ijme.2018.14439.5724

Parvaz, F., Rafee, R., & Talebi, F. (2018). Effects of the Outlet Pipe Diameter on the Performance of Aerocyclone in Gas Droplet Two-Phase Flow. https://doi.org/10.1016/j.cep.2019.107645

Parvaz, F., Hosseini, S. H., Elsayed, K., & Ahmadi, G. (2018). Numerical investigation of effects of inner cone on flow field, performance and erosion rate of cyclone separators. Separation and Purification Technology, 201, 223-237. https://doi.org/10.1016/j.seppur.2018.03.030

Parvaz, F., Hosseini, S. H., Elsayed, K., & Ahmadi, G. (2020). Influence of the dipleg shape on the performance of gas cyclones. Separation and Purification Technology, 233, 116000. https://doi.org/10.1016/j.seppur.2019.116000

Parvaz, F., Hosseini, S. H., Bastan, A. R., Foroozesh, J., Babaoğlu, N. U., Elsayed, K., & Ahmadi, G. (2023). Influence of gas exhaust geometry on flow pattern, performance, and erosion rate of a gas cyclone. Korean Journal of Chemical Engineering, 40(7), 1587-1597. https://doi.org/10.1007/s11814-023-1430-2

Rahimi, A., & Singh, P. (2025). CFD-based optimization of axial cyclone geometry for dual-phase separation. Journal of Fluids Engineering, 147(3), 031501. https://doi.org/10.1115/1.4054932

Vahedi, S. M., Parvaz, F., Kamali, M., & Jafari Jebeli, H. (2018). Numerical investigation of the impact of inlet channel numbers on the flow pattern, performance, and erosion of gas-particle cyclone. Iranian Journal of Oil and Gas Science and Technology, 7(4), 59-78. https://doi.org/10.22050/ijogst.2018.16066.1300

Vahedi, S. M., Parvaz, F., Rafee, R., & Khandan Bakavoli, M. (2018). Computational fluid dynamics simulation of the flow patterns and performance of conventional and dual-cone gas-particle cyclones. Journal of Heat and Mass Transfer Research, 5(1), 27-38. https://doi.org/10.22075/jhmtr.2017.11918.1170

Vahedi, S. M., Parvaz, F., Khandan Bakavoli, M., & Kamali, M. (2020). Effect of Surface Roughness on Vortex Length and Efficiency of Gas-oil Cyclones through CFD Modelling. Iranian Journal of Oil and Gas Science and Technology, 9(1), 68-84. https://doi.org/10.22050/ijogst.2020.19460.1543

Xiong, Z., Ji, Z., & Wu, X. (2014). Development of a cyclone separator with high efficiency and low pressure drop in axial inlet cyclones. Powder Technology, 253, 644-649. https://doi.org/10.1016/j.powtec.2013.12.016

Zhang, S., Shin, M., & Shin, W. G. (2021). Comparison of models to predict the collection efficiency of an axial cyclone with a spindle vane. Journal of Aerosol Science, 157, 105817. https://doi.org/10.1016/j.jaerosci.2021.105817

شناسایی و رتبه‌بندی عوامل مؤثر بر تعیین نقطه تحویل در قراردادهای بین‌المللی فروش گاز طبیعی (مورد مطالعه: قراردادهای فروش گاز طبیعی با روش ال ان جی)

- محمدرضا علیمردان[۱]، عباس کاظمی نجف‌آبادی[۲*]، محمدرضا سیدهاشمی تولون[۳]، سید اصغر هندی[۴]، محمدمهدی حاجیان[۵]

۱. دانشجوی دکتری، گروه حقوق خصوصی، دانشکده حقوق و علوم سیاسی، دانشگاه علامه طباطبایی، تهران، ایران

۲. دانشیار، گروه حقوق خصوصی، دانشکده حقوق و علوم سیاسی، دانشگاه علامه طباطبایی، تهران، ایران

۳. االستادیار، گروه مدیریت، موسسه آموزش عالی سهروردی، قزوین، ایران

۴. عضو هیئت علمی، پژوهشگاه صنعت نفت، تهران، ایران

۵. استادیار، گروه حقوق خصوصی، دانشکده حقوق و علوم سیاسی، دانشگاه علامه طباطبایی، تهران، ایران

(ایمیل نویسنده مسئول: kazemi_najaf@atu.ac.ir)

چکیـــــــده

تحلیل محیط جهانی صنعت انرژی و تحولات آن نشان می‌دهد که گاز طبیعی شکل دهنده آینده انرژی جهان است. آینده ایران به‌عنوان صاحب اولین منابع گازی جهان، انکارناپذیر با مقوله‌ای به نام «گاز طبیعی» گره‌خورده است. تحولات جدید از جمله شرایط محیطی جهان، پیامدهای جنگ روسیه و اوکراین، تنش‌های منطقه خاورمیانه و پیش‌بینی افزایش قیمت جهانی نفت خام در آینده نزدیک نیز بر نقش و اهمیت گاز طبیعی افزوده است. بر اساس تحلیل بریتیش پترولیوم (BP) و آژانس بین‌المللی انرژی (IEA)، روند مصرف گاز طبیعی تا سال ۰۳۰۲ با سرعت بیشتری ادامه خواهد داشت؛ بنابراین برای حفظ موقعیت برتر ایران در بازارهای جهانی و استفاده به‌موقع از مزیت ذخایر گاز کشور به‌منظور تبدیل این ذخایر به سرمایه با ارزش‌افزوده بیشتر، نیازمند توسعه بیشتر زیرساخت‌های فنی، سیاسی، بازاریابی، حقوقی، زیرساختی و غیره کشور هستیم. روش و تنگناهای اساسی در آن. یکی از مهم‌ترین گلوگاه‌های قراردادهای بین‌المللی فروش گاز طبیعی، طراحی و تعیین «نقطه تحویل» است که با توجه به نحوه واگذاری و عوامل احتمالی هر قرارداد، می‌تواند در قراردادهای مختلف متفاوت باشد. در این تحقیق به‌منظور شناسایی عوامل مؤثر بر تعیین «نقطه تحویل» در قراردادهای بین‌المللی فروش گاز طبیعی به‌صورت LNG، ادبیات تحقیق بررسی و با کارشناسان مصاحبه صورت گرفت و مدل مفهومی تحقیق و شاخص‌های اندازه‌گیری آن‌ها طراحی شد. شاخص‌های جمع آوری شده در قالب پرسشنامه محقق ساخته بین اعضای جامعه آماری توزیع و نظرات آن‌ها جمع‌آوری شد. با توجه به یافته‌های این تحقیق، نتایج آزمون T حاکی از آن است که پنج عامل اصلی تعریف شده برای این تحقیق، به گفته اعضای جامعه آماری پژوهش، در تعیین نقطه تحویل در قراردادهای بین‌المللی فروش گاز طبیعی با تأکید بر روش LNG مؤثر است. از طرفی برای رتبه‌بندی این عوامل از نظر میزان اهمیت از آزمون رتبه‌بندی فریدمن استفاده شد. بر اساس نتایج آزمون، عامل قراردادی بالاترین میانگین رتبه و در نتیجه بیشترین اهمیت را داشت. عوامل سیاسی، جغرافیایی، فنی و اقتصادی به ترتیب از نظر اهمیت دنبال شدند.

واژگان کلیدی: گاز طبیعی، گاز طبیعی مایع (LNG)، قرارداد فروش و انتقال گاز طبیعی، نقطه تحویل، عوامل قراردادی، عوامل اقتضایی

جداسازی CO_2 ارتقا یافته با استفاده از غشای Pebax اصلاح شده با اتیلن گلایکول مونو فنیل اتر

- مهدی الیاسی کجاباد[1*]، پریا امیرعابدی[1]، مسعود درفشان[2]

۱. استادیار، گروه مهندسی شیمی، دانشکده فنی و مهندسی، دانشگاه صنعتی خاتم‌الانبیا بهبهان، بهبهان، ایران

۲. استادیار، گروه مهندسی مکانیک، دانشکده فنی و مهندسی، دانشگاه صنعتی خاتم‌الانبیا بهبهان، بهبهان، ایران

(ایمیل نویسنده مسئول: m.elyasi@bkatu.ac.ir)

چکیـــــــده

جداسازی CO_2 یکی از چالش‌های اساسی دنیای امروز می‌باشد که به دلیل رشد صنایع اتفاق افتاده است. روش جداسازی غشایی روشی نوین برای جداسازی CO_2 می‌باشد که غشای پلیمری پلی اتر بلاک آمید (Pebax) یکی از غشاهای صنعتی در این راستا می‌باشد. این نوع غشا محدودیتی به نام محدودیت Trade-off دارد که مانع از کاربرد گسترده آن در صنعت می‌شود. در این مطالعه به‌منظور غلبه بر این محدودیت، از اتیلن گلایکول مونو فنیل اتر (EGME) به‌عنوان پرکننده در زمینه Pebax استفاده شده و تأثیر آن بر روی ساختار شیمیایی، موفولوژی، خواص فیزیکی و حرارتی و نیز خواص جداسازی این پلیمر مورد بررسی قرار گرفت. نتایج نشان داد با افزودن EGME غشای تهیه شده تردتر و سفت‌تر شده و استحکام کششی و مدول یانگ برای غشای حاوی EGME نسبت به غشای خالص به ترتیب ۵۳ و ۹۹/۵ درصد افزایش داشت. علاوه بر این عبور دهی CO_2 و انتخاب‌گری CO_2/N_2 به دلیل برهمکنش‌های اسید-باز لوئیس، دوقطبی- چهارقطبی و π-چهارقطبی برقرار شده بین مولکول‌های EGME و CO_2 به ترتیب ۲۴۷ و ۴۹ درصد ارتقا یافت به‌طوری که با این بهبود عملکرد، غشای Pebax حاوی EGME توانست از مرز بالایی رابسون عبور کرده و بر محدودیت Trade-off غلبه کند که نشانی بر نقش کلیدی EGME در بهبود عملکرد جداسازی Pebax بود. علاوه بر این، عملکرد جداسازی غشاهای تهیه شده با غشاهای ساخته شده توسط دیگر محققان قابل مقایسه بود و از اکثرشان بهتر بود.

واژگان کلیدی: جداسازی CO_2، غشای پلیمری، پلی اتر بلاک آمید، اتیلن گلایکول مونو فنیل اتر، محدودیت Trade-off

مکاربرد امواج فراصوت در امولسیون زدایی (آب‌گیری) از نفت خام

- آسیه حافظی[۱]، امیرحسین سعیدی دهاقانی[۲]، سروه عبدالهی[۳]، مهدی رضوی فر[۴*]

۱. دانشجو دکتری، دانشکده شیمی و مهندسی شیمی، دانشگاه آزاد اسلامی، رشت، ایران

۲. دانشیار، گروه مهندسی نفت، دانشکده مهندسی شیمی، نام دانشگاه تربیت مدرس، تهران، ایران

۳. استادیار، دانشکده شیمی و مهندسی شیمی، دانشگاه آزاد اسلامی، رشت، ایران

۴. استادیار، دانشکده مهندسی شیمی و نفت، دانشگاه تبریز، تبریز، ایران

(ایمیل نویسنده مسئول: m.razavifar@tabrizu.ac.ir)

چکیـــــــده

امولسیون زدایی (آب‌زدایی) نفت خام نقش مهمی در کاهش آلودگی نفتی در محیط متخلخل خاک و سازه‌های سنگی و جلوگیری از خوردگی خطوط لوله و تأسیسات سطحی دارد. در طول دو دهه گذشته، استفاده از تابش امواج مافوق صوت برای امولسیون زدایی و نمک‌زدایی نفت خام به دلیل مزایای زیست‌محیطی و اقتصادی قابل‌توجهی که دارد، توجه روزافزونی را به خود جلب کرده است. بااین‌حال، یک شکاف تحقیقاتی در مورد مقایسه روش‌های متداول امولسیون زدایی با درمان اولتراسونیک (UST) وجود دارد. در این مطالعه، یک بررسی جامع برای ارزیابی اثرات UST بر امولسیون زدایی از نفت خام انجام شد. UST پایداری امولسیون‌های آب در نفت را کاهش می‌دهد، به‌ویژه هنگامی که امواج فرکانس پایین اعمال می‌شود. بر اساس یافته‌ها، UST به‌عنوان یک روش امیدوارکننده هم برای امولسیون زدایی و هم نمک‌زدایی نفت خام مطرح شده است. بر اساس نتایج، UST باعث می‌شود که میزان حذف نمک بیش از ۰۹ درصد و محتوای آب باقیمانده به‌طور مداوم زیر ۰/۳ درصد حجم باشد، حتی برای مواد اولیه خام سنگین با گرانروی بالا. هنگامی که این فناوری در سیستم‌های پیش‌تصفیه پالایشگاه مستقر می‌شود، کارایی نمک‌زدایی را افزایش می‌دهد و در عین حال مصرف دمولسیفایر شیمیایی را ۰۴ تا ۰۶ درصد کاهش می‌دهد. نتایج یک مزیت دوگانه را برجسته می‌کند: عملکرد عملیاتی قوی در شرایط سخت و کاهش قابل‌توجه وابستگی شیمیایی. مکانیسم‌های اولیه امولسیون زدایی مبتنی بر UST کاویتاسیون و ارتعاشات ناشی از موج هستند. این مکانیسم‌ها کشش سطحی (IFT) بین نفت خام و آب را تغییر می‌دهند، گرانروی نفت را کاهش می‌دهند، فشار و دما را افزایش می‌دهند و اجزای نفت خام سنگین، به‌ویژه خوشه‌های آسفالتین را می‌شکنند. ترکیب UST با روش‌های متداول امولسیون زدایی می‌تواند عملکرد را افزایش دهد. به‌عنوان مثال، کاربرد هم‌زمان UST و نانوتکنولوژی یک رویکرد عملی برای امولسیون زدایی کارآمد ارائه می‌دهد. علاوه بر این، اثرات هم‌افزایی UST و افزودنی‌های شیمیایی باید به‌طور جامع بررسی شود تا شرایط عملیاتی بهینه شناسایی شود. نتایج این تحقیق بینش‌هایی را برای صنعت نفت به‌منظور بهبود راندمان امولسیون زدایی و کاهش آلودگی محیطی مرتبط با نفت خام ارائه می‌کند.

واژگان کلیدی: امواج فراصوت، نفت خام، امولسیون، امولسیون زدایی، آبگیری

بهینه‌سازی سازه‌های پایپرک لوله فولادی در صنعت نفت با استفاده از الگوریتم‌های فرا اکتشافی

- روح الامین چترآذر[۱]، حامد قوهانی عرب[۲*]، محمود میری[۳]

۱. ۱-دانشجوی کارشناسی ارشد، گروه مهندسی عمران، دانشکده مهندسی، دانشگاه سیستان و بلوچستان، زاهدان، ایران

۲. ۲-دانشیار، گروه مهندسی عمران، دانشکده مهندسی، دانشگاه سیستان و بلوچستان، زاهدان، ایران

۳. ۳-استاد، گروه مهندسی عمران، دانشکده مهندسی، دانشگاه سیستان و بلوچستان، زاهدان، ایران

(ایمیل نویسنده مسئول: ghohani@eng.usb.ac.ir)

چکیـــــــده

پایپرک‌های فولادی یکی از سازه‌های مهم در صنایع مختلف از جمله نفت و پتروشیمی هستند که برای انتقال سیالات، گازها و مواد شیمیایی، مورد استفاده قرار می‌گیرند. با توجه به کاربرد وسیع این نوع سازه‌ها در صنایع نفت و گاز، بهینه‌سازی آن‌ها از اهمیت ویژه‌ای برخوردار است. هدف این تحقیق، کاهش هزینه‌ی ساخت پایپرک‌های فولادی از طریق بهینه‌سازی وزن به صورت کاربردی با استفاده از الگوریتم‌های فرا ابتکاری گرگ خاکستری و نهنگ و همچنین مقایسه‌ی پاسخ‌های آن‌ها می‌باشد. در این پژوهش، الگوریتم‌های نامبرده به‌صورت خودکار و با استفاده از برنامه‌نویسی در محیط MATLAB توسعه یافته‌اند و از طریق ارتباط با نرم‌افزار ETABS، طراحی بهینه‌ی پایپرک‌های فولادی با رعایت قیود آیین‌نامه‌ای امکان‌پذیر می‌باشد. پژوهش حاضر با بهره‌گیری از الگوریتم‌های فرا ابتکاری و رعایت الزامات آیین‌نامه‌های طراحی، در پی ارائه راهکاری عملی برای طراحی بهینه و ایمن سازه‌های پایپرک فولادی است تا از این طریق هزینه‌های ساخت در صنعت نفت و گاز را کاهش دهد. کارکرد طرح پیشنهادی بر روی دو پایپرک فولادی با رعایت نکات طراحی، ارزیابی شده است. نتایج نشان می‌دهد که هر دو روش بهینه‌سازی فرا ابتکاری گرگ خاکستری و نهنگ، می‌توانند به‌عنوان یک ابزار کارآمد برای مهندسان، در دستیابی به طرح‌های اقتصادی مورد استفاده قرار بگیرند.

واژگان کلیدی: سازه پایپرک فولادی، بهینه‌سازی، الگوریتم‌های فرا ابتکاری، الگوریتم بهینه‌سازی گرگ خاکستری، الگوریتم بهینه‌سازی نهنگ

تأثیر زبری دیواره بر الگوی جریان و عملکرد سیکلون گازی محوری به همراه نرخ فرسایش

- مسعود درفشان[1*]، ستار مقدم[2]، فرزاد پرواز[3]

۱. استادیار، گروه مهندسی مکانیک، دانشکده فنی و مهندسی، دانشگاه صنعتی خاتم‌الانبیا بهبهان، بهبهان، ایران

۲. دانشجو کارشناسی ارشد، گروه مهندسی مکانیک، دانشکده فنی و مهندسی، دانشگاه صنعتی خاتم الانبیا بهبهان، بهبهان، ایران

۳. کارشناسی ارشد، گروه مهندسی مکانیک، دانشکده فنی و مهندسی، دانشگاه سمنان، سمنان، ایران

(ایمیل نویسنده مسئول: dorfeshan@bkatu.ac.ir)

چکیـــــــده

در این مطالعه، تأثیر زبری دیواره بر الگوی جریان، عملکرد و نرخ فرسایش در یک سیکلون گازی محوری بررسی شده است. سیکلون‌های گازی به دلیل انعطاف‌پذیری، هزینه‌های نگهداری پایین و کارایی در کنترل آلودگی هوا، به‌طور گسترده در صنایع مختلف مانند فرآوری مواد غذایی، خشک‌کن‌ها و صنعت سیمان برای جداسازی ذرات جامد از جریان گاز استفاده می‌شوند. مدل‌سازی عددی با استفاده از مدل‌های آشوبناکی، مدل‌های زبری سطح، مدل فاز گسسته و مدل فرسایش انجام شده است تا پارامترهای کلیدی مانند افت فشار، سرعت مماسی، سرعت محوری، راندمان جداسازی و نرخ فرسایش دیواره تحلیل شوند. نتایج نشان می‌دهد که افزایش زبری دیواره باعث کاهش سرعت مماسی و در نتیجه کاهش نیروی گریز از مرکز می‌شود که این امر تأثیر منفی بر راندمان جداسازی ذرات دارد. از سوی دیگر، افزایش زبری دیواره منجر به کاهش افت فشار می‌شود که در طراحی سیکلون یک مزیت محسوب می‌گردد. تحلیل نرخ فرسایش نیز نشان می‌دهد که بیشترین فرسایش در بخش مخروطی پایین سیکلون رخ می‌دهد و افزایش زبری دیواره می‌تواند فرسایش را کاهش دهد. به‌طور کلی، این مطالعه نشان می‌دهد که زبری دیواره تأثیرات متضادی بر عملکرد سیکلون دارد—از یک سو افت فشار را کاهش می‌دهد و از سوی دیگر راندمان جداسازی را کم می‌کند؛ بنابراین، بهینه‌سازی زبری سطح برای دستیابی به تعادل بین این دو عامل در طراحی سیکلون‌های گازی محوری ضروری است. نتایج نشان داد که افزایش ناهمواری دیوار، سرعت مماسی را تا ۸۱ درصد کاهش داد، بازده جمع‌آوری سیکلون برای ذرات بزرگ‌تر از ۵۲ میکرومتر تقریباً ۲۱ درصد کاهش یافت، در حالی که افت فشار حدود ۹ درصد کاهش یافت که این موضوع در کاربردهای حساس به انرژی مفید محسوب می‌شود. بیشترین نرخ فرسایش در نوک مخروط سیکلون مشاهده شد و ناهمواری دیوار به کاهش میانگین فرسایش تقریباً ۵۱ درصد کمک کرد.

واژگان کلیدی: سیکلون گازی محوری، زبری دیواره، افت فشار، فرسایش دیواره، مدل فاز گسسته

JOURNAL OF GAS TECHNOLOGY
VOLUME 9 • ISSUE 2 • WINTER 2024
EISSN: 2588-5596

Contents

1 **Identifying and Ranking the Factors Influencing the Determination of the "Delivery Point" in International Natural Gas Sales Contracts (Case Study: Natural Gas Sales Contracts in LNG state)**

Mohammad Reza Alimardan, Abbas Kazemi Najafabadi, Mohammad Reza Seyed Hashemi Touloun, Seyed Asghar Hendi, Mohamad Mahdi Hajian

2 **Enhanced CO^2 Separation Using Pebax Membrane Modified with Ethylene Glycol Monophenyl Ether**

Mahdi Elyasi Kojabad, Parya Amirabedi, Masoud Dorfeshan

3 **Application of Ultrasonic Waves on the Demulsification (Dehydration) of Crude Oil**

Asieh Hafezi, Amir Hossein Saeedi Dehaghani, Serveh Abdollahi, Mehdi Razavifar

4 **Optimisation of Steel Pipe-Rack Structures in the Oil Industry Using Metaheuristic Algorithms**

Ruholamin Chatrazar, Hamed Ghohani Arab, Mahmoud Miri

5 **The Impression of Roughness on Flow Pattern and Performance of Axial Gas Cyclone Along with Erosion Rate**

Masoud Dorfeshan, Sattar Moghaddam, Farzad Parvaz